ADDIS ABABA UNIVERSITY

ADDIS ABABA INSTITUTE OF TECHNOLOGY

SCHOOL OF CIVIL AND ENVIRONMENTAL ENGINEERING

Estimation of Sediment Yield under the Impact of Climate Change (Case of Mille River Watershed, Lower Awash Sub-Basin, Ethiopia)

A Thesis Submitted and Presented to the School of Graduate Studies of Addis Ababa University in Partial Fulfillment of the Requirement for the Degree of Masters of Science in Civil Engineering (Major Hydraulic Engineering)

By

Samuel Tadesse

Advisor

Bayou Chane (PhD)

March, 2022

Addis Ababa University

Addis Ababa Institute of Technology

School of Civil and Environmental Engineering

Estimation of Sediment Yield under the Impact of Climate Change

(Case of Mille River Watershed, Lower Awash Sub-Basin, Ethiopia)

A Thesis Submitted to the School of Graduate Studies of Addis Ababa University in Partial Fulfillment of the Degree of Masters of Science in Civil Engineering (Major Hydraulic Engineering)

By

Samuel Tadesse

Approval by Board of Examiners

_______________	_______________	_______________
Advisor	Signature	Date
_______________	_______________	_______________
Internal Examiner	Signature	Date
_______________	_______________	_______________
External Examiner	Signature	Date
_______________	_______________	_______________
Chairman (Department of Graduate Committee)	Signature	Date

CERTIFICATION

The undersigned certify that I have read and here by recommend for acceptance by Addis Ababa University Institute of Technology a thesis entitled "Estimation of Sediment Yield under the Impact of Climate Change (Case of Mille River Watershed, Lower Awash Sub-basin, Ethiopia)" in partial fulfillment of the requirement for the degree of Masters of Science in civil engineering specialization in Hydraulic Engineering.

____

Dr. Bayou Chane

____

Date

DECLARATION

I, the undersigned, hereby declare that this thesis entitled, “Estimation of Sediment Yield under the Impact of Climate Change (Case of Mille River Watershed, Lower Awash Sub-basin, Ethiopia” is my own work, and that all the sources I have quoted indicated or acknowledge by means of completed reference.

Samuel Tadesse

ACKNOWLEDGMENT

First of all my thank to Above all, creator and governor of the two worlds, the almighty GOD, Jesus Christ, his mother Saint Marry, all his Angels and Saints for his priceless and miracle gifts to me.

Special thanks to my advisor, Dr. Bayou Chane (PhD) for his support and encouragement during all research time for his critical comments and valuable advices helped me to take this study in the right direction.

Next my deepest gratitude goes to Addis Ababa University institute of Technology, school of civil and environmental engineering staffs who help me by facilitating data requesting letters for different organization during data collection and I would also to thank Ethiopian Ministry of Water, Irrigation and Energy, Awash Basin Authority and National Meteorological Service for their providing me all necessary data for my study.

Finally, I wish to express deep gratitude to all my family members especially to my Mam Birtukan Tadesse Haile and my sister Hana Tadesse for their support, motivation and encouragements to achieve this work and to my precious friends Mubarek Mudesir, Biniyam Lulu, Shemelies Gia, Tekalegn Amanuel, Mastewal Girma, Micheal Lemma, Biniyam Sheleshi, Natnael Negusse and Henok Berhane.

ABSTRACT

Climate change impact and its variability on stream flows and sediment yield are now becoming one of the significant challenges. Hence evaluation of the impact and the trends of the climate change on hydrological process is very important at watershed level. The aim of this study was to assess the impact of climate change on the sediment yield of Mille river watershed at the lower Awash sub-basin using both climate and SWAT hydrological model. The climate model variables (precipitation and temperature) were obtained from Coordinated Regional Downscaling Experiment (CORDEX) of RACMO22 RCM climate model under HadGEM2-ES GCM and CCLM4 regional Climate model under ICHEC-ES global climate model with representative concentration pathway (RCP4.5) and (RCP8.5) scenarios. Bias correction was applied to climate variables and average value of the two RCM models arranged before future climate data's transferred to hydrological model (SWAT) to simulate discharge and sediment for future time period. For model performance evaluation; Coefficient of determination (R^2) and Nash Sutcliffe Efficiency (NSE) were used during calibration (1989-1997) and validated (1998-2002) period. The result of calibration and validation flow (R^2 and NSE) are 0.68, 0.54 and 0.7, 0.6 respectively. Calibration and validation of sediment also provided a result of 0.81, 0.81 during calibration and 0.8, 0.79 during validation for R^2, NSE respectively. Stream flow was simulated for two consecutive thirty years periods of (2031–2060) and (2061-2090) for both scenarios and compared with the base period (1986–2015) to investigate impact of climate change on hydrological process. The result obtained shows that overall mean annual precipitation projected to increase by 3.86% in 2050s and 7.82% during 2070s under RCP 4.5. For RCP 8.5 climate scenario precipitation increase by 4.61% during 2050s and 10.57% during 2070s. The hydrological response of a catchment also show an increment for the increasing precipitation amount such as sediment yield increase by 5.85% and 10.11% during 2050s and 2070s respectively under RCP 4.5 and 8.99% and 14.25% of increment occur in 2050s and 2070s respectively for RCP 8.5 climate scenario.

Temperature maximum also shows an increment with a magnitude of 0.11^{o}c and 0.09^{o}c under RCP 4.5 of the 2050s and 2070s on the other hand 0.2^{o}c and 0.15^{o}c increment was observed with in the same period of RCP 8.5. Temperature minimum will be increase for the future over the Mille watershed by 0.09^{o}c and 0.15^{o}c Under RCP 4.5 and by 0.13^{o}c and 0.18^{o}c under RCP 8.5 for the *same time horizons of 2050s and 2070s.Overall there will be a variations of precipitation, temperature and sediment yield month to month and season to season. Therefore, it is important to consider this variation of sediment yield and climatic variable to draw appropriate guidelines for planning and management of different water resources project.*

Key words: SWAT; GCM; RCM; Climate model; Bias correction; Climate Change;

Table of Contents

LIST OF FIGURES

LIST OF TABLES

ABBREVIATION AND ACRONYMS

AR4	Assessment Report 4
ARBA	Awash River Basin Authority
CCLM	Climate Community limited Area Modeling
CMIP	Coupled Model Inter-Comparison Project
CORDEX	Coordinated Regional Downscaling Experiment
DEM	Digital Elevation Model
DM	Distribution Mapping
GCM	Global Climate Model
GHGs	Greenhouse Gases
HRU	Hydrologic Response Unit
IPCC	Inter-Governmental Panel on Climate Change
ITCZ	Intertropical Convergence Zone
LULC	Land Use Land Cover
MoWIE	Ministry of water, Irrigation & Electricity
NMA	Nation Meteorology Agency
NSE	Nash and Sutcliffe Efficiency
PBIAS	Percent Bias
PT	Power Transformation
QM	Quantile Mapping
RCM	Regional Climate Model
RCPs	Representative Concentration Pathways
RMSE	Root Mean Square Error
SRES	Special Report on Emission Scenario
SWAT	Soil and Water Assessment Tool
UNDP	United Nation Development Program
USDA	United State Department of Agriculture

1. INTRODUCTION

1.1 Background

A comprehensive study of the enormous figure of observation pertaining to different parts of the climate system by the intergovernmental panel on climate change (IPCC) demonstrated that global warming is indeed occurring IPCC (2013, 2014). Since the 1990s, the global average temperature has increase by about 0.8^{o}c and is projected to raise another 1.4^{o}c-2.0^{o}c by the end of the twenty-first century IPCC (2013). This change poses frequent flood, drought, reduction of rainfall potential, and shift in minimal agricultural system Corner et al.,(2012), Kumar et al., (2010), Thornton et al., (2011).

The intergovernmental panel on climate change (IPCC) report confirm that "global warming" is occurring IPCC, (2007). This global warming leads to changes in precipitation and temperature, then affects the hydrological cycle, and thus changes in stream flow and also modifies the transformation and transport characteristics of sediment as well as water pollutants TU T. et al., (2009). Therefore, climate change is an important factor influencing hydrological condition and sediment yield. Understand the hydrologic and sediment responses to climate change is important for water resources planning and management.

The change in climate mainly due to precipitation and temperature pattern could significantly influence soil erosion rate, stream flow and sediment yield which (directly or indirectly) adversely affects water resource availability and ecosystem Shrestha B. et al., (2013). In connection to this, numerous studies have indicated that change in precipitation and temperature and the interaction of these with land use and land cover change (LULCC) will be the main climate change related stress expected to exacerbate soil loss and sediment transport Nearing M., Pruski F. et al., (2004).

Sediment yield estimations are needed for studies of reservoir sedimentation, river morphology, soil and water conservation planning, water quality modelling and design of efficient erosion control structures. Sediment yield refers to the quantity of sediment transported to the basin outlet over a period. It is also referred as the amount, which would enter into reservoir located at the downstream limit of the basin Morries and Fan et al., (1998). The process of soil erosion by rainfall and runoff mainly consists of the detachment and transport by raindrops and runoff.

The sediment load of a river is sensitive to both climate and a wide range of human activities within its drainage basin. These factors could influence sediment mobilization and transfer through actions like clearing of land, agricultural development, mineral extraction, urbanization and infrastructure development, dam and reservoir construction and soil conservation and sediment control programs Walling el al., (2008).

Farmers in the horn of Africa, including Ethiopia are vulnerable to climate change extremes such as flood and droughts, both of which are the most common hydro-meteorological extremes in tropical countries Di Falco S. et al., (2011). Ethiopia is a country which the economy largely depends on rain-fed agriculture, which is highly vulnerable to the impact of climate change, mainly changes in precipitation patterns Deresse T. et al., (2011). Precipitation pattern and character in Ethiopia area predominantly controlled by the oscillation of the intertropical convergence zone. This precipitation has a strong impact on soil erosion. A change in precipitation intensity and seasonal distribution results in a significant impact on soil erosion rate Nearing M., Pruski F. et al., (2004). According to Zhang X. et al., (2005), precipitation and soil erosion are directly proportional to each other.

Reliable prediction of the quantity and rate of runoff, and sediment transport from land surface into streams, rivers and other water bodies are needed to help decision makers in developing watershed management plans for better soil and water conservation measures Setegn S. et al., (2010) and to assess potential future implication due to the factors driving the changes. In order to examine the non-linear interplay between climate induced processes that influence sediment discharge at the watershed level, hydrological and sediment models can be used in combination with climate projection from global circulation models regional climate models Francipane A., Fatichi S. et al., (2015).

Several studies have been conducted to assess flooding and droughts caused by climate change in the lower Awash sub-basin (LARB), including the Mille watershed ACCRA, (2011). However, none of these studies addressed the climate change impact on sediment yield both in the lower

Awash sub-basin and the Mille watershed. Precipitation and temperature of the watershed both fluctuate, which subsequently results in a variation of river flow in the watershed under climate conditions. The Mille watershed is characterized by severe land degradation and desertification, but high flood also occurs, mostly in the upstream areas during high rain seasons ACCRA, (2011). The magnitude of climate change effects on sediment yield varies depending on the region in focus and the climate scenario taken into consideration IPCC, (2001). Understanding the peculiar effects of climate change on sediment load is critical for watershed management LU X. et al., (2013).

Therefore, a comprehensive understanding of hydrological process in the watershed is a prerequisite for water management and environmental restoration. Due to the spatial and temporal heterogeneity of climate condition, soil properties, vegetation and land use practices, a hydrologic cycle is a complex system. As a result, mathematical model and geospatial analysis tool are required for studying climate change, hydrological process and hydrological response to land use and climate change. Hence analyzing the climate change of lower Awash sub-basin at Mille river watershed with respect to the hydrological response is essential for sustainable and important planning and development of water resources project with in the watershed as well as proper management and utilization of Tendaho dam in which Mille River join main Awash river just few kilometers upstream of reservoir. Because of great functionalities of the dam for protection of flooding for downstream areas and for the development of sugar industry for the country the dam needs proper management of sediment deposition and other safety works in order to increase the useful life of the dam and to increase its sustainability. Therefore under this study representative concentration pathways (RCPs), which supersede the Spatial Report on Emission Scenario (SRES), a newly developed climate scenarios that provides input for climate models and a distributed hydrological model, soil and water assessment tool (SWAT) was used to estimate the potential impact on climate change on sediment yield in the lower Awash sub-basin especially at Mille watershed.

1.2 Problem Statement

One of the most important consequences of climate change is alterations in major climate variables, such as temperature, precipitation, and evapotranspiration. This in turn will lead to changes in the hydrological cycle, influencing the components of water balance of drainage basins in several ways such as the availability and distribution of water resources in space and time, stream flow, frequency of extreme events.

A warmer climate will accelerate the hydrological cycle, altering rainfall and the magnitude and timing of runoff. Changes in climate are also expected to have noticeable effects on the soil since rainfall and runoff are the factors controlling soil erosion and sediment transport within landscapes. The changes in flow characteristics resulting from climate change depend on individual catchment characteristics.

The Lower Awash River basin are characterized by sever land degradation and desertification, but high flood also occurs, mostly in upstream areas during high rain seasons ACCRA (2011). Manifestations of desertification in Lower Awash Basin include accelerated soil erosion by wind and water, increasing salinity of soils and near -surface groundwater supplies, a reduction in soil moisture retention, an increase in surface runoff and stream flow variability, a reduction in species diversity, plant biomass and overall productivity. Thus, understanding the impact of climate change and looking for the solution to minimize the problem is essential and also effective measurement can be implemented.

Local perspectives can be combined with scientific climate scenarios to draw policy recommendations for future estimation strategies. Future climate change impact assessment researches conducted using regional climate model and new RCPs at finer resolution scale so far in the study area are limited. Most of it focuses on water resource availability and planning, water resource and extreme events, policy responses to climate change assessment in the sub-basin. Therefore, to fill this gap, this study focuses on assessing the effect of climate change on sediment yield of Mille watershed by considering projected future climate from finer resolution and downscaled regional climate model under different RCPs climate scenarios.

1.3 Research Questions

- What are the likely change of precipitation and temperature for future time period under different RCPs climate scenarios?
- What is the impact of changing climate on sediment yield of the watershed?
- How much sediment is yielded from each sub watershed under different RCPs climate scenarios?

- How much sediment will generate from the change in climate variables under different RCPs climate scenarios over the Mille watershed?

1.4 Objective of the Study

1.4.1 General Objective

The overall objective of this study is to estimate the amount of sediment yield which is generated from Mille watershed under the impact of climate change using downscaled climate model under different RCP scenarios and Arc-GIS interface SWAT hydrologic model.

1.4.2 Specific Objective

I. To estimate the annual sediment yield of the watershed
II. To assess the amount of sediment yield under different RCP climate scenarios
III. To assess the spatial variation of sediment yield under different RCP climate scenarios

1.5 Significance of the Study

Application of hydrological model in the watershed at spatial and temporal scale would be essential to know the hydrological process and to study the impact of climate change on the watershed which helps to set different management scenarios that will lead to sound environmental sustainability.

The effect of climate change on stream flow and sediment yield is crucial and sensitive issue over the entire world today. Therefor identifying and understanding such effects makes water resource planner, decision makers and any concerned body to understand the consequences of climate change impacts on the water resource potential and sediment yielded of the watershed is very important, hence climatic parameters most importantly precipitation and temperature are the key element on the overall hydrological process of a watershed.

In addition, the output of this research will likely used as an input in planning approach and decision support tool in planning, developing and managing of water resources in Awash river basin particularly for Mille watershed.

1.6 Thesis Layout

The organization of the thesis is as follows:

1. Chapter one contain introduction on the issues related with climate change and climate change impact on sediment yield at global level, African continent level, Ethiopia level and Awash basin and lower Awash sub-basin and also this chapter includes the formulated problem statement which uses as a base for the study and identification of the gap, general and specific objectives research questions and significance of the study.
2. Chapter two contains Literature Reviews which includes climate change and climate models as well as the different RCP scenarios. In addition to this in this section SWAT hydrologic model and the general situation which is occurred on sedimentation process also discussed.
3. Chapter three contains material and methodology including description of the study area. In material section the type and source of material which is used for the study with their importance are discussed. And the methodology section describe the procedure which is followed and their process to achieve the specified objectives are elaborated.
4. Chapter four result and discussion that summarized the main findings of the research work. It deals with the performance evaluation of the climate model for their bias correction methods, the change of climate variables (such as precipitation and temperature maximum and minimum) for future period in reference with the base period time and the change in the sediment yield of the watershed due to the impact of climate change and their spatial variation under different RCP scenarios.
5. Chapter five contain the conclusion and recommendation that summarizes the whole research work.

2. LITERATURE REVIEW

2.1 Climate Change

Climate is "average" weather (current atmospheric condition) for a given place or a region. It describes typical weather conditions for a given area based on long-term average, usually decades or longer IPCC, (2007).

Climate change refers to a change of climate that is attributed directly or indirectly to human activity that alter the composition of the global atmospheric and that is in addition to natural climate variability observed over comparable time period, whether due to natural variability or as a result of human activity IPCC, (2007) .

Climate change is facing the entire world nowadays. It is now widely received that climate change is by now happening and further change is unavoidable; the global average combined land and ocean surface temperature data calculated shows a warming of 0.85^{o}c over the period 1880 to 2012 IPCC, (2014). This is more strongly after 1970; many studies discovery specifies that most of the increase in average global surface temperature over the last 50 years is attributed by human activities Endalkachew G. et al., (2012).

It was estimated that, change and sea level is expected to rise at rate of about 1.7 mm/yr as the ocean expands as heat is gradually diffused downwards in the ocean Endalkachew G. et al., (2012). The IPCC also noted observations over the past century shows, change were occurring in the amount, intensity, frequency and types of precipitation globally IPCC, (2007a).

The IPCC was established in 1988 by the world meteorological organization and the united nation environmental program, and its role is to "assess on a comprehensive, objective, open and transparent basis the scientific, technical and socio-economic information relevant to understanding the scientific basis of risk of human induced climate change, its potential impacts and options for adaptation and mitigation". Among the different assessment that were carried out by the IPCC, the most recent which published in 2007, states the projected global surface warming lies within the range 0.6 to 4.0^{o}c, whereas the projected see level rise lies within the range 18 to 59 cm at the end of the next century IPCC, (2007a).

Over the past decade, the impact of climate change on sediment yield have been widely studied around the globe Shrestha B. et al., (2013). Also studies show that sediment transport is highly influenced by extreme precipitation and river discharge due to the non-linear relationship between water discharge and sediment transportation rate Adem A. et al., (2015). Moreover, Francipane A., Fatichi S. et al., (2015) reported that the magnitude of mean and extreme events of sediment yield are expected to decrease with a high probability in Walnut Gulch experimental watershed in southeastern Arizona, USA. However, on their part, Zhang S. et al., (2019) indicated that climate change is expected to increase the annual average sediment yield by 4-32% when compared to the base period for the Zhenjiangguan watershed, in China. Azim F.et al., (2018) examined the impact of climate change on sediment yield of the Naran watershed, Pakistan using global climate model (GCM) predictors from Special Report on Emission Scenarios (SRES) A2 and B2 and scenarios for time horizons of 2011-2040 and 2041-2070, respectively. Likewise, Shrestha B. et al., (2013) used Soil and Water Assessment Tool (SWAT) model in the Nam Ou basin in northern Laos to predict the impact of climate change on sediment yield and reported changes in an annual sediment yield ranging from a 27% decrease to about a 160% increase. Further, Azari M. et al., (2016) conducted a similar study focusing on the Gorganroud river basin in Iran and found that the annual sediment yield would increase by 47.7%, 44.5% and 35.9% for the 2040-2069 time serious of the A1F1, A2 and B1 emission scenarios, respectively. Parry M. et al., (2007) imagines that under future climate condition with increased precipitation in the great horn of Africa, direct runoff and more erosion will be initiated.

2.1.1 Climate Change in Ethiopia

For the past four decades, the average annual temperature in Ethiopia has been increasing by 0.37oc every ten years, which is slightly lower than the average global temperature rising Emerta A. et al., (2013). According to Emerta, the greater part of the temperature rise was observed during the second half of the 1990's and temperature rise is more pronounced in the dry and hot spots of the country, which are located in the northern, northeastern and eastern parts of the country. The lowland areas are most affected, as these areas are largely dry and exposed to flooding during extreme precipitation in the highlands.

Future temperature projection of the IPCC mid-range scenario show that the mean annual temperature will increase in the range 0.9 to 1.1oc by 2030, in the range of 1.7 to 2.1^{o}c by 2050, and in the range of 2.7 to 3.4oc by 2080 in Ethiopia compared to the 1961 to 1990 Emerta A. et al., (2013).

However the has both dry and wet periods over the past four decades, precipitation has a general decreasing trend since the 1990s Abayneh A. et al., (2011). The decrease in precipitation has multiple effect on water availability for irrigation and other farming uses, especially in the north, northeastern, and eastern low lands of the country. The average change in rainfall is projected to be in the range of 1.4 to 4.5 percent, 3.1 to 8.4 percent and 5.1 to 13.8 percent over 20, 30 and 50 years respectively, compared to the 1961 to 1990 usual. According to Abayneh, the overall trend in the entire country is more or less constant. Related with rainfall and temperature change and variability, there was recurrent draught and flood events in the country. There was also observation of water level rise and dry up of lakes in some part of the country depending on the general trend of the temperature and rainfall pattern of the regions.

The economy of Ethiopia is heavily dependent on rain-fed agriculture that is highly vulnerable to climate change Deresse T. et al., (2011). According to NMA (2001) studies, using historical data of temperature and precipitation from 1951-2005 for selected stations in Ethiopia showed that, from year to year variation of precipitation was observed. Over the country, during this period both wet and dry were occurred.

Trend analysis of annual precipitation in Ethiopia shows that precipitation remained more or less constant when average over the whole country while a declining trend has been observed over the northern and southwestern and the spatial variation of precipitation was influenced by the change in intensity, position and movement of direction rain-producing systems over the country IPCC, (2007). According to NMA, (2001) revealed that in Ethiopia climate variability and change in the country, is mainly manifested through the variability and decreasing trend in precipitation and increasing trend in temperature.

A study McSweenet C. et al., (2008) reported that, historical climate data from (1960-2006) for the country indicated that, mean annual temperature has been increased by 1.3^{oc} and 0.28^{oc} per decade and an average rate was increased. The authors also explained that, increase in temperature in Ethiopia has been most rapid in June, August and September at a rate of 0.322^{oc} per decade and also precipitation in historically highly variable and there is no clear trend in amount of precipitation over time. The wide range of these different scenarios highlights the uncertainty in future projections for climate change in Ethiopia. Clearly, Ethiopia is highly vulnerable to current variability and there are also indicate that climate change will increase precipitation variability which will likely increase losses form rain-fed agriculture. McSweenet C. et al., (2008) suggested that, projection from different climate models in the collaborative are broadly consistent in indicating increase in annual precipitation in Ethiopia. These increase are largely a result of increased precipitation in the short precipitation season (October, November and December) in shouter Ethiopia. In this projected precipitation change by 10% to 70% as average over the whole of the country. However eastern part of the country in these season decreases precipitation.

Haile A., Rietjes T. et al., (2015) findings on upper Blue Nile basin shows that, under 2oc global warming threshold the projected future yearly rainfall vary between -2.8% to 2.7%. However the direction of this projected precipitation was not clearly understood. The authors also defined that, in the period of minor rainy season future precipitation will reduced. Daba M. et al., (2017) also conclude that in the upper Awash sun-basin projected future maximum and minimum temperature will show an increment in all time periods.

Based on the UNDP climate change study which has been done in the university of Oxford allover Ethiopia have indicated that, the recent climate trend shows that the annual average temperature has increase by 1.30oc between 1960 and 2006, with a mean value of 0.28oc per decade. The temperature in Ethiopia accelerate and get higher mostly in July, August and September (JAS) with a magnitude of 0.32oc per decade. Daily temperature data shows significant increasing trend in the frequency of hot days and considerable increasing trend mostly in hot nights. The frequency of cold seven days shows a huge decrement in all seasons except December, January and February (DJF). The frequency of cold nights (Temperature below which 10% of days or nights are recorded in current climate of that region or season) has decreased more rapidly and significant in all seasons.

In addition to the recent climate change trend UNDP climate change research about the future climate change; the research based on GCM projection of future climate in Ethiopia. Based on the result, the annual average temperature is increased by 1.1^{oc} to 3.1^{oc} by the 2060s and by 1.5^{oc} to 5.1^{oc} by 2090s.under specific emissions scenario, the projected change from different models extended up to 2.1oc. Moreover, a small increment in annual precipitation is expected over the country NMS, (2012).

Investigation on climate change of the Awash river basin shows, the basin would be considerably affected by climate change and significant water stress is estimated by using GCM models. All the models recommended that global warming has an overall output on the increase in dryness, which would decease availability of water. Moreover, Belete B., Semu A. et al., (2013) findings indicate that a 20% decrease in precipitation in the together with a 20oc increase in temperature would result in 41% decrease in the annual surface runoff. Even a temperature rise of 20^{oc} without precipitation change would result in a 9% decrement in yearly surface runoff amount. In addition an increment of 10% precipitation would offset a 2^{oc} to 4^{oc} increment in temperature and result in excess amount of surface runoff ranging from 4% to 12%.

2.1.2.1 General Circulation Model (GCM)

Climate models, both global and regional are the primary device which guided our understanding of the various approach that derive the climate system Jeremy H. et al., (2007). Climate is the most difficult geophysical system to be simulated due to the number of interacting components and the vast rage of temporal and spatial scale of relevant process and their complexity Laprise R. et al ., (2008). Global climate model also known as general circulation models (GCMs) are the prior and widely used sophisticated climate models, since they considered to show the primary parameters of the climate system in three directions.

According to IPCC, (2011), global climate models (GCMs) are the quintessential aid used to operate climate change experiments regionally and worldwide with a very finer scale up to point climate pattern from which climate change scenarios are derived; but they have basic demerits due to their large (courser) resolution. In most cases they lack generating present day climate trend having most important statistical parameters like mean and variance.

2.1.2.2 Regional Climate Model

A regional climate model (RCM) is a climate model with high resolution than GCMs. It can be adjusted within a global model to provide highly explained simulated for a particular area. Local climate change is affected mainly by local terrain property like mountain. Because of their courser resolution, small scale topographical features are not considered by GCMs. RCMs have finer resolution than GCMs ((~ 25 km) even less and are affected by a smaller scale of topographical features IPCC, (2013). It is much more sophistication in its process, running of RCMs usually taken over a limited area.

2.1.3 Downscaling Techniques

Downscaling or regionalization is the term provided to the analysis of deriving finer resolution data for a specific point from coarser resolution GCM data set. Although regional climate models (RCMs) are strong tools for expressing regional and even finer scale climate conditions, they still contains severe systematic defects Jakob T., et al (2011). The projections of the estimates of GCM and RCM climate variables either for now or future period resulted direct forward from simulation of GCM and RCM outputs are of limited value for any study as the spatial resolution of both results are coarse in nature to resolve many sub-grid scales. These property makes the results are always unreliable at particular grid. Therefore spatial downscaling methods have been developed to solve such problem.

The approach used to change GCM or RCM results into regional climate parameters used for hydrological modeling or any other local climate study are known as downscaling techniques Wood A. et al., (2004). Recently, there are various types of downscaling approaches to give very fine scale GCM and RCM outputs at finer scale; for instance some of the approaches are discussed in Jakob T., et al (2011). The other downscaling method which is referred to as dynamical downscaling method is mostly used to derive regional scale data from GCMs. specifically, small-scale patterns of daily precipitation are highly dependent on model resolution and parameterization and can often not be used directly in climate change impact assessment studies Fowler H. et al., (2007).

2.1.4 Climate Scenarios

Socio-economic and emission scenarios provide possible clarification of how the future can also evolve with regard to a range of parameters combined with socio-economic change, technological change, energy and land use, and emission of greenhouse gases and air pollutants Van V. et al., (2011). These future scenarios of driving agents are fed in to the climate models as input, and the output of these climate models is further used in climate change analysis and hence, the assessment of impacts, adaptation and mitigation.

RCP–Emission scenarios

Within the research community, now a days there has been an increasing interest in scenarios that explicitly investigate the impact of various climate-policies in addition to the no climate policy scenarios such as SRES Moss R. et al., (2010). Therefore, a collection of new scenarios is developed having emission, concentration and land use projections known as “Representative Concentration Pathways (RCPs)”. Based on the name given, the word “representative” elaborates that each of the RCPs represents a larger set of scenarios in the literature. This indicates that this set of RCPs should be compatible with the full range of emission scenarios (with and without climate policy) accessible in the current scientific literature.

The word “concentration pathway” describes that RCPs are not the final new, fully integrated scenarios, but instead are internally consistent sets of projections of the components of radiative forcing that are used for the input to climate models. The word “concentration” also explain that instead of emissions, concentrations are used as the key product of the RCPs, designed as input to climate models. There are four categories of RCPs scenarios based on their radiative forcing target level for 2100.

RCP2.6: This scenario has also been referred to as RCP3PD representing the radiative forcing trajectory which goes to a peak level of 3 W/m^2 (~490 ppm CO_2 eq) before 2100, followed by a decline (PD = Peak-Decline). The selected pathway declines to 2.6 W/m^2 by 2100 Van V. et al., (2011). Its main objective is to limit the increase of global mean temperature to 2°C above the pre-industrial period.

RCP4.5: This scenario explain the stabilization without overshoot pathway to 4.5 W/m^2 (~650 ppm CO_2 eq) at stabilization after 2100 Clarke L. et al., (2007). RCP4.5 grouped to that category scenarios in AR4 which contains the far majority of the scenarios assessed.

RCP6: This scenario is also similar to RCP4.5, with stabilization without overshoot pathway to 6 W/m^2 (~850 ppm CO_2 eq) at stabilization after 2100 Fujino J. et al., (2006). The number of mitigation scenarios concerning to 6 W/m^2 in the literature is comparatively less however, in similar situation many baseline scenarios (no climate policy) correspond to this forcing level.

RCP8.5: This scenario corresponds to the rising radiative forcing pathway leading to 8.5 W/m^2 (~1370 ppm CO_2 eq) by 2100 Riahi K. et al, (2007). It corresponds to a scenario with no-climate policy baseline and comparatively high greenhouse gas emissions.

RCPs represent pathways of radiative forcing, not linked with exclusive socio-economic assumption in contrary to Special Report on Emission Scenarios (SRES). A particular radiative forcing pathway can result from a wide range of socio-economic and technological development scenarios. RCPs are the new climate change scenarios established by CMIP5, which can depict a wide range of the actual future climate scenarios. The fifth assessment report (AR5) scientific literature identify one mitigation scenario (RCP2.6), two stabilization scenarios (RCP4.5 and RCP6) and one high emission scenario (RCP8.5). RCP2.6 implies that emission rise early, then decrease show technically feasible. But one of the main assumption is full participation of all developed and developing countries in the world in the short run to reduce all the main emitters, which is not possible in real case. RCP4.5 is a mid-range scenario that stabilizes radiative forcing at 4.5 W/m^2 (approximately 650 ppm CO2-equivalent) in the year 2100 without passing this magnitude, but this does not indicate that the climate system are stable. Whereas RCP8.5 is upper bound of all RCP scenarios that stabilizes radiative forcing at 8.5 W/m^2 (greater than 1370 ppm CO2-equivalent) in the year 2100) Fikru F. et al., (2018). According to the above explanation for this finding one low to medium mitigation scenario which is RCP4.5 and one high emission scenario RCP8.5 selected to assess the impact of climate change over the watershed.

2.1.5 Bias Correction Methods

A number bias correction methods, starting from simple scaling method up to the more complex distribution mapping method, have been developed to correct biased RCM outputs Teutschbein. C, Seibert J. et al., (2012). Zollo, A.L., et al., (2014) and Ramos M., et al., (2016) the scaling method basically having linear or nonlinear alternatives that adjust the climatic factors based on the change between observed and model simulated means in a linear or nonlinear equations, such as the linear scaling method (LS) and the power transpiration technique (PT) Lenderink G. Buishand A. et al., (2007). Distribution mapping also include distribution-based and distribution-free quantile mapping methods, comparing the statistical distribution of RCM-simulated climatic factors to the distribution of recorded data. Distribution-based quantile mapping is considered that climatic factors follows a certain distribution, such as Gamma and Gaussian distributions Chen J. et al., (2013) and White R., et al (2013), while the distribution-free quantile mapping method applies the empirical distribution Chen J. et al., (2013). Choosing an appropriate bias correction method is important for arranging proper and reliable inputs for impact analysis of an area.

Based on G.H.Fang, et al., (2015) uses five precipitation bias correction (LS, LOCI, PT, QM, DM) and three temperature bias correction (LS, VARI, DM) methods for correct the row RCM data and to evaluate their performance for hydrological impact study and conclude that Different precipitation correction methods show a big difference in downscaled precipitations while different temperature correction methods show similar results in downscaled temperatures. For precipitation, the PT and QM methods carried out efficiently in terms of the frequency-based indices; while the LOCI method satisfactorily achieved in terms of the time-series-based indices for temperature, all correction options worked in similar in adjusting raw temperature.

Biases in climate model simulations are commonly detected by validation with observations where the observations were considered to be “true” and unbiased Ménard R.et al., (2010). Sahilu G. and Nigussie A. et al., (2015) can validate that bias correction efficiently reduce any tendency to overestimate or underestimate the mean of downscaled variables.

Under this investigation the power transformation method for precipitation and variance scaling bias correction method for temperature used and perform well in adjusting the row RCM data in comparison with the observed metrological data for each stations.

2.1.6 Performance Evaluation of Bias Correction Methods

The ability of RCMs to simulate climate conditions at a particular location can be evaluated using a variety of techniques Flato G. et al., (2013). However, no single evaluation method or performance criteria is considered superior; rather, the integrated application of different methods and measures that result a comprehensive overview of model ability.

The performance evaluation of corrected precipitation data sets was checked with frequency-based indices and time serious performance against the recorded precipitation data. The frequency-based indices considering mean, median, standard deviation (SD), 90^{th} percentile, probability of wet days and intensity of wet days Belete B. et al., (2016). The time serious-based includes the Nash-

Sutcliffe measure of efficiency (NSE) Nash and Sutcliffe, (1970), the root-mean-square error (RMSE) and the percent bias (PBIAS).

2.1.7 Climate Change Projections

Due to the inherent uncertainty of the climate system and the inevitable existence of model errors, multi-model ensemble is the recommended approach for climate change projections Nikulin G. et al, (2012). IPCC has used several models in its coupled model inter-comparison projects (CMIP3, CMIP5) to make the various projections. There is also regional model inter comparison projects, like the Coordinated Regional Climate Downscaling Experiment (CORDEX). CORDEX project (http://wcrpcordex.ipsl.jussieu.fr/) is an initiative of the World Climate Research Program (WCRP) performed with the intention of producing an ensemble of high-resolution climate change projections by dynamically downscaling GCM simulations from Coupled Model Inter-comparison Project Phase 5 (CMIP5) data archive Jones C. et al., (2011).

The major aims of the CORDEX initiative are to provide a quality-controlled dataset of downscaled information, coordinated model evaluation framework, and an interface to the applicants of the climate simulations for further climate change impact, adaptation, and mitigation studies Giorgi F. et al., (2009). Recent analyses in relation to CORDEX simulations over Africa can be found in Nikulin G. et al, (2012). Hernández Diaz L. et al., (2013); Jacob G. et al., (2012). Jones C. et al., (2011) evaluate the ability of ten RCMs over Africa and conclude that all RCMs simulate the seasonal mean and annual cycle quite accurately. Likewise, it is verified that the mean of multi-model outputs does better than individual simulation. Hernández Diaz L. et al., (2013) strengthen the achievement of Nikulin G. et al, (2012). They successfully reproduce the overall features of geographical and seasonal distribution over most Africa. In their report, CORDEX simulations succeed in reproducing the average distribution of precipitation and its large geographical differences.

2.2 Soil Erosion and Sedimentation Processes

Soil erosion due to water encompass removal of individual soil particle from the soil mass, transport of some or all of the eroded soil as sediment downslope, and throughout its transit depositing some of the sediment or picking up more eroded soil. In following a droplet of runoff down the hillslope, three typical forms of erosion are considered in the upland areas. These are sheet erosion, rill erosion, and gully erosion Marcelo et al., (2008).

A. Sheet Erosion

It also recognized as inter-rill erosion, it occur uniformly between rills or gullies and outcomes basically from raindrop effect. The washing away of a thin layer of the land surface and erosive capacity of this effect relies upon on size of the rain drop, fall velocity, and total mass at impact, however can be devastating. In the absence of vegetation, mulch, or different cover to soak up the impact, raindrops can detach large quantities of soil.

B. Rill Erosion

Rills may also be very shallow or very deep, but normally produce parallel channels moving downslope on the planar surface. Their location is controlled somewhat randomly with the aid of small irregularities in the micro-topography, so if they are destroyed via tillage they will reform in various places. Rill erosion thicker than interrill erosion. These small channels transport runoff and sediment from interrill locations, the rain that falls directly on them, and any sediment generated from erosion inside the rill. Rill erosion increases rapidly as the slope steepens or lengthens and as the runoff rate increases.

C. Gully Erosion

It is considerable detachment of soil by excess concentration of runoff. This situation happened in the low part of the macro-topography where the planar hillslops converge, so they are suitable thought of as the upper most part of the watershed channel system. The phenomena is basically occurred in the upland areas and upper channels of the watershed. After the flow stream flow has reached the watershed channel system, sediment may also yielded from rivers or channels due to streambed and river side bank erosion, in which case the channel is said to be degrading. On the other side, if some additional extra sediment is contributed from the upland portions than the channel flow can transit significant deposition and storage of upland sediment may exist within the channel system, in this case the channel is said to be aggrading. On stable channel, insignificant amount of net erosion occur due to balancing between the sediment moved out of the channel system and that added by the upland erosion. Rainfall makes increasing water saturation or the formation of seal on soil surface. Due to the two process, movement of water down to the soil surface is decreased. Water on the soil surface exist immediately as the rain intensity began to passes the infiltration rate Nille D. et al, (1996)

2.2.1 Modes and Mechanisms of Sediment Transport

Sediment is the disintegrated material basically formed by means of mechanical and chemical weathering of the parent material from the earth crust. Mechanical weathering of material may induced by human or animal activity or some other movement on the soil surface. On the other hand chemical weathering of parent material may exist through chemical reaction of fluids, wind, and water/moisture or by the force of gravity acting on the particle itself Bhuiyan F. et al., (2011)

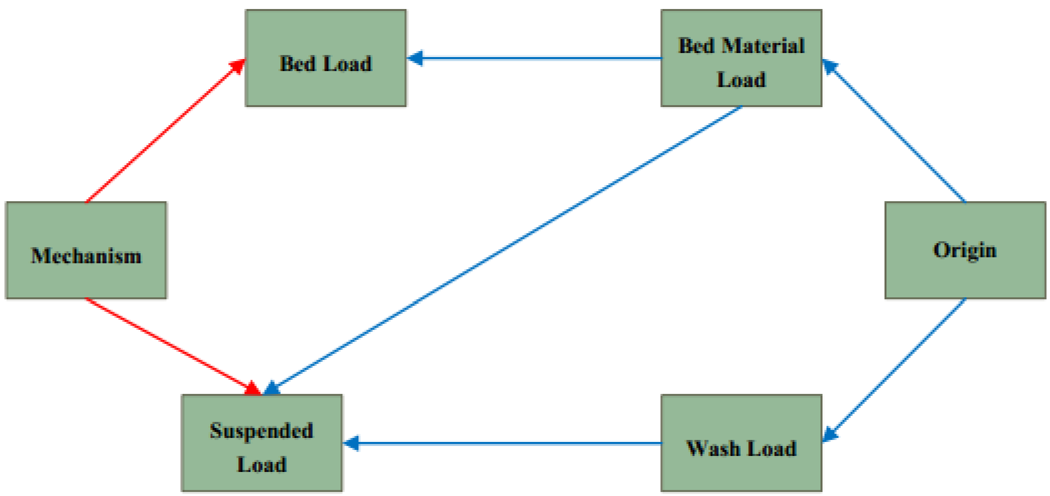

(Breusers, H. N. C,1974)

Figure 2.1: Mechanism and Origin of Sediment Transport

2.2.1.1 Bed Load Transport

Transport of bed load implies to the sediment particle, which is in most cases movement of soil particles with continuous contact with channel bed and moving forward through sliding, rolling and hopping. Bed material began to slide or rolling in non-stop contact with the bed when the magnitude of shear velocity start to exceed critical value at the initiation of motion. Hopping also occur for increased value of bed shear velocity, which transport individual soil particle along the bed with similar jumping pattern.

2.2.1.2 Suspended Load Transport

Suspended load transport can be described as a part of total sediment, portion of the eroded soil which is remain in suspension by the turbulence of the flowing water for considerable time duration with out in touch the bed of the channel. Such materials mostly consists sand and silt that can stay in suspension by the upward flux of turbulence exist at the bed of the channel Vortag et al., (2010). Suspended sediment load remains in suspension, if the soil particle fall velocity is less or equal to the opposite up ward current Van Hieu Bui et al., (2019).

2.2.2 Origin of Transported Material

I) **Bed Material Load** Bed material originate from channel bed and channel sides, which contain both bed and suspended load. The type of stream flow determine the amount of sediment yield and the type of material transported in the form of rolling and sliding on the channel bed as well as bed material transported near to the bed as saltation or suspension..

II) **Wash Load** Fine sediment material which is originated from outside the channel basically by land erosion that does not have direct interaction with surrounding condition. This load included soil particles finer than that exist in considerable amount in the bed material. As long as they exist in near-permanent suspension, they are transported along the stream without deposition. The amount of sediment yield along the channel reach is governed by the rate at which these particles become available Bhuiyan F. et al., (2011).

2.2.3 Sediment Properties

The sediment transported through natural channels consists in most cases particles vary from gravel or sand up to very small particles which is categorized as silt or clay. The very fine portion are transported as wash load or even as colloidal suspension in which electrochemical forces have a great impact.

For the alluvial stream hydraulics, the most important particles are those found in range of sand (0. 06 mm to 2 mm), gravel (2 mm to 20mm). From a hydraulic point of view the most important sediment properties are related to size, shape and specific gravity Frank et al, (1967).

Size determination The American Geo Physical Union (AGU) for clay, silt, sand, gravel, cobbles and boulders gives classification of particles according to size.

Table 2.1: Grain Size Determination

Type of Sediment Material	Method of Size Determination
Boulders and Cobbles	Direct Measurement
Gravel and Sand	Sieving
Fine Sand, Silt and Clay	Sedimentation or Microscopic Analysis

Particle size distribution The most usual and convenient method for particle size distribution analysis is the sieve analysis, which is applicable for particle sizes not smaller than 0.06 mm. Sufficient number of representative sediment samples are analyzed, and the result is presented as a frequency curve (figure a) or as a cumulative frequency curve (distribution curve, figure b) Frank. E and Eggert. H, (1967).

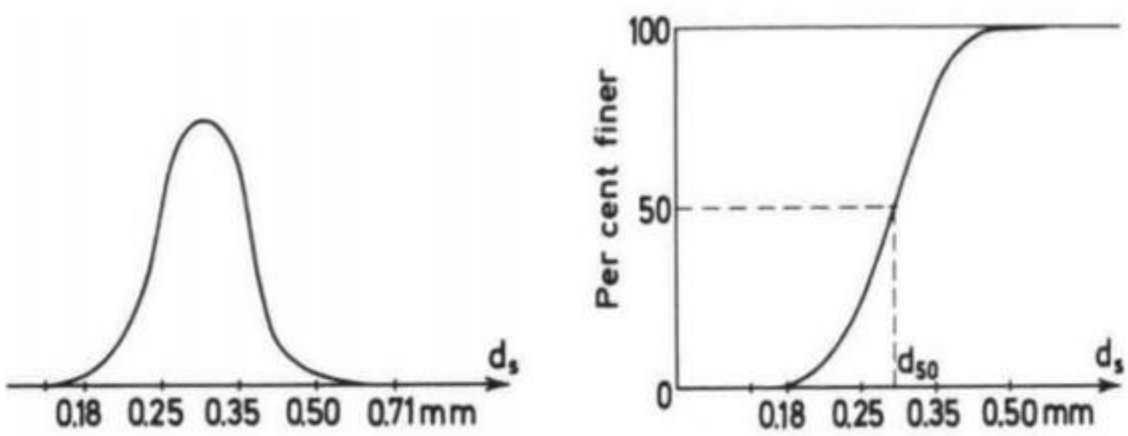

Figure 2.2: Particle Size Distribution

Where the abscissa represents sieve diameter ds and the ordinate indicates how many percent (by weight) of the total sample finer than the diameter ds.

Shape Besides the grain diameter, also the shape is of great importance. A flat particle has a smaller fall velocity and more difficult to transport as a rounded particle. Breusers, (1974). Several definitions can be used to characterize the shape:

a. **Roundness** Roundness depicts average curvature of radius of the edges and the radius of circle inscribed in the maximum projected area of the particle. Roundness is a function of abrasion induced by transport and it increases slowly with distance. Thousands of kilometers of transport in a river are required to achieve even moderate rounding. Beaches where sand moves in and out with each wave are ideal places for rounding of sand particles if they stay there for any length of time (L. C.Van Rijn).
b. **Sphericity** It is the ratio of surface area of sphere and surface area of particle at the same volume.
c. **Shape factor** Generally represented by the Corey shape factor, defined as:

$$SF = \frac{c}{\sqrt{ab}} \quad \ldots\ldots\ldots\ldots\ldots\ldots\ldots\ldots 2.1$$

In which a, b, c are three mutually perpendicular axes from which a is major, b is intermediate and c is minor axis. The shape factor for natural sand is approximately SF≈ 0.7 and for sphere SF=1.

Density Most sediments originate from disintegration or decomposition of rock. Table 2.2 Origin of sediment

Table 2.2: Origin of Sediment

Clay	Fragments of feldspars and Micas
Silt	Silca's
Sand	Quartz
Gravel	Fragments of Original Rock
Boulders	All Components of Original Rock

The density of most sediment particles (<4 mm) varies between narrow limits. Since quartz is predominant in natural sediments, average density can be assumed 2650 Kg/m3 (specific gravity 2.65). Sometimes heavy minerals are present which can be segregated during ripple formation or other modes of transport. Clay minerals range from 2500-2700 Kg/m3.

Fall velocity Fall velocity is an important parameter in studies on suspension and sedimentation of sediments. The fall velocity is obtained from equilibrium between gravity force and flow resistance:

$$\frac{\pi}{6} * D^3 (\rho_s - \rho_w) g = C_D * \frac{1}{2} \rho_w * \omega^2 * \frac{\pi}{4} D^2 \ldots\ldots\ldots\ldots\ldots\ldots 2.2$$

Gravity Force = Flow Resistance ………………………2.2

In which Drag Coefficient (C_D) and fall velocity (ω), from the above relation follows

$$\omega = \sqrt{\frac{4}{3} * \frac{gD}{C_D} * \Delta} \ldots\ldots\ldots\ldots\ldots\ldots\ldots\ldots\ldots\ldots\ldots 2.3$$

Where

$$\Delta = \frac{\rho_s - \rho_w}{\rho_w} \ldots\ldots\ldots\ldots\ldots\ldots\ldots\ldots\ldots\ldots\ldots\ldots\ldots\ldots\ldots\ldots 2.4$$

Values of C_D depends on Reynold number ω*D/υ and the shape of the particle (expressed by $SF = \frac{c}{\sqrt{ab}}$)

For spherical particle and low Reynold number (Re < 1), C_D can be given by C_D = 24/Re so that;

$$\omega = \frac{\rho_s - \rho_w}{18\upsilon} gD^2 \quad \text{Stokes Low} \ldots\ldots\ldots\ldots\ldots\ldots\ldots\ldots\ldots 2.5$$

For larger Reynold number C_D becomes constant so that W varies as $(\Delta gD)^{0.5}$ therefore W varies with $D^{0.5\text{-}2}$. Relation between C_D, Re and SF are also given by Albertson (1953).

Bulk density and porosity In estimating the life of a reservoir and similar cases, the calculated weight of the sediment transported to the reservoir has to be converted in to volume. For this the sediment dry weight per unit volume in place, bulk density ρb has to be estimated. Bulk density express mass of dry sedimentary material within a unit of volume (Kg/m3). The volume taken by the sediment depends on the conditions of settling and is a function of consolidation time.

According to Lane et al., (1953), bulk density of deposits in reservoirs is estimated by the empirical relation,

$$\rho_{bt} = \rho_{bi} + B \log t \ldots\ldots\ldots\ldots\ldots\ldots\ldots\ldots 2.6$$

Where t – time in years

ρ_i - initial bulk density taken to be the value after one year of consolidation

B – Consolidation coefficient

Table 2.3: Initial Bulk Density for Sediment

Reservoir Operation	Sand		Silt		Clay	
	ρ_i	B	ρ_i	B	ρ_i	B
Sediment always submerged or nearly submerged	1500	0	1050	90	500	250
Normally a moderate reservoir drawdown	1500	0	1185	45	750	170
Normally considerable reservoir drawdown	1500	0	1275	15	950	100
Reservoir normally Empty	1500	0	1320	0	1250	0
Breusers, H. N. C, (1974)						

For sediments of containing material of more than one size class proportional addition of the fractions can be made. Data given in table are based on normal conditions and applicable for first estimate.

2.2.4 Sediment Accumulation

Sediment accumulation in the reservoir is determined by using the bathymetric survey data collected. The base line was considered as the planed storage capacity of the reservoir at the various stage in the 1966. The storage capacity in the various bathymetric survey compared to that of 19966 at different level capable estimation of sediment accumulation rate. Thus, the competition between stored silt volumes deposited between the different surveys is obtained Ahmed et al., (2009).

2.2.5 Temporal and Spatial Variability in Sediment Yields

The amount of sediment yield differ both spatially and temporally. Understanding the vast range of variability in space and time is important in related with resource allocation for sediment management. Based on the findings Guyota et al., (1994) on the transport of sediment in Rio Grande, the Andean river of the Bolivian Amazon drainage basin, it was found that dominant transport of sediment occurs in period of the three months of the year in which the river gets maximum flow, during this period 90% of the annual load generated. The influential parameter for the increment and decrement of sediment yield with time depend on the particular site situation. In some conditions, annual variation in sediment generation can just be the result of the variation in precipitation and runoff amount.

Batalla et al., (1994) reported about a research on the time variability of suspended sediment load in a Mediterranean sandy gravel-bed river where considerable temporal variability was occurred due to the seasonal impact, gradual exhaustion of sediment availability to be moved in the period of consecutive storm event and extremely large concentration during individual floods. A plot of total observed sediment load has the capacity to implicate the temporal variation of sediment yield by inspecting the slope in the graph of cumulative water discharge versus cumulative sediment discharge. The same factors that have been discussed to be responsible for the temporal variation of sediment yield have the capacity to affect the spatial variation in sediment generation as long as there is accessibility of spatial variation in the controlling parameter within the watershed area. The variation based on time can be seasonally, annually and monthly. Therefore it is important to give attention for longer term sample record for better understanding of the temporal variation of sediment yield and in order to point out realistic summarization from the observation Hampson. , (1997).

2.2.6 Sediment Yield Estimation of the Watershed

Sediment yield describe the quantity of the eroded sediment which is discharged by a stream at any given place over a certain period of time, which is also the quantity that will enter to a reservoir located at the downstream limit of its tributary watershed. The known usual unit for sediment yield is tones/ year. The particular sediment yield is the generated sediment over a unit area of land most of the time given by tones/ km2/year. Long-term sediment yield estimation have been used for determination of the size of the reservoir storage and estimating the life span of the reservoir Morris et al., (2009). Exact estimation of sediment yield is very crucial in order to design a reservoir and for efficient management of its sediment so that the reservoir can satisfy its requirements. Sediment yield is influenced by geology, slope, climate, drainage density and frequency of human disturbance and therefore, no single factor or a group of simple parameters explain the vast range of sediment yield variability. Sediment yield from arid location tends to be limited due to low runoff and yield in wetter areas is constrained by the soil top cover which protect and reduce the erodability of humid zone soils Vanoni et al., (2006).

2.2.7 Sediment Transport Equation

Sediment transport equations are used to determine the sediment transport capacity for a specific set of flow condition. The first step in evaluating sediment transport is to select one or more of available equations for use in solving the problem. The selection is not straight forward, since the result of different formulas can give drastically different results and it is usually not possible to determine the one providing best result. Additionally, some of the methods are considerably more complex than the other. According to Bagnold, (1962), the initial consideration is to decide what portion of sediment transport need to be estimated. If it is desirable to know the contribution of bed load and suspended load to the bed-material discharge, formula for each are available. Other formulas provide direct determination of bed material discharge. According with in ISO standard ISO, (2002.) Wash load consists of fine materials that are finer than those found in the bed. The amount of wash load depends mainly on the supply from the watershed, not on the hydraulics of the river. Consequently, it is difficult to predict the wash load based on the hydraulic characteristics of a river. Most total load equations are therefore, total bed material load equation

In Modified universal soil loss equation (MUSLE), the rainfall energy factor is replaced with a runoff factor. This improves the sediment yield prediction, eliminates the need for delivery ratios, and allows the equation to be applied to individual storm events. Sediment yield prediction is improved because runoff is a function of antecedent moisture condition as well as rainfall energy. Delivery rations (the sediment yield at any point along the channel divided by the source erosion above that point) are required by the USLE because the rainfall factor represents energy used in detachment only. Delivery ratios are not needed with MUSLE because the runoff factor represents energy used in detaching and transporting sediment. Erosion caused by rainfall and runoff is computed with the Modified Universal Soil Loss Equation (MUSLE) Neitsch et al., (2011). MUSLE is a modified version of the Universal Soil Loss Equation (USLE) develop by Wischmeier (1965)

$$Sed = 1.292\ EI_{USLE} * K_{USLE} * C_{USLE} * P_{USLE} * L_{USLE} * CFRG \ldots\ldots\ldots\ldots 2.7$$

Where, Sed is the sediment yield on a given day (metric ton/ha)

EI_{USLE} is the rainfall erosive index (0.017 m-metric ton cm/ (m2hr.)),

K_{USLE} is the USLE soil erodibility factor (0.013 metric ton m2 hr/ (m3-metric ton cm)),

C_{USLE} is the USLE cover and management factor,

P_{USLE} is the USLE practice factor,

LS_{USLE} is the USLE topographic factor,

CFRG is the coarse fragment factor

USLE predicts the average annual gross erosion as a function of rainfall energy. Whereas in MUSLE the rainfall energy is replaced with a runoff factor which improves the sediment yield prediction, eliminates the need for delivery ratios, and allows the equation to be applied to individual storm events. Sediment yield prediction is improved because runoff is a function of antecedent moisture condition as well as rainfall energy. Delivery ratios (the sediment yield at any point along the channel divided by the source erosion above that point) are required by the USLE because the rainfall factor used by USLE represents energy used in detachment only Neitsch et al., (2011).

$$Sed = 11.8\ (Q_{surf} * q_{peak} * Area_{hru})^{0.56} * K_{USLE} * C_{USLE} * P_{USLE} * L_{USLE} * CFRG \ldots 2.8$$

Where, Q_{surf} is the surface runoff volume (mm), q_{peak} is the peak runoff rate (m / s ^{3}), hru Area is the area of the HRU (ha), and the other variables in the equation carries the same meaning as described in USLE equation.

2.2.8 Sediment Transport Modelling

To better understand the parameterization process, some fundamental concepts and definitions on sediment transport will be covered briefly. The Brahmaputra is a braided river which is a pattern defined as flow paths constantly changing around smaller unstable or semi-permanent alluvial bars and islands Campos, (2001). At low discharge levels the river is flowing in several smaller braided channels, while at high discharge levels it submerges most of the bars and is lands and is transformed into a few larger channels Vanoni et al., (2006). The number and size of the braided channels are therefore varying, with the exception for more stable node points where the riverbanks are made up by more consolidated material. To compensate for a changing width and still transport the same discharge, the scour depth is affected. When distributing the flow over several channels in a braided system, the wetted cross-sectional area of the combined channels should be equal to that of the nodal pointed. Braided rivers have evolved from combination of a relatively steep slope and an overabundance of sediment load Vanoni et al., (2006). In contrast to a meandering river, a braided river has a lower sinuosity and does not scour on one bank and deposit on the other, it may affect both banks equally. Depositional processes can be summarized as various bed formations such as bars and dunes, and sedimentation in overbank areas during floods Campos et al., (2001). Sediment transport within the channel is commonly divided into groups. Bed load is characterized by grains commonly larger than 0.1 mm that moves along the bottom of the channel by rolling, sliding and saltation. Suspended load is of smaller grain sizes that can be sustained by the flow without settling Meyer et al., (1969). The mobility of coarse non-cohesive grains, like sand and gravel, depends on the threshold of entrainment (i.e. the incorporation into the flow), and is also referred to as the dimensionless bed shear tress. The bed shear stress, and thus bed scouring, varies depending on factors such as bed slope, grain size and degree of immersion in sub layer. Due to this critical threshold, some grains are picked up and due to different settling velocities of the grain sizes, a sorting process is evolving. Thus, when bed erosion occurs, the finer grains on top are carried away first, while other potentially mobile fine particles may be trapped by coarser grains creating an armor effect. This leads to less material transported while the bed surface becomes rougher. Finer cohesive particles, like silt and clay, depend on bed processes such as electrochemical forces and are transported as composite particle aggregations Meyer et al., (1969).

2.3 Hydrological Model

Hydrologic models classified into three different categories V. P. Singh et al. (2002).

- **A.** Physically based models that depend on solving governing equations such as mass conservation and momentum equations. Parameters and state variables are directly measured either in the field or reasonably assumed based on site characteristics.
- **B.** Conceptual models utilize simple mathematical equations to express the core hydrological processes such as runoff, base flow, surface storage, evapotranspiration, percolation and

snowmelt. The merit of this approach is that the model is much simpler from a mathematical point of view. The processes are predicted with simple equations rather than solving governing partial differential equations. To replace partial differential equations with simple statements, varieties of different model parameters are introduced into model that may have little physical meaning.

C. Empirical models, which are based on analyzing observed input and output then after linking them through statistical or other similar techniques. Empirical models are normally mathematically simpler than their conceptual and physical counterparts, and reasonably good outcomes can be quickly gained by using techniques such as regression and neural networks.

2.3.1 Selection Criteria of the Model

There are a range of possible model structures within each class of models. Hence, choosing a particular model structure for a particular application is one of the challenges of the model user community. Beven, (2001) suggested four criterions for selecting model structures as below.

1. Consider models which are readily available and whose investment of time and money appeared worthwhile.
2. Decide whether the model under consideration will produce the outputs needed to meet the aims of a particular project.
3. Prepare a list of assumptions made by the model and check the assumptions likely to be limiting in terms of what is known about the response of the catchment. This assessment will generally be a relative one, or at best a screen to reject those models that are obviously based on incorrect representations of the catchment processes.
4. Make a list of the inputs required by the model and decide whether all the information required by the model can be provided within the time and cost constraints of the project.

Therefore, an appropriate model for those specific objectives can be select and can achieve those expected out-puts.

2.3.2 SWAT Model Description

Soil and Water Assessment Tool (SWAT) is a physically-based continuous-event hydrologic model developed to predict the impact of land management practices on water, sediment and agricultural chemical yields in large complex watersheds with varying soils, land use and management conditions over long periods of time Arnold et al., (1998).

The SWAT (Soil and Water Assessment Tool) Arnold et al. (1998) model developed in the early 1990's by the U.S. Department of Agriculture, Agricultural Research Service (USDA-ARS) to overcome all limitations of previous model.

In the SWAT model, the modeling or estimation of flow, sediment or nutrient transport of the watershed is done by dividing the watershed into sub basins and the land areas in the sub basins are also sub-divided again into one or more land units, possessing similar land use, soil type and applied management strategies. These similar land units in land use, management and soil attributes are called Hydrologic Response Units (HRUs). The HRUs are helpful for a better estimation of the loadings (flow, sediment, pollutants) from the sub basins. The Arc SWAT extension of Arc GIS is a graphical user interface for the SWAT model Arnold et al. (1998). To create a SWAT dataset, the interface will need to access Arc GIS compatible raster (GRIDs) and vector datasets (shape files or feature classes) and database files which provide certain types of information about the watershed. SWAT model designed to route water and sediments from individual watersheds through the river systems. It can incorporate the tanks and the reservoirs/check dam off-stream in addition to streams. The agricultural areas can be integrated with respect to their management practices Arnold et al., (1998).

SWAT model can satisfactorily estimate sediment yield for even poorly gauged catchments Ndomba and Griensven, et al., (2011). The model uses SCS curve number and Green Ampt method having daily rainfall data as input to generate surface run off whereas modified universal soil-loss equation (MUSLE) used to predict sediment loss. Soil Conservation Service curve number use land use ,soil permeability and antecedent moisture conditions (SCS, 1972) whereas Green Ampt computes infiltration as function of wetting front metric potential and effective hydraulic conductivity Green Ampt et al., (1911).

2.3.3 Hydrological Process in SWAT

SWAT simulates different hydrological processes through integrating spatial variation in topography, soil, land use, slope and other watershed characteristics. The simulated hydrological process encompasses runoff, infiltration, Lateral flow, channel routing, percolation to shallow aquifers, deep aquifers and evapotranspiration Arnold et al., (1998). From these hydrological process the surface runoff, lateral flow (subsurface flow), base flow (return flow) contribute to the stream flow in the main channel whereas water that enters deep aquifer is assumed to be lost out of watershed under investigation. All the hydrological process raised above are simulated in surface, soil, vadose (intermediate) zone, shallow and deep aquifers as shown in Figure 2.3.

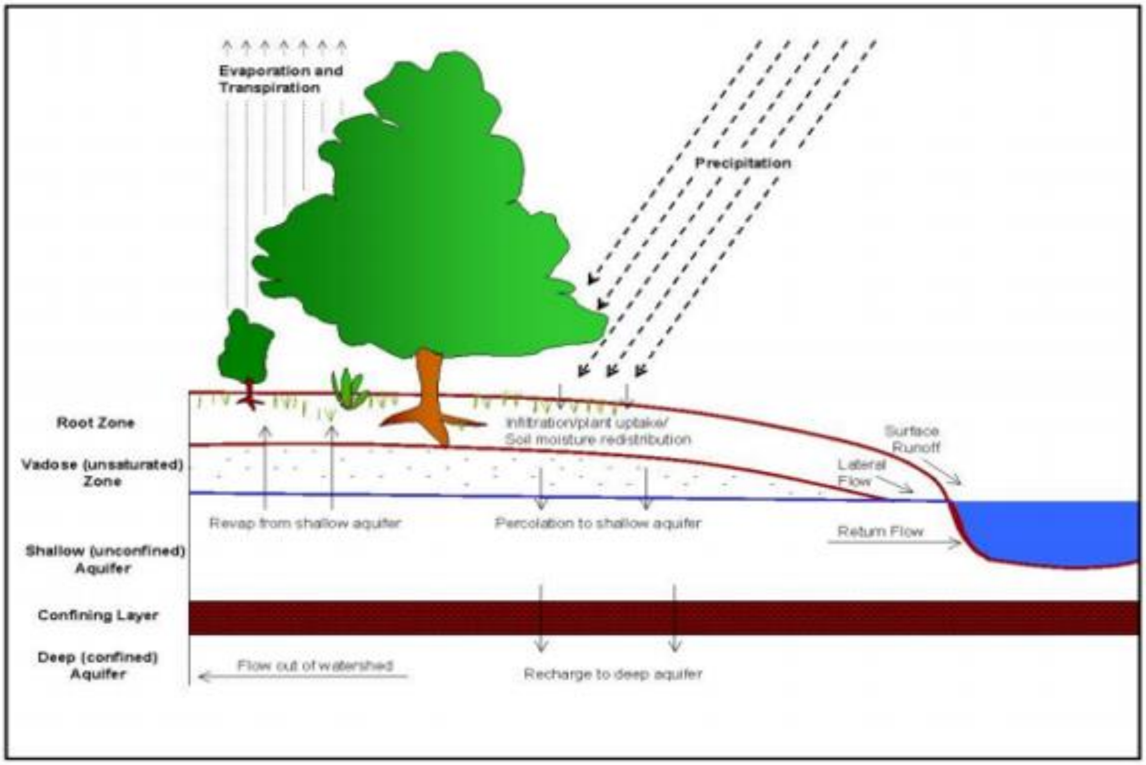

Figure 2.3: Schematic Illustration of Hydrologic Cycle

2.3.4 SWAT Model Evaluation

The performance of SWAT is evaluated using statistical measures to determine the quality and reliability of predictions when compared to observed values. Coefficient of determination (R^2). and Nash-Sutcliffe simulation efficiency (E_{NS}) are the goodness of fit measures used to evaluate model prediction. The R^2 value is an indicator of strength of relationship between the observed and simulated values. The Nash-Sutcliffe simulation efficiency (E_{NS}) indicates how well the plot of observed versus simulated value fits the 1:1 line. If the measured value is the same as all predictions, E_{NS} is 1. If the E_{NS} is between 0 and 1, it indicates deviations between measured and predicted values. If E_{NS} is negative, predictions are very poor, and the average value of output is a better estimate than the model prediction Nash and Sutcliffe, (1970).

2.3.5 Performance of the SWAT Model

Mahtsente Tibebe, Assefa M. Melesse and Dereje Hailu, (2016) The hydrology of Holetta River and its seasonal variability is not fully studied. In addition to this, due to scarcity of the available surface water and increase in water demand for irrigation, the major users of the river are facing a problem of allocating the available water. Therefore, the aim of this research was to investigate the water availability of Holetta River using Geographical Information Systems (GIS) tool and hydrological model. The rainfall runoff process of the catchment was modeled by using Soil and Water Assessment Tool (SWAT). According to SWAT classification, the watershed was divided in to 6 sub-basins and 33 hydrological response units (HRUs). The only gauged sub-basin in the catchment is sub-basin one that is found in the upper part of the area. Therefore, sensitivity analysis, calibration and validation of the model were performed at sub-basin one and then the calibrated model was used to estimate runoff at the un-gauged part of the catchment. The performance of SWAT model was evaluated by using statistical (coefficient of determination [R^2], Nash-Sutcliffe Efficiency Coefficient [NSE] and Index of Volumetric Fit [IVF]) and graphical methods. The result showed that R^2, NSE and IVF were 0.85, 0.84 and 102.8, respectively for monthly calibration and 0.73, 0.67 and 108.9, respectively for monthly validation. These indicated that SWAT model performed well for simulation of the hydrology of the watershed.

Meqaunint T. Asres and Seleshi B Awulachew, (2010) SWAT (Soil and Water Assessment Tool) model was applied to the Gumara watershed to predict sediment yield and runoff, to establish the spatial distribution of sediment yield and to test the potential of watershed management measures to reduce sediment loadings from hotspot areas. The model calibrated using five years of flow and sediment record and validated using data for the next three years. Out of 30 SWAT sub-basins, 18 sub-watersheds (72%) were identified as erosion prone areas contributing to a mean annual sediment load ranging from 11 to 12 ton/ha/year. Flow calibration resulted in Nash –Sutcliffe simulation efficiency index (Ens) of 0.76, a correlation coefficient (R^2) of 0.87 and a mean deviation of 3.29% showing a good agreement between measured and simulated monthly flow. Foe the validation, a good match between monthly measured and simulated flow was demonstrated by the correlation coefficient (R^2) of 0.83, a Nash –Sutcliffe simulation efficiency index (Ens) of

0.68 and mean deviation of measured and simulated monthly flows of -5.4%. in calibrating the sediment response, a good agreement between simulated and measured monthly sediment yield was demonstrated by a correlation coefficient (R^2) of 0.85, a Nash –Sutcliffe model efficiency index (Ens) of 0.74 and a mean deviation (D) of -14.2%. when validating the model for sediment, a good match between simulated and measured sediment was demonstrated by a correlation coefficient (R^2) of 0.79, a Nash –Sutcliffe simulation efficiency index (Ens) of 0.62 and mean deviation (D) of -16.9%.

Tesfa Gebre and Minichil Jemberie, (2016) The study mainly focused on predicting the amount of sediment yield and stream flow of the Didessa sub basin of the Abay basin was made. A physical-based, semi-distributed hydrological model, SWAT was used to simulate hydrological response (sediment and stream flow) of Didessa sub-basin. The simulated Stream flow and sediment yield results were utilized to analyze seasonal variability of sediment and stream flow of the sub basin. The performance of SWAT model was evaluated through sensitivity analysis, calibration, and validation. Both the calibration and validation result show good agreement between observed and simulated stream flow and sediment yield. Sensitivity analysis using the SWAT model has pointed out some crucial parameters that control the stream flow and sediment yield in the catchment. The result of calibration using the average monthly stream flow showed good agreement between observed and simulated stream flow with Nash –Sutcliffe efficiency of 0.76 and coefficient of determination (R^2) of 0.80. The validation of model simulation also showed a good agreement between simulated and measured monthly flow with the NSE value 0.70 and R^2 0.79 respectively. The model sediment yield calibration for the period of 8 years from 1987 to 1994 revealed good agreement between observed and simulated average monthly sediment inflow with NSE of 0.78 and R^2 of 0.83. The validation of the model from 1995 to 1998 also indicated good agreement between simulated and measured monthly flow with the NSE value 0.73 and R^2 0.81. During the study the sediment yield from the sub basin was determined using spatially semi-distributed SWAT model. The model evaluation statistics of sediment yield prediction and stream flow gave a good result since NSE and R^2 of the model were greater than 0.7. Therefore, SWAT model was good predictor of stream flow and sediment yield for Dedissa sub basin.

2.3.6 Benefits of SWAT Model Approach

- Watersheds with no monitoring data (e.g., stream gage or water quality data) can be modeled.
- The relative impact of alternative input data (e.g. changes in management practices, climate, vegetation, or land use) on water quality or another variable of interest can be quantified.
- The model uses readily available inputs. While SWAT can be used to study more specialized processes such as bacteria transport, the minimum data required to run the model are commonly available from government agencies.
- SWAT is computationally efficient. Simulation of very large basins or a variety of management strategies can be performed without excessive investment. The model enables users to study long-term impacts. Many of the problems currently addressed by users involve the gradual buildup of pollutants and the impact on downstream water bodies. To study these types of problems, results are needed from runs with output spanning several decades. Ideally, however, inputs from many years (5+) are desirable to calibrate the model. The SWAT model can be applied to support various watershed and water quality modeling studies. Applications include national and regional scale water resource assessment.
- SWAT explicitly incorporates elevation or orographic effects on precipitation and temperature.
- SWAT was developed for and has been widely applied to simulation of watersheds in arid regions.
- SWAT explicitly incorporates routines for agricultural diversions and irrigation.
- SWAT includes routines designed to address the impacts on flow and pollutant loading of multiple small (or large) farm ponds within a basin.
- ❖ SWAT is designed to use either observed meteorological data or statistically generated meteorology, facilitating the development of long-term analyses. Because the model is physically based and uses commonly available geographic data, it is claimed "Watersheds with no monitoring data…can be modeled", allowing the efficient evaluation of "relative impact of alternative input data (e.g., changes in management practices, climate, vegetation, etc.) on water quality…".

2.3.7 Limitation of SWAT Model

The following are some of the limitations using SWAT for hydrological modeling:

- Due to the heterogeneity of the catchments, a number of meteorological observation stations are required to represent the spatial variation in the hydro-meteorological characteristics in the area. The lack of adequate number of observation stations affects the model output.
- In order to calibrate the model for the historic land use scenarios, the corresponding land use maps are needed. In order to get the real time picture of the land use pattern, this information can be extracted from the remote sensing satellite imageries by using digital image processing technique. However, acquisition of satellite imageries is expensive and also the expertise required for the image interpretation is another major limitation.
- Though SWAT is a free software tool, in order to represent the spatial variation in the catchments characteristics, GIS software is the prerequisite to run the model.
- While SWAT is a process-based model, it intentionally incorporates simplified representations of most processes so that many parameters can be obtained from readily available geo spatial coverage. For upland generation of flow and sediment, SWAT relies on the well-tested, semi-empirical approaches of the SCS Curve Number and MUSLE. The basic time step of the model is one day (although hydrology can be simulated at a finer scale using Green-Ampt infiltration); so actual flow hydrographs are not represented. The MUSLE approach is most applicable to the estimation of cumulative loads, rather than loads from individual events. It should also be noted that the default SWAT algorithm may yield unrealistic results from HRUs that contain a mix of urban pervious and impervious land cover because MUSLE is calculated with the peak flow from the entire HRU, using a weighted curve number, and not from the flow from the previous section. This is equivalent to assuming that all impervious area runoff proceeds as sheet flow across the pervious sections, rather than being piped or channelized, and can result in a significant over-estimation of sediment load from developed areas.

3. MATERIALS AND METHODS

3.1 Description of the Study Area

3.1.1 Location of the Study Area

Awash Basin is located between $7^0$53’42’’ to $12^0$07’20’’ North and $37^0$56’56’’ to $43^0$17’04’’ East. The basin is bordered by Danakil, Abbay, Omo- Gibe, Rift-Valley lakes and Wabi-Shebele basins and Republic of Djibouti. The river originates from the central highlands of Ethiopia, and flows north east through the northern section of the Rift Valley to eventually discharging into Lake Abbe near Djibouti boarder, traveling a distance of about 1200km. The total catchment area of the basin is about 116,000 square kilometers.

The Mille River is one the tributary of the Awash river at the lower section of the lower Awash river basin and joined Main Awash up stream of Tendaho reservoir. Mille river originates and drain from the high lands of North Wollo to the low land of the Afar Region. Mille watershed is among the sub-watersheds of Lower Awash Sub Basin and is situated in the western part of the basin and located between 11°32’31.73’’N 39°35’07.24’’E at the North high land of Wollo and 11°26’38.83’’N and 40°55’32.43’’E at the confluence of main Awash river (Figure 3.1). The watershed drainage area is about 4640.43 km^2 up to the outlet point. The elevation of the study area ranges from 3635m to 410m a.m.s.l.

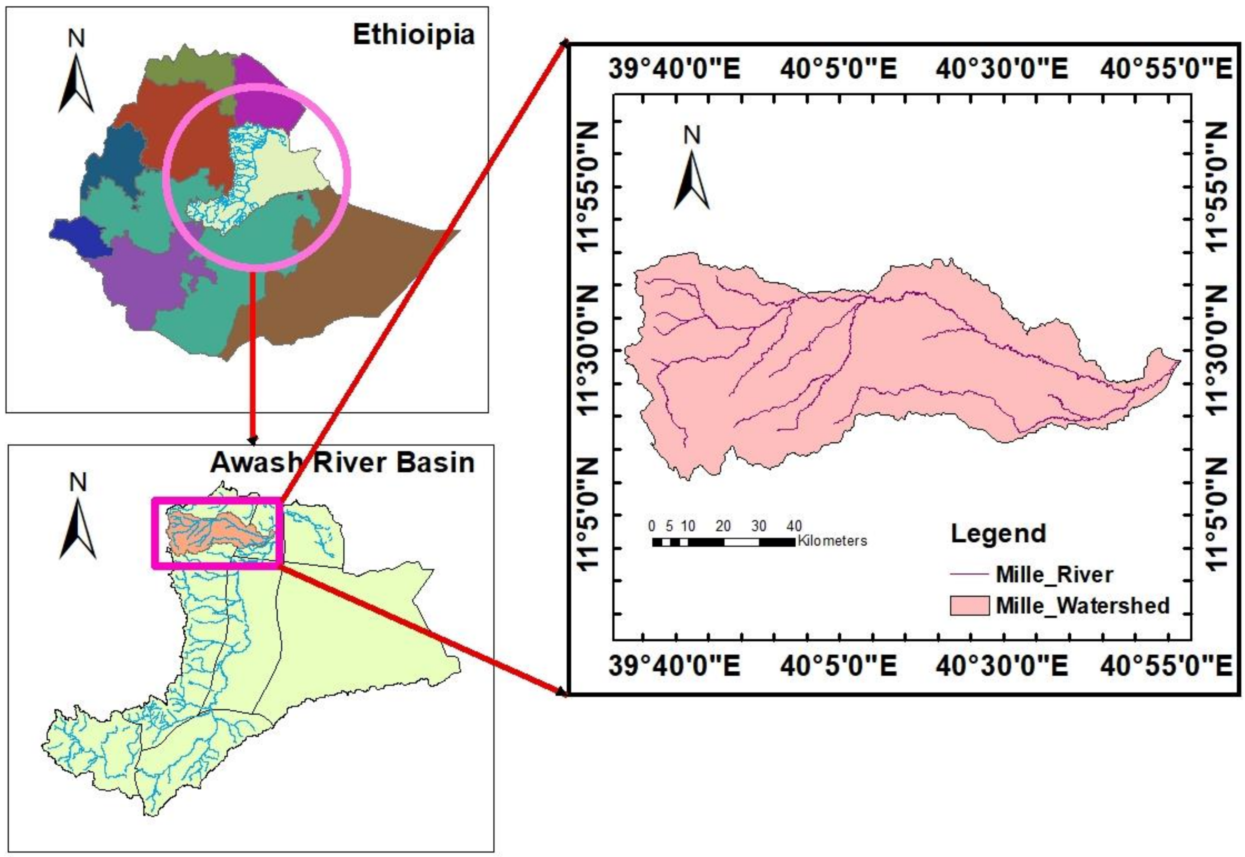

Figure 3.1: Location of the Study Area

3.1.2 Geology and Topography

Lower Awash River is characterized by extensive floodplain (including terrace) stretching from Logia town in the northwest to Asayita town and as far as Buri Plain in the southeast, few km northwest of Asmara hill/volcano. Awash creates broad meander belt as wide as 12 to 15 km around Dubti area and Det-Bahari – Galifage areas. The floodplain is mainly underlain by silty clay/clayey silt, across which the Awash River laterally wanders forming meandering channel pattern.

Generally, the floodplain and terraces are covered by thick riparian vegetation (riverine forest) mainly of prosopis, spiny trees and shrubs, except areas covered by old cotton plantations and new sugarcane plantations. Extensive areas on both sides of the present-day courses of Awash River are covered by natural riparian vegetation, which commonly occur in the Ethiopian Rift valley, Back swamps, naturally recharged floodplain by floodwater, support riparian vegetation.

3.1.3 Climate

Awash River Basin ranges from cold high mountainous zones to semi-desert lowlands with extreme ranges of temperature and precipitation Getahen Y. et al., (2015). There are three seasons in the Awash River Basin based on the movement of the Intertropical Convergence Zone (ITCZ) and the amount of precipitation timing. The three seasons are named: Kiremt, which is the main rainy season (June–September), Bega, which is the dry season (October–January), and Belg, the small rainy season (February–May). Therefore, the precipitation was categorized under bi-modal pattern. The mean annual precipitation varies from 1600 mm in the elevated areas to 160 mm in the LARB. In the same way, the mean annual temperature of Awash River Basin ranges from 20.8 ◦C in the upper part to 29 ◦C in the lower part.

The weather system of the Lower Awash sub-basin in general influenced by position of the Inter-Tropical Convergence Zone (ITCZ). The rainy season begins in July when the position of ITCZ is to the most north. Based on climatic classification of the country, the sub-basin has hot arid type of climate. Both distributions of precipitation and temperature over the sub-basin are strongly related to the altitude.

There are few meteorological stations with in and around the catchment with different length and type of record mainly concentrated in the upper part of the watershed. Some of the rainfall stations considered for the watershed area are Bati, Merssa, Serinka, Weldiya, Haike, Mille and Dubit.

3.2 Data Collection

3.2.1 Data Types and Sources

The data used for this research were varied in types and sources. Spatial data that included DEM, Land Use Land Cover and Soil Map also collected from Ministry of Water, Irrigation and Electricity (MoWIE) and Awash River Basin Authority (ARBA). Daily climate variables of (Rainfall, temperature, Relative humidity, Wind speed and Sunshine hour) were collected from Ethiopian National Meteorological service (NMA) while Daily discharge and sediment concentration of Mille River at Mille near Mille Village gauging Station were obtained from Ministry of Water, Irrigation and Electricity (MoWIE). Regional climate model data from Coordinated Regional Downscaling Experiment for Africa domain (CORDEX-Africa) with a horizontal grid resolution of 0.44º * 0.44º (50km * 50km) were downloaded via the download node (https://esgf-data.dkrz.de/search/cordex- dkrz). The climate model data includes simulated historical (1951-2005) and Future projected (2006-2100) precipitation and temperature data under RCP4.5 and RCP8.5 scenarios.

To get a better result, it is critical to use all relevant and good quality data required. The outcome depends on the quality and quantity of data used because the spatial and temporal resolution of data used in modelling will greatly influence the model performance. All the data type used for the study and their sources are summarized with a table below.

Table 3. 1: Data Types and Sources Used in the Study

I	**Spatial Data**		
1	DEM	30m*30m	MoWIE/ARBA
2	Soil Map	30m*30m	MoWIE/ARBA
3	Land Use Land Cover Map	30m*30m	MoWIE/ARBA
II	**Meteorological Data**		
	Data Type	Time Step	Data Sources
1	Rainfall		NMA
2	Temperature	1986-2017	NMA
3	Wind Speed	Base Period	NMA
4	Sun Shine Hr.	1986-2005	NMA
5	Relative Humidity		NMA
III	**Hydrological Data**		
1	Stream Flow Data	1989-2002	MoWIE/ARBA
2	Sediment concentration	1989-2002	MoWIE/ARBA
Iv	**Climate Data**		
1	CORDEX-RCP Climate Data	1986-2090	http://esgf-data.dkrz.de/search/cordex-dkrz

3.2.2 Digital Elevation Model (DEM)

The DEM (Digital Elevation Model) data with (30mx30m) resolution was collected from ministry of water irrigation and electricity (MoWIE) GIS Department. DEM is used in the SWAT model along with soil and land use/land cover data to delineate the watershed and to further divide the watershed into sub-watersheds and hydrologic response units (HRUs). The resolution of the digital elevation model (DEM) is the most critical input parameter when developing a SWAT model Gassman, (2007). DEM resolution affects the watershed delineation, stream network and sub basin classification in the SWAT model. It affects the number of sub-basins and HRUs. According to Chaubey, (2005) a decrease in DEM resolution resulted in decreased stream flow and watershed area. Since the runoff volume and total sediment load depends on the watershed area, the decrease in the DEM resolution results in large Error in the predicted output. In this study a digital elevation model (DEM) of 30mX30m resolution was used to delineate the watershed and for future HRU analysis. Fig.3.2 shows the digital elevation model (DEM) of the Mille watershed.

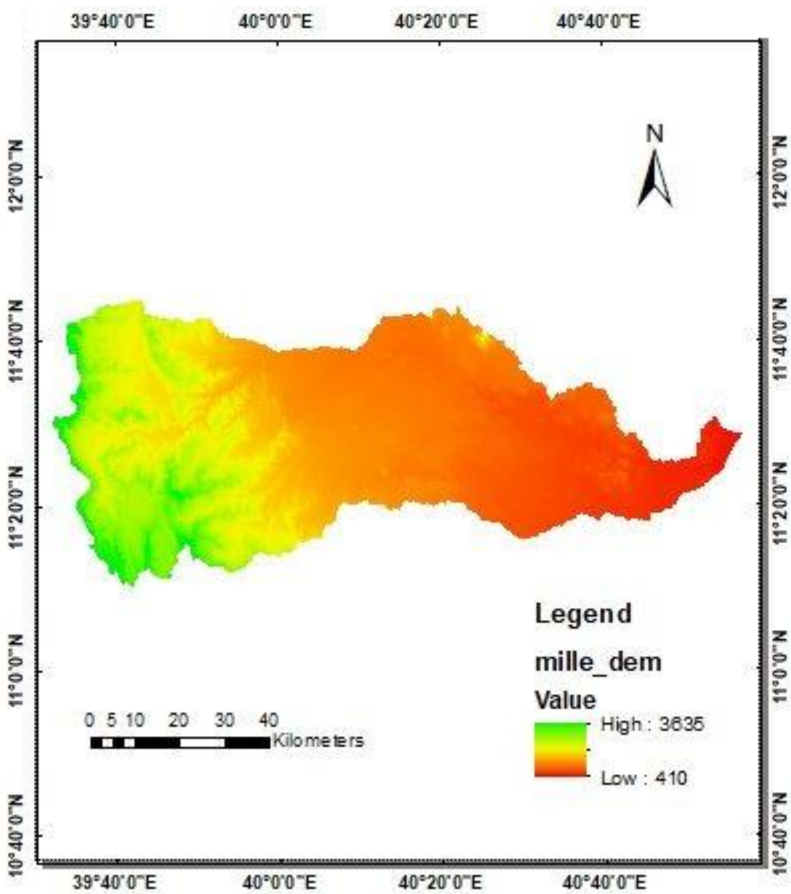

Figure 3. 2: DEM of Mille Watershed

3.2.3 Land Use Land Cover Map

Land use land cover of a watershed is a highly influencing factor of hydrological properties of watershed. It is one of the main input data of the SWAT model to describe the hydrological response units (HRUs) of the watersheds. The SWAT model has predefined four letter codes for each land use these codes were used to link or associate the land use map of the study area to

SWAT land use databases. Hence, while preparing the lookup-table, the land use types were made compatible with the input needs of the model. The LULC map of study area was obtained from Ministry of Water, Irrigation and Electricity (MoWIE) GIS Department for the year of 2013. The land covers of the watershed are dominated by 39.08% of barren land, 42.95% of range brush, forest mixed and pasture area with 7.69% and 4.27% respectively. The LULC classification of the watershed and percent of area coverage presented in tables (3.2).

Table 3. 2: LULC Classification of Mille Watershed

No.	LULC Name	SWAT Code	Area Coverage (%)
1	Agricultural land -generic	AGRL	1.37
2	Agricultural land -Row Crops	AGRR	0.1
3	Barren Land	BARR	39.08
4	Forest Evergreen	FRSE	3.46
5	Forest Mixed	FRST	7.69
6	Range- Brush	RNGB	42.95
7	Pasture	PAST	4.27
8	Water body	WATR	0.88
9	Wet land non-Forested	WETN	0.2
	Total		100

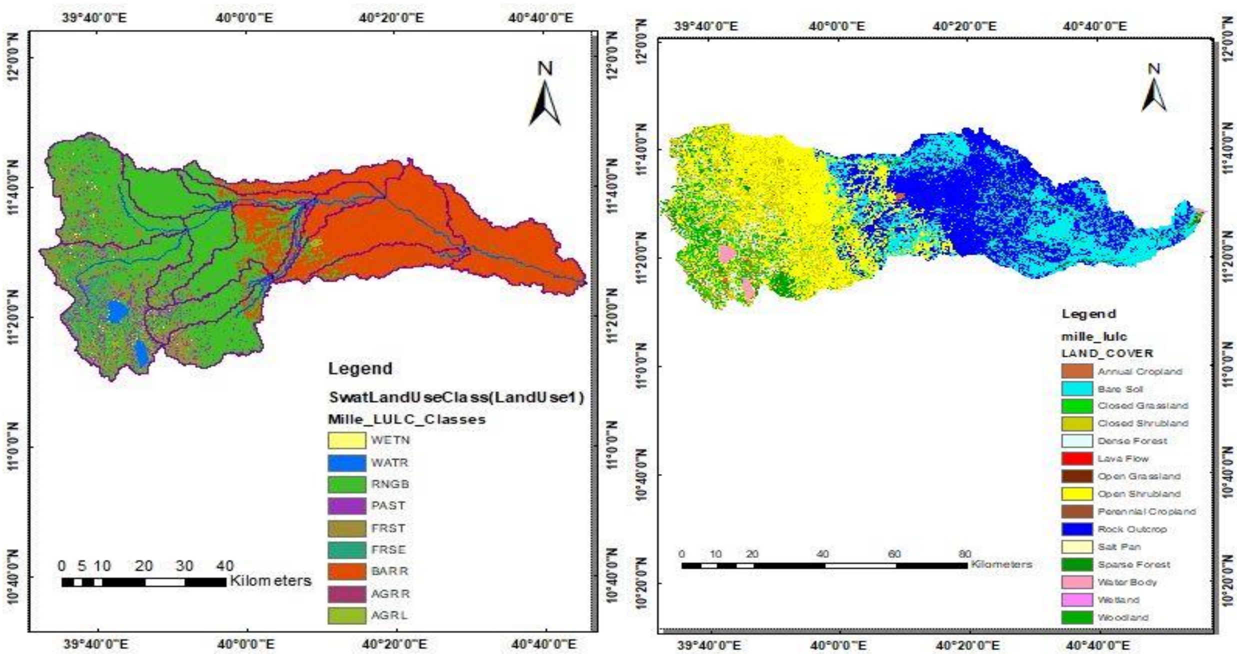

Figure 3. 3: Land use Land Cover Map of Mille Watershed

3.2.4 Soil Map

Soil data is one of the major input data for the SWAT model with inclusive physical and chemical properties. The soil map of the study area was also obtain from Ministry of Water, Irrigation and Electricity (MoWIE) GIS Department and the physical and chemical properties of the soil collected from Awash River Basin Authority (ARBA). Based on the data acquired, the soil map of the watershed was developed by overlying the soil map shape file during HRU definitions. As shown in the figure 3.5, the watershed is dominantly covered by calcaric flubosols, eutric regosols, haplic xerosols, eutric cambisols and leptosols. Table 3.3 shows the major soil types and their percentage of area coverage obtained during overlying of soil maps.

Table 3. 3: Major Soil Types and their Percentage of Area Coverage

No.	Soil Name	Area Coverage (%)
1	Calcaric Flubisols	21.23
2	Chromic Luvisols	0.37
3	Dystric Nitisols	4.29
4	Eutric Cambisols	10.03
5	Eutric Regosols	24.68
6	Haplic Xerosols	20.45
7	Leptosols	8.07
8	Orthic Solonchaks	3.21
9	Vertic Cambisols	4.52
10	Vertic Andosols	3.15
	Total	100

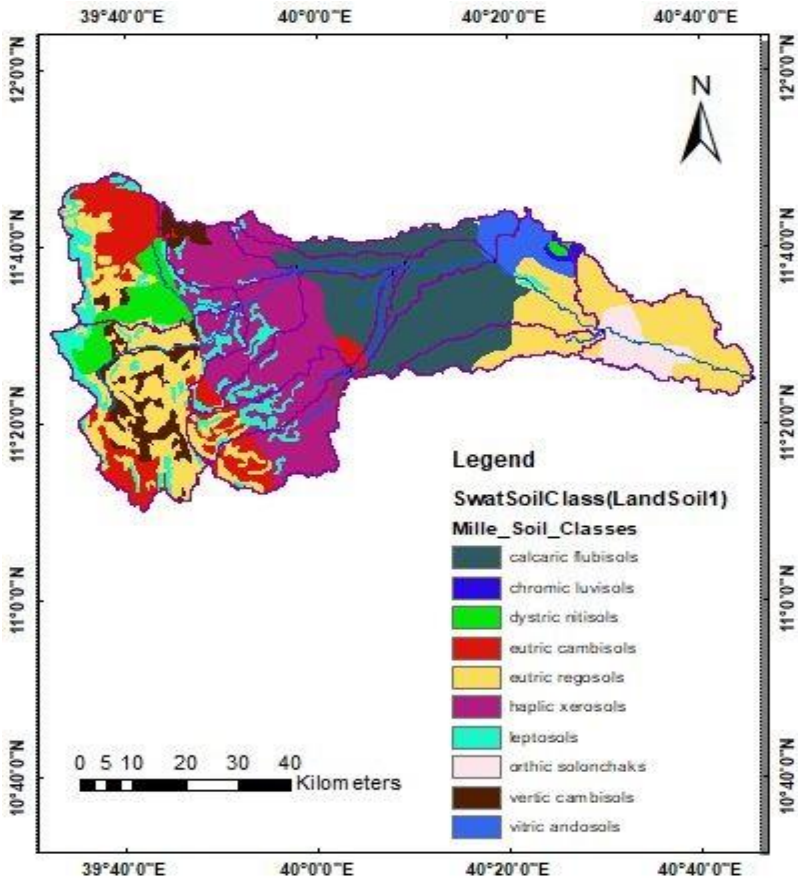

Figure 3. 4: Map of the soil types of Mille watershed

3.2.5 Slope Class

The land slope classification is categorized based on Stegn, (2008) for best sediment yield class and it has 5 main category starting from 0-2, 2-8, 8-15, 15-30 and >30 percent slope. Table 3.4 shows the percentage of each slope class over the Mille watershed.

Table 3.4: Slope Class of Mille Watershed

No.	Slope Class	Area Coverage (%)
1	0-2	10.32
2	2-8	37.87
3	8-15	16.26
4	15-30	19.17
5	>30	16.39

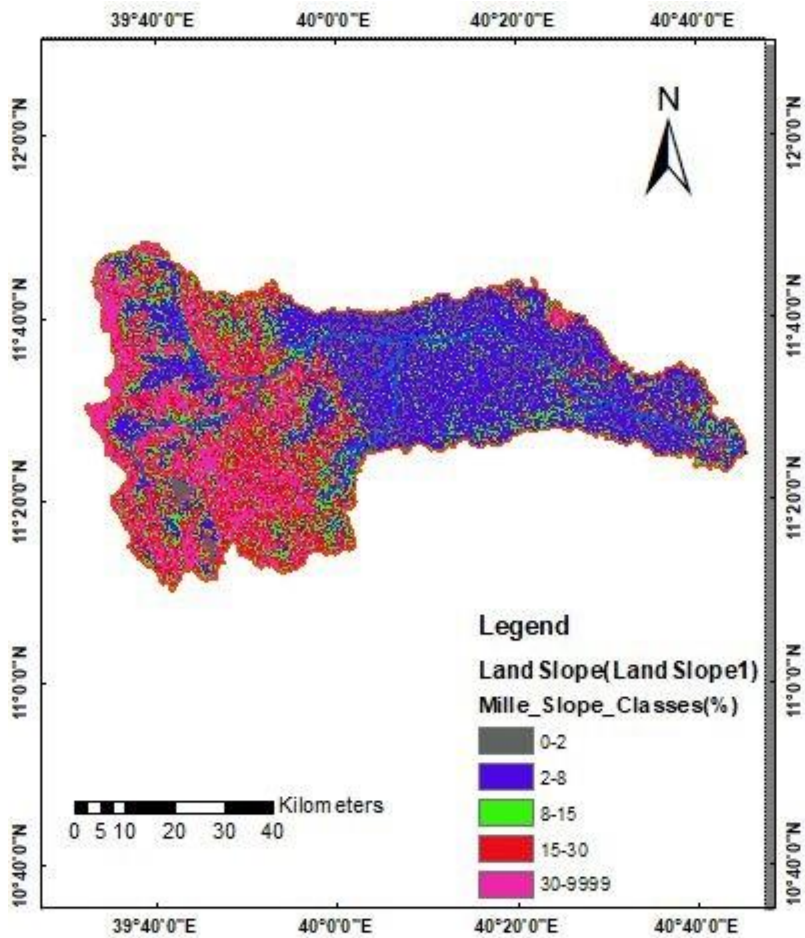

Figure 3.5: Slope Class of Mille watershed

3.2.6 Meteorological Data

In this study more than five metrological station data were collected from Ethiopian National Meteorological Agency (NMA), however only 5 stations were selected for detail analysis due to the quality and quantity of data. Due to low quality and short period of recording data (2007-2010) stations such as Mille and Weldiya were not utilized for further analysis, thus the selected five station has good quality of data that contain the necessary meteorological parameters such as precipitation, maximum and minimum temperature, relative humidity sunshine hours and wind Speed.

Table 3. 5: Meteorological Station Locations and Length of Data Series.

No.	Name of Stations	Latitude	Longitude	Elevation	Data Serious
1	Bati	11.19667	40.01539	1660	1986-2017
2	Dubity	11.723	41.01	376	1986-2017
3	Haike	11.30532	39.68021	1985	1986-2017
4	Merssa	11.66605	39.66605	1578	1986-2017
5	Serinka	11.751	39.61428	1861	1986-2017

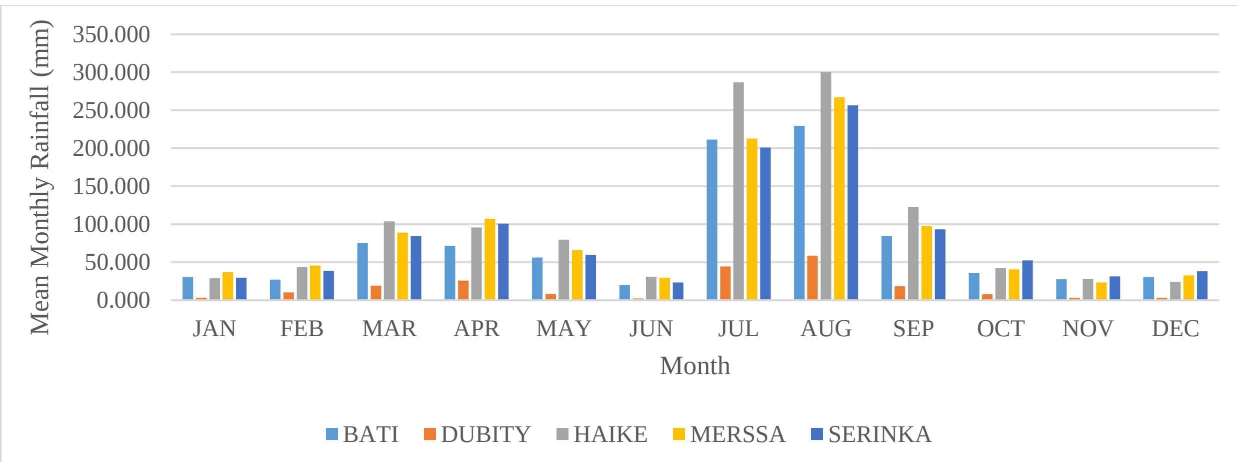

Figure 3.6: Mean Monthly Rainfall of Selected Stations

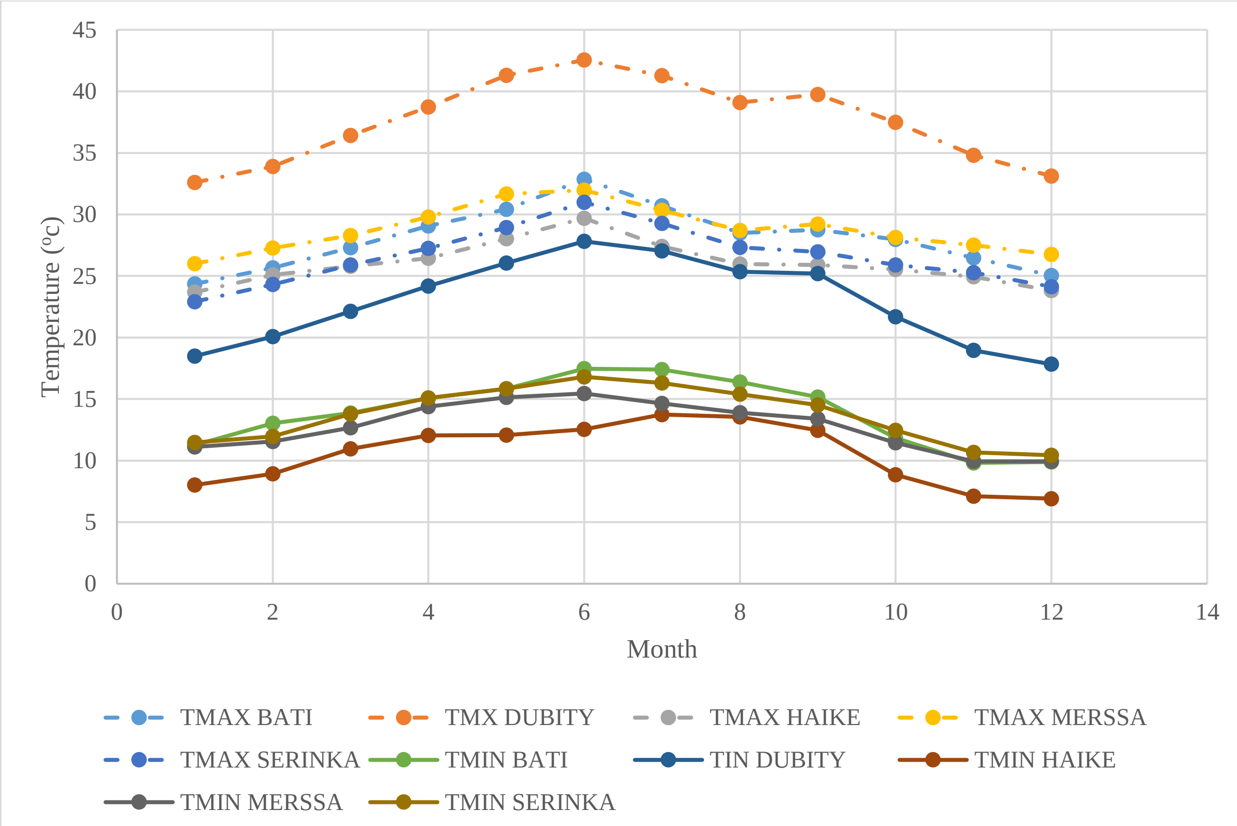

Figure 3. 7: Mean Monthly Temperature Maximum and Minimum of Selected Stations

3.2.7 Hydrological Data

3.2.7.1 Stream Flow Data

SWAT simulates stream flow and sediment yield transport at watershed scale, on a Continuous, daily time step Neitsch, (2011). SWAT CUP uses this data values for comparing the observed values and simulated output. Daily flow data for Mille River for a period of 14 years from 1989-2002 (time period of data with no missing value) recorded at Mille gauging station near Mille Village collected from Ministry of Water Irrigation & Electricity (MoWIE).

3.2.7.2 Sediment Data

Sediment data collected from Ministry of Water Irrigation and Electricity hydrology department, but which recorded data of the station with different year had been missing data. To fill this gap, developed sediment rating curve is one of the options. Many researchers have also used sediment rating curve to estimate suspended sediment when measured data has missing values or not valid Asselman, (2000.). Sediment rating curve expresses the average relation between river discharge and suspended sediment concentration for a certain existing data. The sediment rating curve usually express as a power function of discharge

$$Qs= a*Q^b \quad ....3.1$$

Where: Qs is suspended sediment (ton/day), a and b is regression coefficient and exponent Q is river discharge.

The sample of suspended sediment measured by (mg/l) to convert sediment load (ton/day) by using the following formula.

$$Qs = 0.0864Cs * Q \quad ....3.2$$

Where: Qs is sediment load (ton/day), Cs is sediment concentration (mg/l), Q river flow (m3/s) and 0.0864 conversion factor. Data for rating curve development appendence (E).

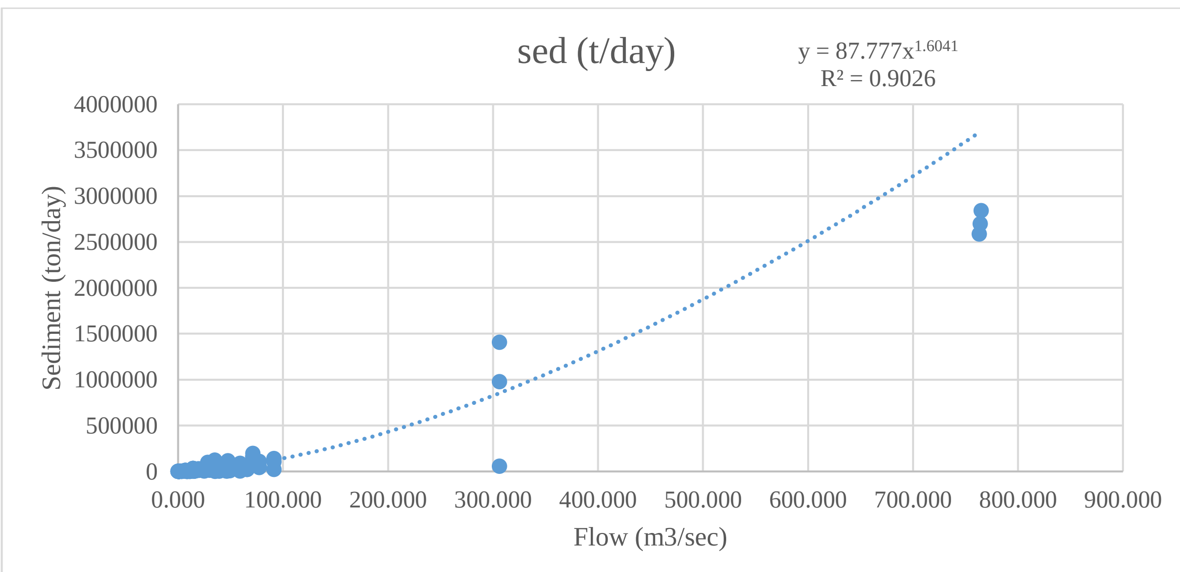

Figure 3.8: Sediment Rating Curve Mille near Mille Village Gauge Station

3.2.8 Climate Model Data

Under this specific study, CORDEX-Africa climate model for African domain projections under Representative Concentration Pathways (RCP4.5 and RCP8.5) were utilized as input for impact assessment of climate change model. CORDEX datasets covered from (1951-2005) as past historical periods and (2006-2100) for future time periods are accessible under different GCM and

RCM climate models and RCP scenarios with spatial resolution of 0.44° * 0.44° (50m * 50m). Dynamical downscaling regional climate models (RCMs) are more preferable than global climate models (GCMs) due to their finer scale resolution at regional level, For this study, precipitation and maximum and minimum temperature datasets were downloaded from CORDEX Africa from http://cordexesg.dmi.dk/esgf-web-fe/ under HADGEM2 and ICHEC-EC-EARTH GCM having RACMO22T and CCLM-4-8-17 RCM model respectively for climate change impact analysis under representative concentration pathways (RCP4.5 and RCP8.5) and the mean of the two RCM model data are arranged for SWAT input in order to reduce the uncertainties resulted from usage of a single climate model after bias correction each RCM model.

3.3 Data Analysis

3.3.1 General

For this specific study the methodology used to achieve the desired objective has different part, the first part was establishment of hydrologic model and checking the performance of the developed model for further impact assessment due to the change in climate variable such as precipitation and air temperature using SWAT model. The second part of the analysis part correcting the biasness of the downloaded climate model data using bias correction methods for each climate variables (such as precipitation and maximum and minimum air temperature and checking the performance of bias correction methods. RACMO22T RCM model from HADGEM-2 GCM and CCLM4 RCM model from ICHEC GCM climate model was selected for climate change impact assessment on sediment yield of Mille watershed. A time period from 1986-2015 was considered as the reference time to compare the bias correction of the climate model with the observed climate data for each meteorological stations at a watershed scale and from 2031-2060 as (2050s) and from 2061-2090 (2070s) the two future period which is considered as the near future and the far future period time. Finally after checking the performance of the hydrologic model and the sediment yield which is generated from the Mille watershed was estimated in related with the change in climate for future time, the spatial variation of sediment yield also checked under different RCP scenarios. The reason for the selection of the SWAT model was that SWAT model is physically semi distributed and continuous time developed to predict the impact of land management practices on water, sediment and agricultural chemical yields from a watershed. After setting the objectives and select the appropriate model, all the necessary data required to run the model was collected and prepared as to the requirement of the SWAT model format. The geospatial data including the digital elevation map, land use/land cover map, soil map, meteorological data such as daily rainfall data maximum and minimum daily air temperature data, relative humidity, solar radiation and wind speed from 1986 to 2015 and hydrological data i.e. daily stream flow data and sediment load concentration (1989-2002) collected and processed as per the input requirement format of the model. The conceptual framework of followed during the study is shown below.

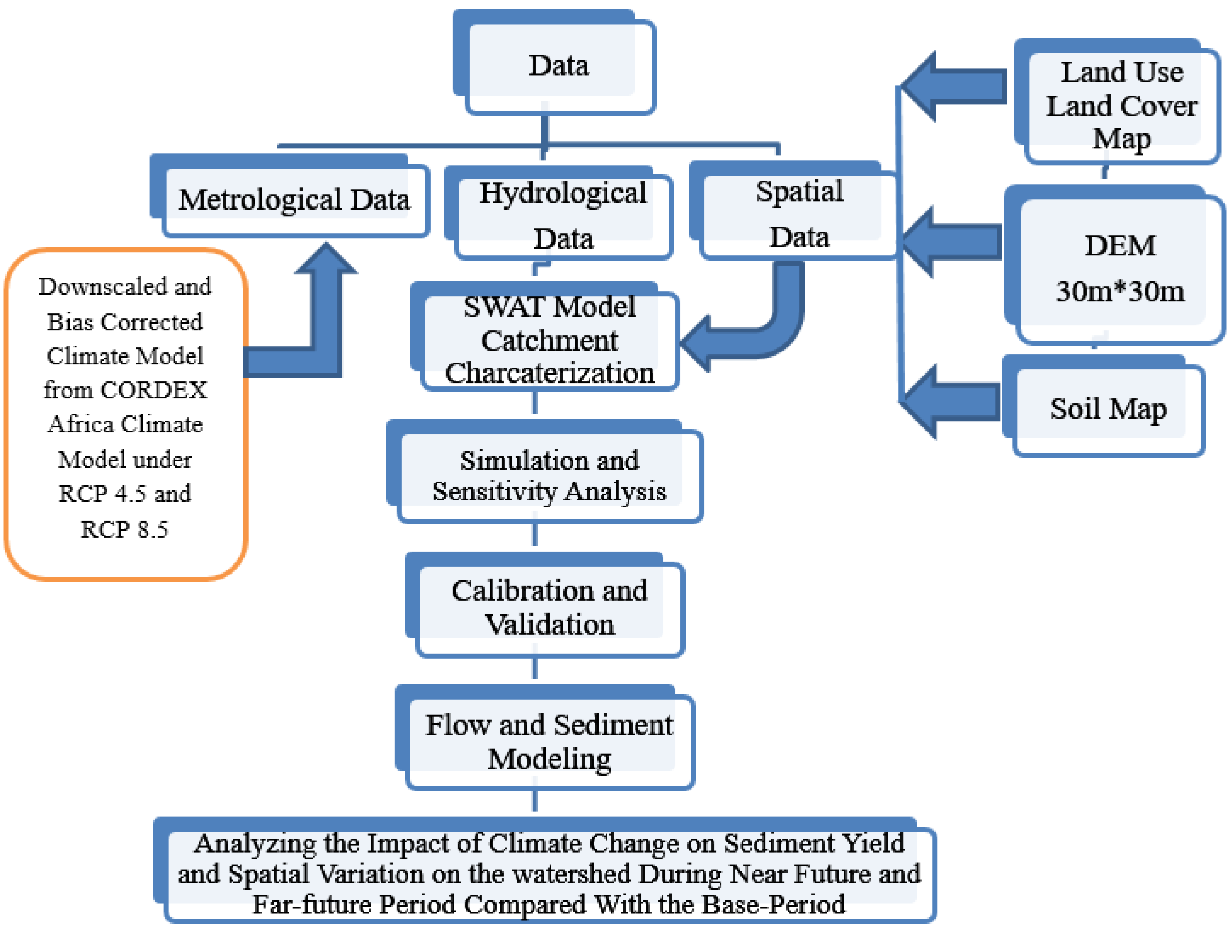

Figure 3. 9: Conceptual Frame Work of Methodology

3.3.2 Data Quality Analysis

The precipitation data must be checked for continuity and consistency before it is used for further analysis. After the rainfall, data is obtained from NMS it must be checked for its quality. The first step in data quality control is by visual inspection. This can be done by checking if date and time record is complete, unphysical values (negatives), flat regions (sensor or transfer system fall out) and unphysical variation patterns (sensor malfunctioning).

3.3.2.1 Filling of Missing Data

Some precipitation stations may have short breaks in the records because of absence of the observer or because of instrumental failures. It is often necessary to estimate or fill in this missing record. The missing precipitation of a station was estimated from the observations of precipitation at some other stations as close to and as evenly spaced around the station with the missing record as possible. Here, the station whose data was missing is called interpolation station and gauging stations whose data are used to calculate the missing station data are called index stations.

For this study normal ratio method were used. After calculating the normal annual value of each station then the missing value of each station calculated using the equation 3.3.

$$P_x = \frac{1}{n} \sum_{i=1}^{n} \frac{N_x}{N_i} * P_i \quad \text{..........} \quad 3.3$$

Where

Px = the missing precipitation for any storm at the interpolation station x,

Pi = the precipitation for the same period for the same storm at the i^{th} station of a group of index stations,

N_x = the normal annual precipitation for station x,

N_i = the normal annual precipitation value for the i^{th} station.

3.3.2.2 Checking Consistency of Gauging Stations (Double Mass Curve)

Double mass curve (DMC) was applied to test the consistency of rainfall for adjustment of inconsistent data. This technique is based on the principle that when each record data comes from the same parent sample, they are consistent. A group of four base stations in the neighborhood of the station was selected. A consistent record is one where the long term data of the record have no deflection with time. A double-mass curve is graph of the cumulative catch of rain gage of interest versus the cumulative catch of one or more gage in the region that has been subjected to similar hydro metrological occurrence and is known to be consistent. If a rainfall record is consistent estimator of the hydro meteorological occurrences over the period of record, the double-mass curve will have a constant slope. A change in the slope of the double mass curves would suggest that an external factor has caused changes in character of the measured values. If a change in slope is evident, then either the record needs to be adjusted with the early or the later period of record adjusted H.Hardision, (1960).

$$P_{CX} = Px\left(\frac{Mc}{Ma}\right) \qquad 3.4$$

Pcx = correct precipitation at any time t_1 at station x

Px = original record precipitation at any time t_1 at station x

Mc = correct slope of the double mass curve

Ma = original slope of double mass curve

According to the double mass curves analysis, all the stations in and around Mille watershed were Consistent. For illustration the double mass curves for some stations are presented below.

Figure 3. 10: Double Mass Curve of Metrological Stations

3.3.2.3 Checking Homogeneity of Selected Stations

Therefore, in order to choose representative meteorological station for the analysis of rainfall estimation, checking homogeneity of several stations are critical and the homogeneity of the selected gauging stations rainfall records were analyzed by non-dimensional.

$$\text{Pi} = \frac{P^{-}}{P} * 100 \qquad 3.5$$

Where:

Pi - is non- dimensional value of precipitation for the month in the station i
Pi¯ - is over year's average monthly precipitation for the station i
P¯ - is over year average yearly precipitation for station i
The selected stations was plotted for comparison and the stations have the same pattern, hence the group of stations selected are homogeneous.

3.3.2.4 Estimation of Areal Precipitation

In order to achieve accurate estimation of the spatial distribution of rainfall the Thiessen polygon method was considered because this method is the most important in engineering practice especially in engineering hydrology. The method weighs each gauge in direct proportion to the area it represents of the total basin without consideration of topography or other basin physical characteristics. Station weights are scalar factors used to distribute point precipitation observed at this rainfall gauging stations into related mean precipitation over the watershed that the station data are likely to represent. If there are n station with rainfall value P1, P2, P3….Pn and A1, A2, A3,….An are the area of the respective Thiessen polygons, the average rainfall over the catchment Pav is computed as:

$$P_{avg} = \sum_{i=1}^{n} Pi \left(\frac{A_i}{A}\right) \ldots\ldots \quad 3.6$$

Where, $\frac{Ai}{A} =$ weight factor for each station

3.3.2.5 Outliers Test

Outliers are data points that depart significantly from the trend of the remaining data. The retention or deletion of these outliers can significantly affect the magnitude of statistical parameters computed from the data, especially for small samples. Procedures for treating outliers require judgment involving both mathematical and hydrologic considerations.

The following frequency equation can be used to detect the outliers from the gathered and filled data using the regression:

$$Y_H = \bar{y} + K_n S_y \ldots\ldots 3.7$$

$$Y_L = \bar{y} - K_n S_y \ldots\ldots 3.8$$

Where

Y_H Is the higher outlier threshold in log unit and Y_L is the log of low outlier limit,

K_n The critical deviate taken from Table for sample n

S_y Is the standard deviation of the logs of the sample flows, and $\bar{y}$ is the mean of the log of the sample flows,

3.3.3 Correction of Biased RCM Simulations

3.3.3.1 Purpose of Bias Correction

Bias correction procedures employ a transformation algorithm for adjusting RCM output. The underlying idea is the identification of possible biases between observed and simulated climate variables, which is the basis for correcting both control and scenario RCM runs. Bias correction methods are assumed to be stationary, i.e., the correction algorithm and its parameterization for current climate conditions are also valid for future conditions. In this study the power transformation of bias correction method for precipitation correction and the variance scaling method for temperature correction of the row RCM data was applied.

3.3.3.2 Power Transformation for Precipitation

The bias correction method used for this study was a non-linear correction to adjust observed and simulated precipitation data. Correction factors were computed from statistics of the observed and simulated variables. The principal of this of this method shows mean and standard deviation of the daily precipitation data becoming equal to those of observed data Teutschbein, C, (2013) The power transformation method is explained in the following equation

$$P^* = aP^b \qquad 3.9$$

where P^* is the corrected value of precipitation, and a and b are power transformation parameters determined for the period of a year, which were obtained from calibration in the baseline period and subsequently applied to the projection period.

3.3.3.3 Variance Scaling for Temperature

Bias correction of temperature only involved shifting and scaling to adjust the mean and the variance. The corrected daily Temperature Tcorr was obtained as:

$$T_{corr} = \overline{T}_{obs} + \frac{\sigma(T_{obs})}{\sigma(T_{rcm})}\left(T_{rcm} - \overline{T}_{obs}\right) + \left(\overline{T}_{obs} - \overline{T}_{rcm}\right) \qquad 3.10$$

Where Tcorr is the corrected daily temperature; $\bar{T}_{rcm}$ is the uncorrected daily temperature from the RCM model; $\bar{T}_{obs}$ is observed daily temperature; $\bar{T}_{obs}$ and $\bar{T}_{rcm}$ are mean temperatures for observed and simulated datasets, respectively. For this particular study, CMhyd (Climate Model data for hydrologic modeling) software program was used to both extract climate model variables from Net-CDF file and correct biases of selected climate variables.

3.3.3.4 Performance Evaluation of Selected Climate Model

The ability of selected RCM to simulate climate variables at a particular location can be evaluated using a various techniques. There is no a single best evaluation technique or performance measure is considered as superior rather, it is combined use of many techniques and measures that provides a comprehensive overview of model performance Gordon & Shaykewich, (2000).

In this study, The performance evaluation of these corrected climate datasets was tested with frequency-based indices and time series performances against observed climate data. Frequency-based indices of the mean and standard deviation and also from the time serious-based matrices percent bias (PBIAS) and root-mean-square error (RMSE) as well as coefficient of variation and correlation coefficient also applied to assess the performance of the bias correction methods and to check the correlation between the row, bias adjusted and observed meteorological data.

$$Mean\ (\overline{P}) = \frac{1}{n} * \sum_{i=1}^{n} Pi \qquad 3.11$$

$$Standared\ Deviation\ (\delta) = \left[\frac{1}{n-1} * \sum_{i=1}^{n} \left(Pi - \overline{P}\right)^2\right]^{1/2} \qquad 3.12$$

$$PBIAS = \frac{\sum_{i=1}^{n}\left(P_{obs}^{i} - P_{rcm}^{i}\right)}{\sum_{i}^{n} p_{obs}^{i}} * 100 \qquad 3.13$$

$$RMSE = \sqrt{\frac{1}{N} * \sum_{i=1}^{n}\left(P_{obs}^{i} - P_{rcm}^{i}\right)^2} \qquad 3.14$$

$$Correl = \frac{\sum_{i}^{n}(P_{obs} - \overline{P}_{obs}) * (P_{rcm} - \overline{P}_{rcm})}{\sqrt{\sum_{i=1}^{n}(P_{obs} - \overline{p}_{rcm})^2 * (P_{rcm} - \overline{P}_{rcm})^2}} \qquad 3.15$$

Where $\overline{P}$ is the average precipitation and the subscript obs. and rcm represent the observed data the climate model data

Mean of a sample data represent shows the mid-point of a data and standard deviation is a number used to tell how measurements for a group are spread out from the average (mean), or expected value. A low standard deviation means that most of the numbers are close to the average. A high standard deviation means that the numbers are more spread out. Percent bias (PBIAS) measures the average tendency of the simulated values to be larger or smaller than their observed ones. Positive bias indicate the under estimation of a model and the negative bias express the over estimation of a model. The root-mean-square deviation (RMSD) or root-mean-square error (RMSE) is a frequently used measure of the differences between values (sample or population values) predicted by a model or an estimator and the values observed. In general the smaller RMSE is better than the higher value. Correlation is a statistic that measures linear correlation between two variables *X* and *Y*. It has a value between +1 and −1, where 1 is total positive linear correlation, 0 is no linear correlation, and −1 is total negative linear correlation. It is widely used in the sciences.

3.3.4 Statistical Test for Trend and Variability Analysis

The Mann Kendall trend test (sometimes called the M-K test) is used to test data collected over time for consistently increasing or decreasing trends (monotonic trends). The null hypothesis test is that, there is no monotonic trend in the series and the alternate hypothesis is that, the trend exists. This trend can be positive, negative, or null. For this study, non-parametric statistical method, the Mann-Kendall (MK) trend test, was used to identify the presence of trend in the time serious at 5% significate level Mann, (1945), Kendall, (1975) Amogne, (2018). The MK trend test analysis was recommended by the World Meteorological Organization (WMO) and has been widely used in practice to evaluate the significance of monotonic trends in hydrological and meteorological time series Adeyeri O.(2017)Birhanu H. (2017) and to determine the changes (increasing, decreasing, or trendless) in the values of climatic variables. For a given time series X ($x_1, x_2, \ldots, x_n$), the statistic S is defined as:

$$S = \sum_{i=1}^{n} \sum_{j=i+1}^{n-1} sgn(x_j - x_i) \qquad \ldots\ldots\ldots\ldots\ldots\ldots\ldots\ldots \quad 3.16$$

Where

$$Sign(X_j - X_i)\begin{cases} 1, & x_j > x_i, \\ 0, & x_j = x_i, \\ -1, & x_i < x_j, \end{cases} \qquad \ldots\ldots\ldots\ldots\ldots\ldots\ldots\ldots \quad 3.17$$

x_i and x_j are the data values in the time series, and n is the number of data points in the time series, The variance S is calculated using the following equation when the value of $n \geq 8$;

$$Var\ (s) = \frac{n(n-1)(2n+s)}{18} \quad \ldots\ldots\ldots \quad 3.18$$

The standard normal test statistic is calculated using the following equation

$$Z = \begin{cases} \frac{(1-S)}{\sqrt{Var(S)}}, & S > 0, \\ 0, & S = 0, \\ \frac{(1+S)}{\sqrt{Var(S)}}, & S < 0. \end{cases} \quad \ldots\ldots\ldots \quad 3.19$$

The statistical test Z is used to determine the significance of trend. If absolute value of Z is greater than tabulated Z at selected significance level say, for this study 5% which is 1.96, the trend is significant either increasing or decreasing based on S sign. If absolute of Z is less than the tabulated significance level the trend is not significant. The slope of n pairs of data points was estimated using the Sen's slope estimator as:

$$T_i = \frac{x_j - x_k}{j-k}\ , For\ i = 1,2,3, \ldots \ldots .. n \quad \ldots\ldots\ldots \quad 3.20$$

Where x_j and x_k are data values at times j and i respectively. Note (j > k). Ti is a Sen's estimator of slope which is the median of these N values. T indicates how much increasing or decreasing in trends. Calculating the trends for each data series manually was difficult. Therefore, AUTO_MK_Sen software program was used for this study to test the trends of both simulated and observed rainfall and discharges in annual based.

3.3.5 Hydrological Modeling Using SWAT

SWAT is one of the most powerful hydrologic models (Manfred, K. et al., 2013). It is physically semi-distributed, conceptually and computationally efficient and operates on a daily time step according to the soil properties, topography, vegetation and land management practices in the watershed Neitsch S.et al., (2005). The model was developed by the United States Department of Agricultural Research Service Arnold (1995) to predict and qualify the impact of agricultural management practices on water, sediment and chemical yields in different size of catchments with varying soils, land use and management conditions over long periods of time .The model has been widely applied to the different sizes of the watersheds and its applications all over the water resources, including the effects of climate and soil erosion Neitsch S. et al., (2005).

3.3.5.1 Surface Runoff Component of SWAT Model

For this study a physically based, continuous time watershed model which simulates hydrological processes in the watershed was used. The details of SWAT were shown in Neitsch S. et al., (2005). SWAT used together with Arc SWAT in ArcGIS (Geographical Information System) interface to process the datasets and construct the required input for the initial modeling setup. In SWAT model application, the study basin/watershed is first sub divided in to sub-basins/sub-watershed based on digital elevation model and channel network, and further delineated into hydrological response units (HRUs) considering dominant soil/land use category in each sub-basin/sub-watershed where each sub-basin/sub-watershed was assumed to be constituted with a homogeneous soil, land use and slope.

Routing of water is simulated from the HRUs to the sub-basin level, and then through the stream network to the basin outlet. The model predicts the hydrology ultimately streamflow Neitsch S. et al., (2005) at each HRU using water balance equation, which contain precipitation, surface runoff, evapo-transpiration, infiltration and sub-surface inflow. The water balance equation of the hydrologic cycle is:

$$SW_t = SW_O + \sum_{i=1}^{t}\left(R_{day} - Q_{surf} - E_a - W_{seep} - Q_{gw}\right) \quad \text{........................} \quad 3.21$$

in which SW_t is the final soil water content (mm), SW_O is the initial soil water content on day I (mm), t is the time in days, R_{day} is the amount of precipitation on day i (mm), $Q_{surf}$is amount of surface runoff on day i (mm), $E_a$is amount of evapotranspiration on day i (mm), W_{seep} is amount of water entering to vadose zone from the soil profile on day i (mm), and Q_{gw} is amount of return flow on day i (mm).

When the rate of precipitation exceeds the rate of infiltration, surface runoff occurs. SWAT offer the methods of the Soil Conservation Service (SCS) curve number procedure United States Soil Conservation Service., (1972), and the Green & Ampt infiltration method Green and Ampt, (1911) to estimate surface runoff. SCS curve number method was selected for this watershed. SWAT model simulation as the SCS curve number procedure uses daily precipitation and the Green & Ampt infiltration method requires precipitation input in sub-daily scale. In the SCS method retention parameter defined by Curve Number (CN) is significant, and it is a sensitive function of the land use, soil's permeability and antecedent soil water conditions. Surface runoff was estimated using Soil Conservation Service Curve Number (SCS-Curve number) method:

$$Q_{surf}= \frac{(Rday-Ia)}{(Rday-Ia+S)}^{2} \text{ ....} \quad 3.22$$

Where R_{day} is rainfall depth, I_a is the initial abstraction which includes surface storage, interception and infiltration prior to runoff and S is the retention parameter (mm) Retention parameter defined by

$$S = 25.4(\frac{1000}{CN} - 10) \text{ ....} \quad 3.23$$

CN is curve number for the day varies from 0 to 100 depending on soil permeability, land use and the antecedent soil water condition.

Initial parameter approximated as 0.2S, Equation (3.22) becomes

$$Qsurf = \frac{(Rday-0.2S)^2}{(Rday+0.8S)} \text{..} \quad 3.24$$

Where R_{surf} is amount of surface runoff on day i (mm).

3.3.5.2 Sediment Component of SWAT Model

Erosion and sediment yield in SWAT are estimated for each HRU with the Modified Universal Soil Loss Equation (MUSLE). It uses the amount of runoff to simulate erosion and sediment yield. The hydrology module/component supplies estimate of runoff volume and peak runoff rate, which, with the sub basin area, are used to calculate the runoff erosive energy variable. The crop management factor is recalculated every day that runoff occurs.

The studies by Setegn et.al, (2008) show that sediment transport in the channel network consists of two components operating simultaneously, which are deposition and degradation. To determine the deposition and degradation process the maximum concentration of sediment is calculated using Equation 3.25 below.

$$Conc_{sed,ch,mx} = C_{sp} * V_{ch,pk}^{spexp} \text{ ....} 3.25$$

Where $concsed,h,mx$ is the maximum concentration of sediment that can be transported by water (ton/m3 or kg/L), Csp is the coefficient defined by the user, Vch,pk is the peak channel velocity (m/s), and spexp is an exponent parameter for calculating sediment re-entrained in channel sediment routing that is defined by the user and set at 1.5 for this particular study. It normal varies between 1 and 2. The peak channel velocity, Vch, is calculated by using equation 3.26.

$$V_{ch,pk} = \frac{prf * q_{ch}}{A_{ch}} \quad \text{………………………………………………….3.26}$$

Where prf, is the peak rate adjustment factor (a user specified parameter), qch is the average rate of flow (m3/ s), and Ach, is the cross-sectional area of flow (m2). The maximum concentration of sediment (Concsed, ch, mx) that is calculated from the previous equation is compared to the concentration of sediment in the reach at the beginning of the time step Conc sed, ch, i. If Conc sed, ch, i > Concsed, ch,mx, deposition is the dominant process in the reach segment, Equation 3.27 below is used to calculate the net amount of sediment deposited in the reach.

$$Sed_{dep} = (Conc_{sed,ch,i} - Conc_{sed,ch,mx}) * V_{ch} \quad \text{………………………………………3.27}$$

Where Sed dep is the amount of sediment deposited in the reach segment (metric tons) and Vch is the volume of water in the reach segment (m3). If Conc. sed, ch, i < Conc. sed, ch, mx degradation is the dominant process in the reach segment and the net amount of sediment re-entrained is calculated by Equation 3.28 below.

$$Sed_{deg} = (Conc_{sed,ch,mx} - Conc_{sed,ch,i}) * V_{ch} * K_{ch} * C_{ch} \quad \text{……………………………..3.28}$$

In which, $Seddeg$ is the amount of sediment re-entrained in the reach segment (metric tons), Kch is the channel erodibility factor (cm/hr/pa), and Cch is the channel cover factor. The channel erodibility factor (Kch) is conceptually similar to the soil erodibility factor in the Universal Soil Loss Equation. Channel erodibility is a function of properties of the bed or bank materials. In general, values for channel erodibility are an order of magnitude smaller than values for soil erodibility. The channel cover can be defined as a ratio of degradation from a channel with a specified vegetative cover to the corresponding degradation from a channel with no vegetative cover. The vegetation affects degradation by reducing the stream velocity, and consequently its erosive power, near the bed surface.

After the amount of deposition and degradation is calculated, equation 3.29 is used to determine the final amount of sediment in a reach.

$$Sed_{ch} = Sed_{ch,i} - Sed_{dep} + Sed_{deg} \quad \ldots\ldots 3.29$$

where, $Sedch$ is the amount of suspended sediment in the reach (metric tons), $Sedch,i$is the amount of suspended sediment in the reach at the beginning of the time period (metric tons), $Seddep$ is the amount of sediment deposited in the reach segment (metric tons), and $Seddeg$ is the amount of Sediment re-entrained in the reach segment (metric tons).

Finally, Equation 3.30. Below is used to calculate the amount of sediment transported out of the reach.

$$Sed_{out} = Sed_{ch} * \frac{V_{out}}{V_{ch}} \quad \ldots\ldots 3.30$$

where, Sed out is the amount of sediment transported out of the reach (t), $Sedch$ is the amount of suspended sediment in the reach (t), Vout is the volume of out flow during the time step (m3), and Vch is the volume of water in the reach segment (m^3).

3.3.6 SWAT Model Setup

3.3.6.1 Watershed Delineation

The watershed and sub watershed delineation was performed using 30m*30m DEM resolution data using Arc SWAT model watershed delineation function. First, the SWAT project set was created. The watershed delineation processes follows five successive steps, DEM setup, stream definition, outlet and inlet definition, watershed outlet selection definition and calculation of sub basin parameters. Once, the DEM setup was completed Flow direction and accumulation are the concepts behind the definition of the stream network of the DEM in SWAT and the location of outlet point (gauge station of Mille River near Mille town) was specified on the DEM, for the final delineation of the entire watershed. Subsequently, stream networks, sub watersheds and topographic parameters were calculated using the respective tools. The stream definition and the size of sub basins were carefully determined by selecting threshold area or minimum drainage area required to form the origin of streams. The Mille watershed was delineated in to 15 sub basins having an estimated total area of 4640.43 km^2 Figure 3.16.

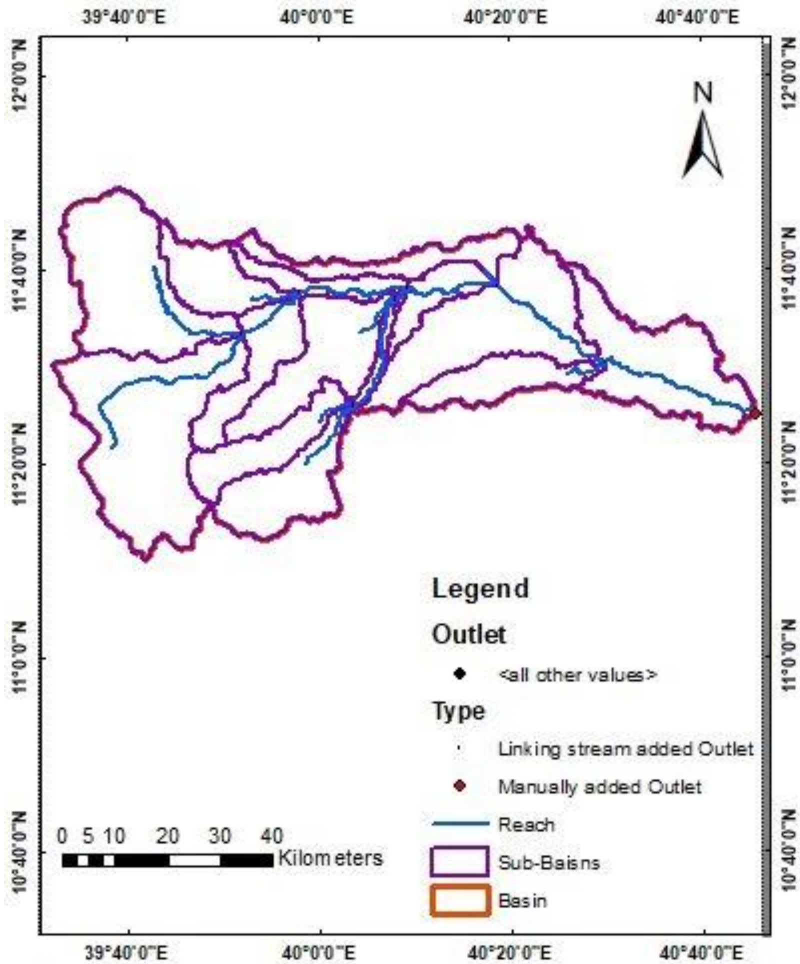

Figure 3. 14: Delineated Watershed of Mille

3.3.6.2 Hydrologic Response Units Analysis

Hydrological Response Unit (HRU) which is the smallest unit of the model to route streamflow was established after reclassification of land use, soil maps and slope classes and then overlaid one upon each other.

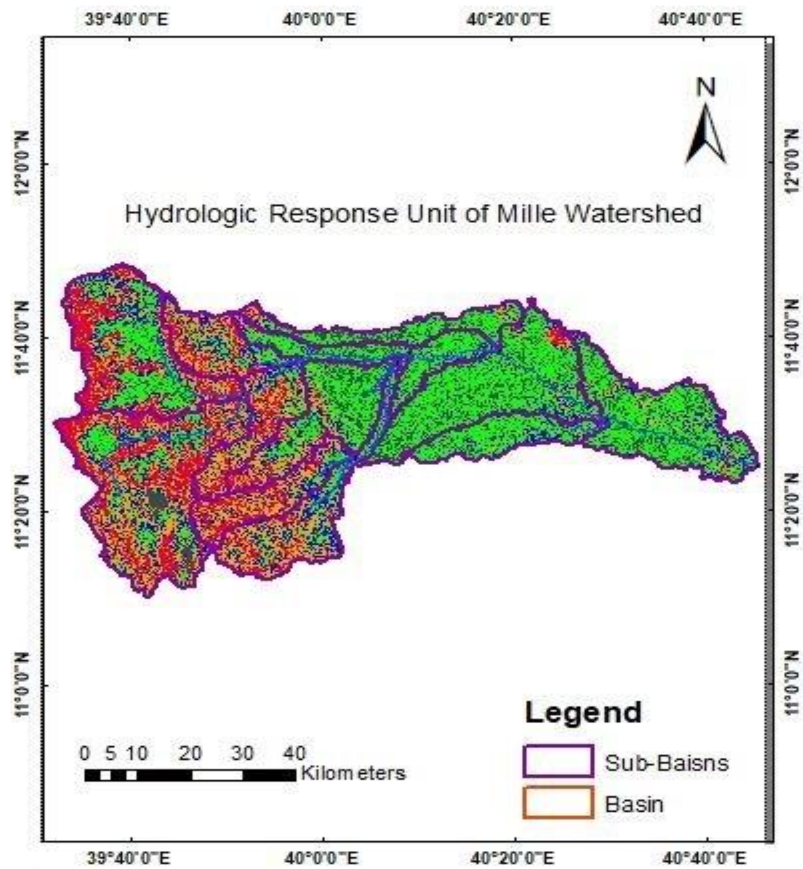

Figure 3. 15: Hydrologic Response Unit of Mille Watershed

The sub watershed were divided into HRUs by assigning the threshold values of land use and land cover, soil and slope percentage. In general the threshold level used to eliminate minor land use and land covers in sub basin, minor soil within land use and land cover area and minor slope categories within a soil on particular land use land cover area. Following minor elimination, the area of remaining land use and land covers, soils and slope cases are reapportioned so that 100% of their respective area modeled by SWAT. Land use, soil and slope characterization for Sub basin was performed using commands from HRU analysis menu on the Arc SWAT Toolbar. These tools allowed loading land use and soil maps which are in raster formats/shape files in to the current project, evaluates slope characteristics and determining the land use/soil/slope class combinations in the delineation sub basin. In the model, there are two options in defining HRU distribution: assign a single HRU to each sub basin or assign multiple HRUs to each sub basin based on a certain threshold values. According to (Arnold, et al. 1998) user manual, the threshold levels set for multiple HRUs is a function of the project goal and the amount of detail desired by the modeler and it was indicated for most applications, the settings for land use threshold

(10 %), soil threshold(10 %) and (5%) slope will be appropriate and this threshold level was applied in this study. Runoff and sediment is generated for individual HRUs and routed to get the cumulative runoff and sediment load for the watershed. This improves the accuracy of runoff predictions of the model and provides a much better physical description of the water balance. All model input data were projected to the same projection of Transverse Mercator projection.

3.3.6.3 Weather Generator`

In developing countries, there is a lack of full and realistic long period of climatic data. Hence, the weather generator eliminate this problem by producing data from the observed one Danuso et al, (2002). The Model requires the daily values of all climatic variables from measured data or generated from values using monthly average data over a number of years. This study used measured data for all climatic variables. However, the weather data obtained for the stations in and around Sub basin had missed records in some of the variables. Therefore, this missed values were filled with the weather generator utility in the Arc SWAT model from the values of weather generator parameters. Weather data of three stations (Bati, Dubity, and Serinka) with continues records were used as input to determine the values of weather generator parameters. Hence, for weather generator data definition, the weather generators data file wgnstations.txt was selected first. Subsequently, rain fall data, temperature data, relative humidity data, solar radiation data and wind speed data were selected and added to model.

The SWAT Model contain weather generator model called WXGEN Shapley and Williams et al., (1990). It is used in SWAT model to generate climatic data or to fill missing data using monthly statistics which is calculated from existing daily data. From the values of weather generator parameters, the weather generator first separately generates precipitation for the day. Maximum temperature, minimum temperature, solar radiation and relative humidity are then calculated. Lastly, the wind speed is generated independently. To generate the data, SWAT Weather Database is designed to be a friendly tool to store and process daily weather data to be used with SWAT projects. It enable of: saving reliable daily weather information; easily producing .txt files that can be applicable as input data during an Arc SWAT project setup; effectively calculating the WGEN statistics of many weather stations in single run Essenfelder, A. H., et al., (2016). As for any SWAT project, missing values must be entered as -99 such values will not be used during the calculation of the WGEN statistics.

3.3.6.4 Sensitivity Analysis

Calibration is necessary to optimize the values of the model parameters which help to reduce the uncertainty in model outputs. However, such type of model with a multiple parameters, the difficult task is to determine which parameters are to be calibrated. In this case, sensitivity analysis is important to identify and rank parameters that have significant impact on the specific model output interest Van Griensven, et al., (2006). Therefore, for this study, sensitivity analysis was done prior to the calibration process in order to identify important parameters for model calibration.

The average monthly stream flow data of nine year from 1989-1997 of the watershed gauging station were used to compute the sensitivity of stream flow parameters. In sensitivity process, by entering the Arc SWAT interface SWAT-CUP sensitivity analysis window, first the SWAT simulation was specified for performing the sensitivity analysis and the location of the sub basin where observed data was compared against simulated output. Then, selected parameters were entered for sensitivity analysis with the default lower and upper parameter bounds. Hence, 20 flow parameters were included for the analysis with default values as recommended by Van Griensven, et al., (2006) and rank of sensitivity was based on the value of t-sat and p-values.

3.3.6.5 Model Calibration and Validation

Following the sensitivity analysis result, model calibration was done to obtain optimum values for sensitive parameters. SWAT provides three options for calibration: manual calibration, auto-calibration and combination of these two methods. For this study, first manual calibration was done to fine tone some of the parameters and some model parameters were adjusted by manual calibration. Then, auto calibration by SWAT-CUP was done on monthly time steps using the average measured stream flow data of the sub basin covering from 1989-1997.There were different calibration procedure methods Generalized Likelihood Uncertainty Estimation (GLUE), Parameter Solution (ParaSol), Sequential Uncertainty Fitting (SUFI2) and Markov chain Monte Carlo (MCMC). For this study, the Sequential Uncertainty Fitting (SUFI2) option was selected. This method was chosen for its applicability to both simple and complex hydrological models. In this procedure, by entering the Arc SWAT interface SWAT_CUP Auto-calibration window, first the SWAT simulation was specified for performing the auto-calibration and the location of the sub basin where observed data could be compared against simulated output. Then, the desired parameters for optimization, observed data file, and methods of calibration were selected.

Hence, seven flow parameters were considered in the calibration process. After the auto calibration runs completed, the model was run using the best parameter output values and the simulations were compared with observed stream flow data using Nash and Sutcliffe coefficient of efficiency (ENS) and coefficient of determination (R^2).Validation was also done to compare the model outputs with an independent data set without making further adjustment of the parameter values. Model validation is comparison of model outputs with an independent data set without making further adjustment which may adjust during calibration process. The measured data of average monthly stream flow data of four years from 1998-2002 were used for the model validation process. In this process, the two model performance values were also checked here to make sure that the simulated values are still within the accurate limits.

3.3.6.6 Performance Evaluation of SWAT Model

After manual and automatic calibration monthly streamflow were compared against the observed data. There are several ways in which SWAT can be calibrated and validated. In this study, the Nash-Sutcliffe coefficient (E_{NS}), coefficient of determination (R^2) were used to evaluate performance of SWAT model simulation in the calibration and validation process Moriasi (2007).

Nash-Sutcliffe Efficiency (E_{NS}): E_{NS} is a normalized statistic that determines the relative magnitude of the residual variance ("noise") compared to the measured data variance ("information") Nash and Sutcliffe, (1970). E_{NS} indicates how well the plot of observed versus simulated data fits the 1:1 line. The optimal values to get best model performance is at E_{NS} =1. E_{NS} is computed as shown in equation 3.31:

$$E_{NS} = 1 - \left[\frac{\sum_{i=1}^{n}\left(Q_i^{obs} - Q_i^{sim}\right)^2}{\sum_{i-1}^{n}\left(Q_i^{obs} - \overline{Q}_{obs}\right)^2}\right] \qquad 3.31$$

Where Qi^{obs} is the i^{th} observed stream flow of day I, Qi^{sim} is the i^{th} simulated stream flow of day I, Q_{obs}^{mean} the mean of observed streamflow, Q_{sim}^{mean} the mean of simulated streamflow.

Coefficient of Determination (R^2): describe the degree of co-linearity between simulated and measured data. The R^2 describes the proportion of the variance in measured data explained by the model. The ranges of R^2 varies from 0 to 1, with higher values indicating less error variance, and typically values greater than 0.5 are considered acceptable. Although R^2 has been widely used for model evaluation, this statistic is over sensitive to high extreme values (outliers), and insensitive to additive and proportional differences between model predictions and measured data.

$$R^2 = \frac{\left[\sum_{i=1}^{n}\left(Q_i^{obs} - \overline{Q}_{obs}\right)\left(Q_i^{sim} - \overline{Q}_{sim}\right)\right]}{\sqrt{\sum_{i=1}^{n}\left(Q_i^{obs} - \overline{Q}_{obs}\right)^2 * \sum_{i=1}^{n}\left(Q_i^{sim} - \overline{Q}_{sim}\right)^2}} \ldots \qquad 3.32$$

Where Qi^{obs} is the i^{th} observed stream flow of day i, Qi^{sim} is the i^{th} simulated stream flow of day i, Q_{obs}^{mean} the mean of observed streamflow.

Table 3. 4: SWAT Model Performance Evaluation Criteria Moriasi (2007).

Model Evaluation	E_{NS}	R^2	PBIAS
Excellent	$0.75 < E_{NS} \leq 1.00$	$0.70 < R^2 \leq 1.00$	PBIAS ≤ ± 10
Good	$0.65 < E_{NS} \leq 0.75$	$0.60 < R^2 \leq 0.70$	±10 < PBIAS ≤ ± 15
Satisfactory	$0.50 < E_{NS} \leq 0.65$	$0.50 < R^2 \leq 0.60$	±15 < PBIAS ≤ ± 25
Unsatisfactory	$0.00 < E_{NS} \leq 0.50$	$0.00 < R^2 \leq 0.50$	PBIAS > ± 25

4. RESULT AND DISCUSSION

4.1 Data Quality Analysis

4.1.1 Checking Consistency of Gauging Stations (Double Mass Curve)

According to the double mass curves analysis, all the stations in and around Mille watershed were Consistent. For illustration the double mass curves for some stations are presented below.

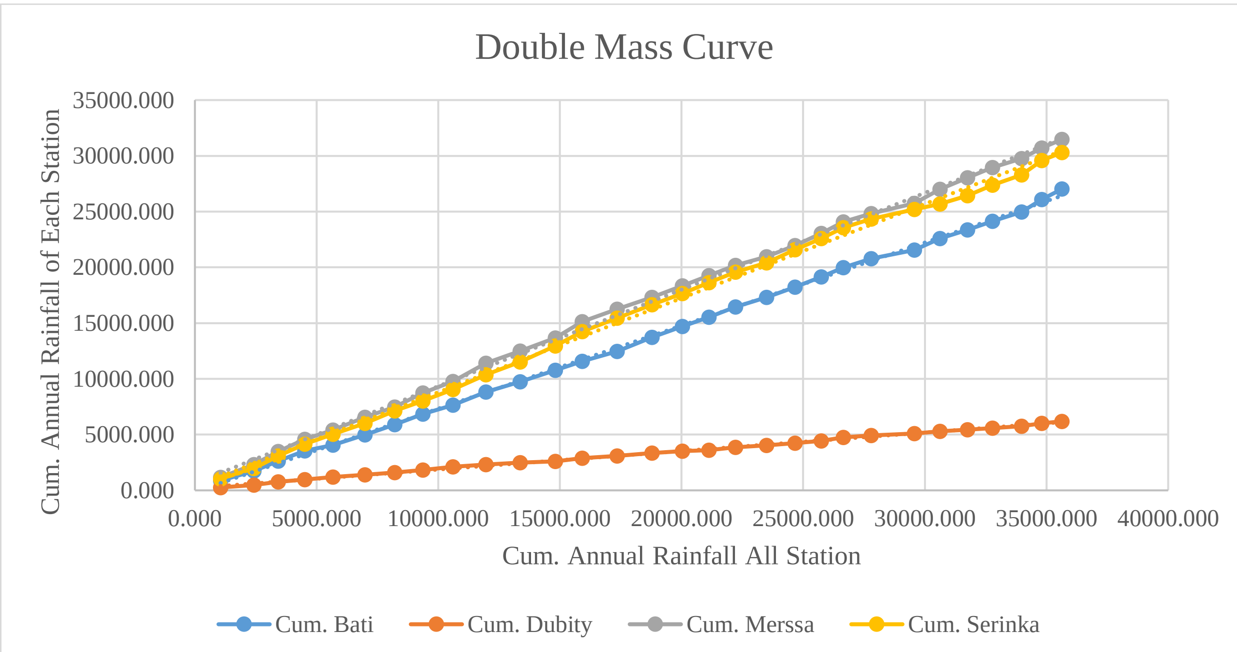

Figure 3. 10: Double Mass Curve of Metrological Stations

4.1.2 Checking Homogeneity of Selected Stations

The homogeneity of parameters analysis is important to the variation of the statistical properties of the time series. The causes of variation can be either human or natural. These include alterations to land use and relocation of the observation station.

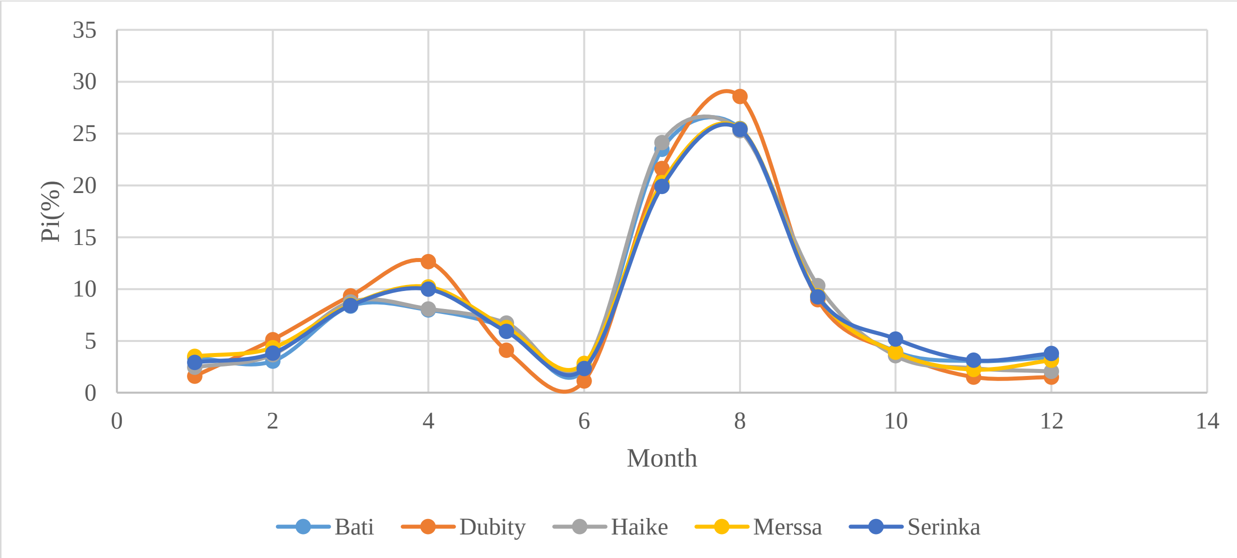

Figure 3.11: Homogeneity Test for Selected Metrological Stations

4.1.3 Estimation of Areal Precipitation

Arial precipitation of the Mille watershed as indicated on Figure 3.15 and Table 3.5 The area represented by each gauge is assumed to be that which is closer to it than to any other gauge.

Table 3. 6: Selected Stations for Thiessen Polygon and their Weight Factors

No.	Station Name	Weight	Area (Km^2)
1	Bati	0.42	2392.715
2	Haike	0.33	1846.252
3	Dubity	0.12	653.906
4	Serinka	0.09	529.293
5	Merssa	0.04	240.445

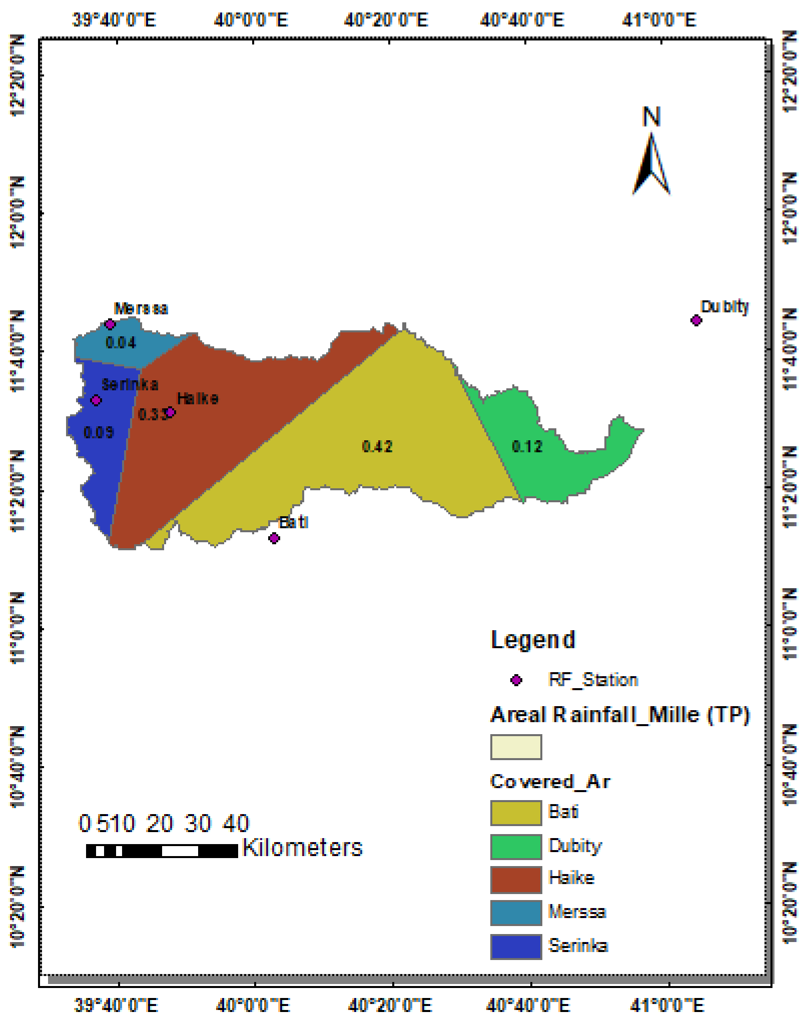

Figure 3. 12: Thiessen Polygon for Selected Station over the Study Area

4.1.4 Outlier Test

After the regression analysis the gauge station record are tested for outlier and hence no outlier set of recorded data is found from the recorded flow data. The regression analysis for higher outlier values is 99.812 m3/sec and the lower outlier value is 8.132 m3/sec. however the maximum flow recorded values is 61.023 m3/sec and the lower values is 10.899 m3/sec thus the result indicate that there is no higher or lower outlier values with in the recorded flow data.

4.2 Evaluation of Bias Correction Method

Impact assessment of climate change necessitates evaluation of the climate model's accuracy. For this reason, in this study, the models performance was evaluated for each GCM and RCM climate model under each RCP scenario using statistical measures such as annual mean, standard deviation, PBIAS, RMSE, CV and CC. Climate change signals for both variables were computed from the differences in the long-term averages for the reference period 1986-2015 and for two future periods. As historical runs of the climate models end in 2005, the climate model data for the reference period included the first years of the scenario runs. Therefore, separate reference scenarios were derived for the two emission scenarios. In the first years of the scenario runs, when emission forcing almost does not diverge yet, model results vary mainly due to the random "model weather" and lead only to small differences in the long-term reference period averages Phillip, (2018). Table 4.1, 4.2 and 4.3 describes the statistical results of the observed, bias corrected and bias uncorrected climate model outputs.

Table 4.1: Statistical Result of Precipitation Bias Correction

GCM	RCM	RCP	ANNUAL RF (mm)	STD DEV	CV (%)	PBIAS	RMSE	CORR
Observed			930.79	102.55	11.02			
Bias Corrected HADGEM2	RACMO22T	RCP 4.5	970.12	106.31	10.96	-4.23	79.00	0.78
		RCP 8.5	925.11	105.98	11.46	0.61	79.96	0.70
Bias Uncorrected HADGEM2	RACMO22T	RCP 4.5	1140.29	192.54	16.88	-22.51	300.98	-0.02
		RCP 8.5	1117.11	193.44	17.32	-20.02	284.68	0.00
Bias Corrected ICHEC	CCLM4-8-17	RCP 4.5	956.50	141.21	14.76	-2.76	107.59	0.66
		RCP 8.5	922.58	131.19	14.22	0.88	92.41	0.70
Bias Uncorrected ICHEC	CCLM4-8-17	RCP 4.5	2714.99	609.51	22.45	-191.69	1883.83	0.03
		RCP 8.5	2457.99	634.62	25.82	-164.08	1644.41	0.22

As shown in the table above the performance of the climate model increase after bias correction for both climate models and for the two RCP scenarios. Slight over estimation of mean annual rain fall is observed for both climate model under RCP 4.5 climate scenario and slight under estimation mean annual rainfall is observed under RCP 8.5 climate scenario of the two climate model after bias correction and such problem may occur due to the resolution of the gird cell data. The correlation between the simulated base period climate data and the observed data of precipitation for historical period shows a better correlation after bias correction was performed. Generally the overall quality of precipitation data shows improvement and better result. On the other hand the row RCM data shows a great overestimation and huge variation of precipitation values that leads to significant error and unrealistic output during impact assessment over the watershed.

Table 4.2: Statistical Result of Temperature Maximum Bias Correction

GCM	RCM	RCP	ANNUAL TEMP MAX(ºc)	STD DEV	CV (%)	PBIAS	RMSE	CORR
Observed			28.40	0.51	1.80			
Bias Corrected HADGEM2	RACMO22T	RCP 4.5	28.40	0.52	1.85	0.02	0.38	0.72
		RCP 8.5	28.41	0.54	1.90	-0.03	0.40	0.70
Bias Uncorrected HADGEM2	RACMO22T	RCP 4.5	25.80	0.58	2.23	9.16	2.66	0.50
		RCP 8.5	25.74	0.57	2.22	9.37	2.73	0.36
Bias Corrected ICHEC	CCLM4-8-17	RCP 4.5	28.31	0.44	1.56	0.31	0.37	0.72
		RCP 8.5	28.41	0.50	1.76	-0.03	0.42	0.64
Bias Uncorrected ICHEC	CCLM4-8-17	RCP 4.5	22.18	0.49	2.21	21.92	6.25	0.40
		RCP 8.5	22.25	0.53	2.37	21.65	6.17	0.55

Table 4.3: Statistical Result of Temperature Minimum Bias Correction

GCM	RCM	RCP	ANNUAL TEMP MIN (ºc)	STD DEV	CV (%)	PBIAS	RMSE	CORR
Observed			13.81	0.54	3.93			
Bias Corrected HADGEM2	RACMO22T	RCP 4.5	13.83	0.57	4.10	-0.14	0.38	0.76
		RCP 8.5	13.82	0.58	4.20	-0.07	0.35	0.80
Bias Uncorrected HADGEM2	RACMO22T	RCP 4.5	14.46	0.40	2.79	-4.69	1.03	-0.48
		RCP 8.5	14.48	0.46	3.17	-4.82	1.08	-0.47
Bias Corrected ICHEC	CCLM4-8-17	RCP 4.5	13.78	0.60	4.37	0.25	0.48	0.64
		RCP 8.5	13.90	0.55	3.97	-0.67	0.49	0.61
Bias Uncorrected ICHEC	CCLM4-8-17	RCP 4.5	14.35	0.32	2.21	-3.88	0.85	-0.15
		RCP 8.5	14.41	0.37	2.60	-4.36	0.99	-0.49

Temperature is the other important climate parameter which is considered for this study and have a significant impact on the hydrological process of a watershed. Variance scaling bias correction method indicate that can improve the quality of row simulated climate data for period of reference as historical time frame and for the two future time. For both climate model row annual average temperature maximum shows under estimated values and annual average temperature minimum of bias uncorrected row data shows over estimated values in both RCP 4.5 and RCP 8.5 climate scenarios for base period time. However; after bias correction was taken these unnecessary over estimation and under estimation of climate data's corrected and the quality as well as correlation of the observed and simulated data improved for both temperature maximum and temperature minimum.

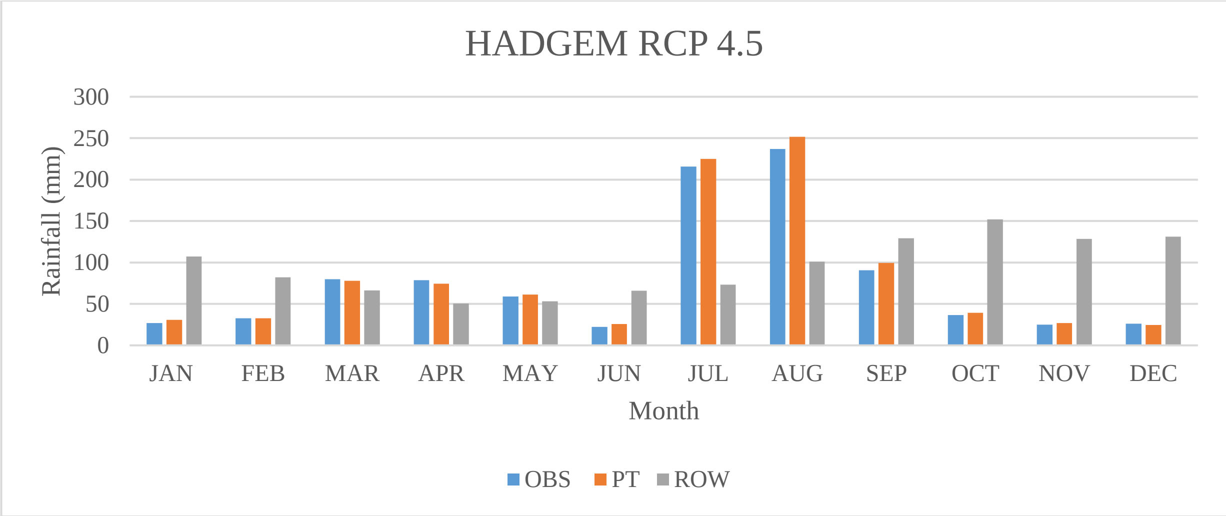

Figure 4.1: Mean Monthly Observed (OBS), Power Transformation (PT) Bias Corrected and Row RCM Bias Uncorrected (ROW) Rainfall of Mille Watershed

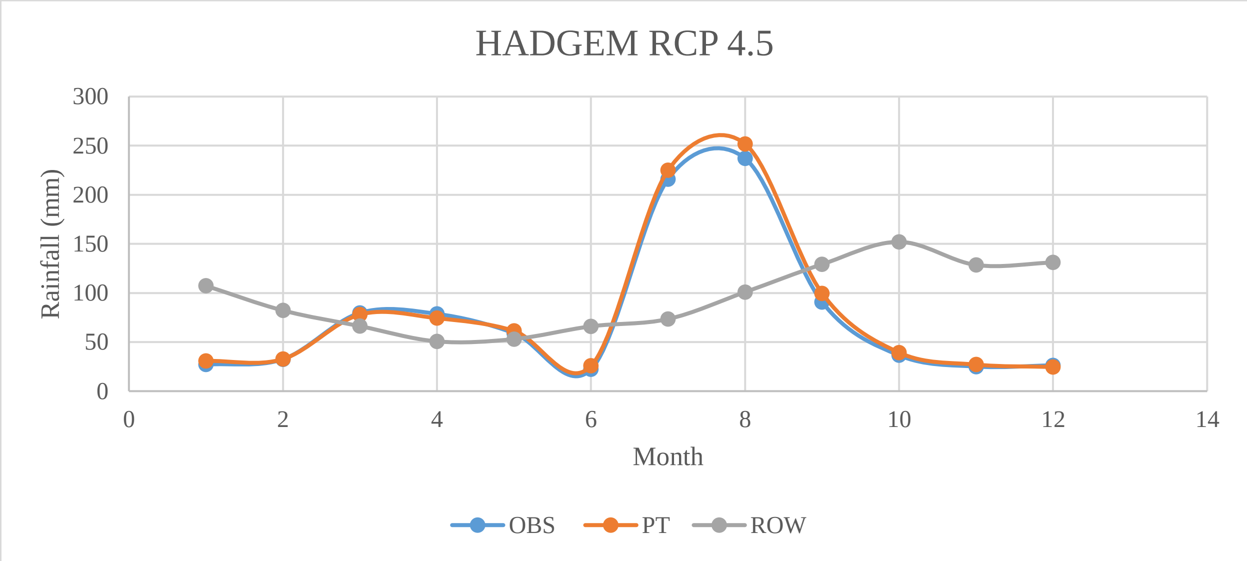

Figure 4.2: Observed (OBS), Power Transformation (PT) Bias Corrected and Row RCM Bias Uncorrected (ROW) Rainfall Pattern of Mille Watershed

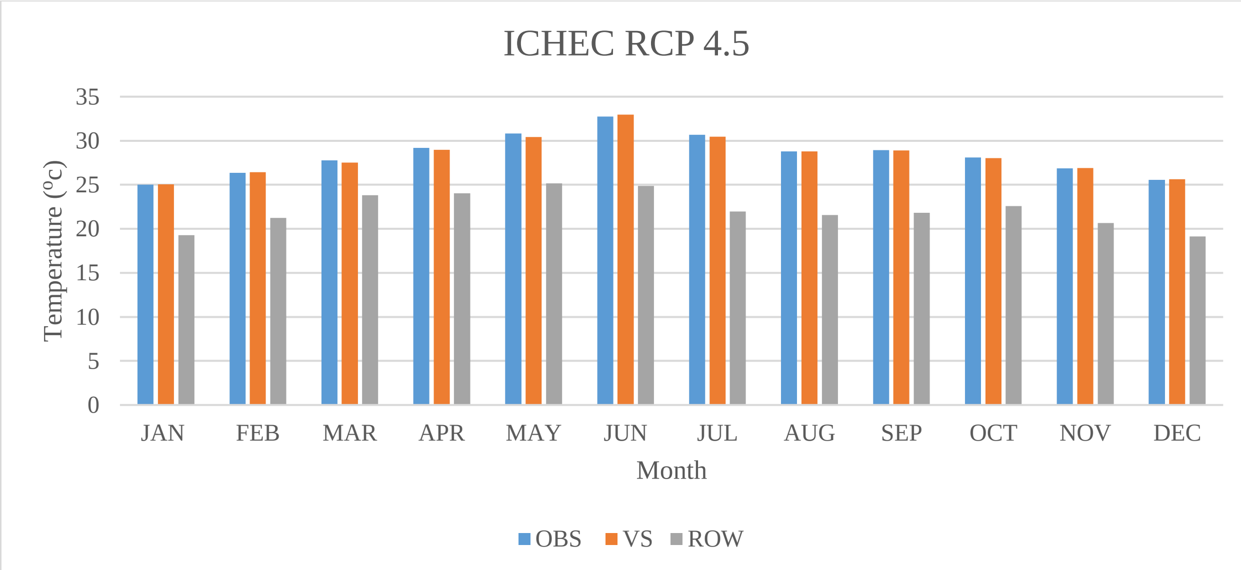

Figure 4.3: Mean Monthly Observed (OBS), Variance Scaling (VS) Bias Corrected and Row RCM Bias Uncorrected (ROW) Maximum Temperature of Mille Watershed

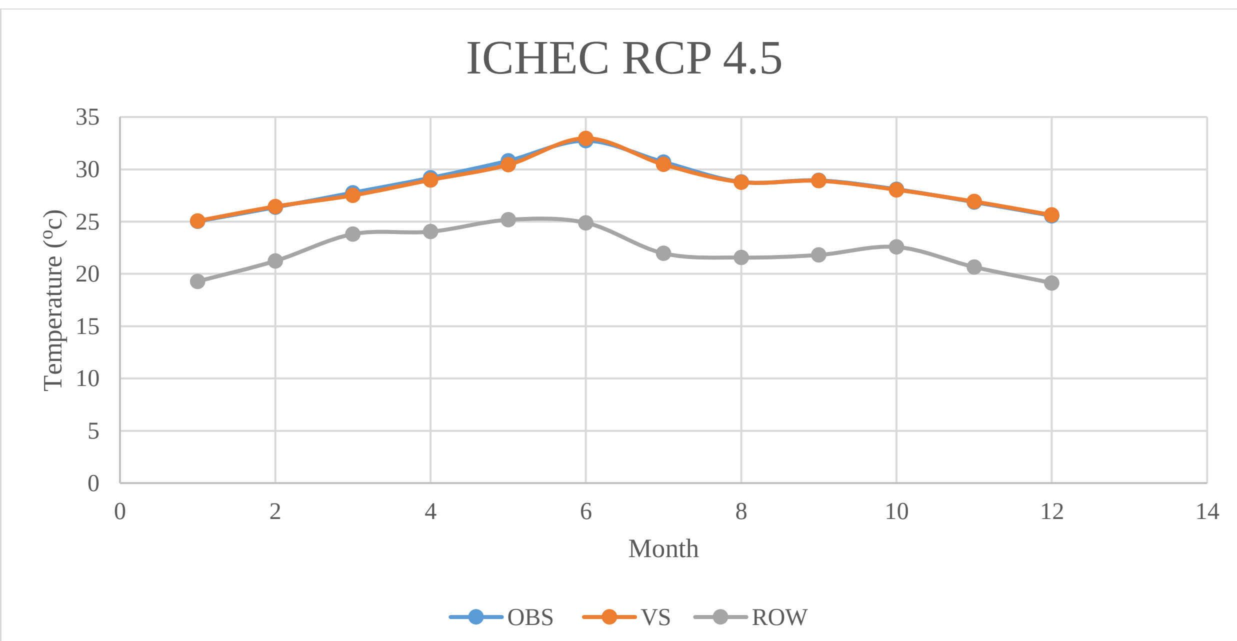

Figure 4.4: Mean Monthly Observed (OBS), Variance Scaling (VS) Bias Corrected and Row RCM Bias Uncorrected Temperature (ROW) Maximum Pattern of Mille Watershed

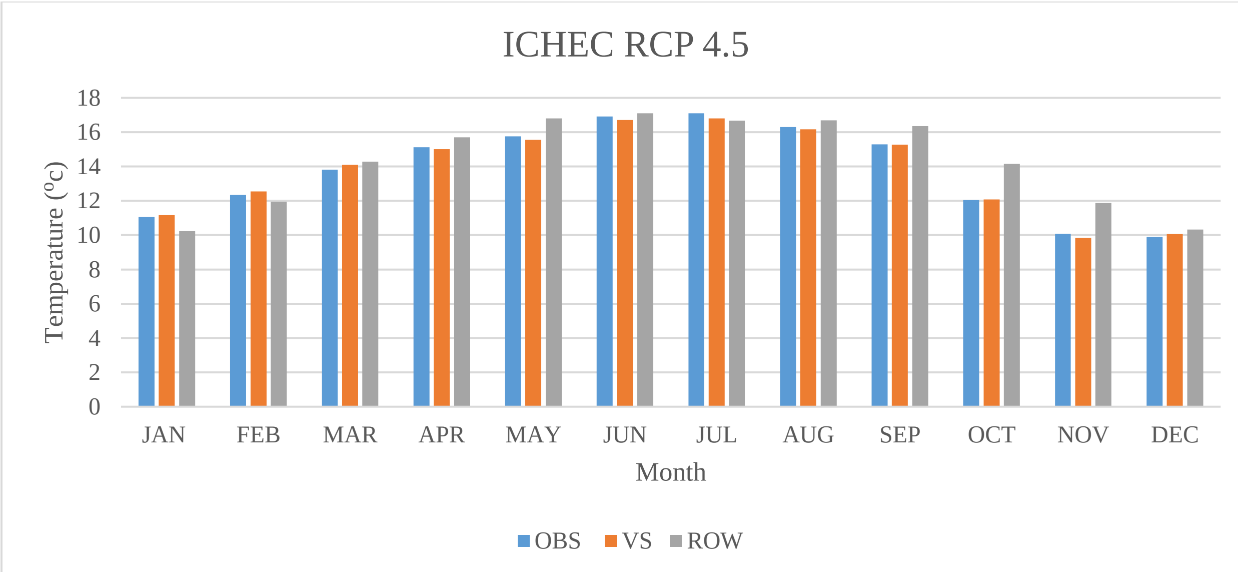

Figure 4.5: Mean Monthly Observed (OBS), Variance Scaling (VS) Bias Corrected and Row RCM Bias Uncorrected (ROW) Minimum Temperature of Mille Watershed

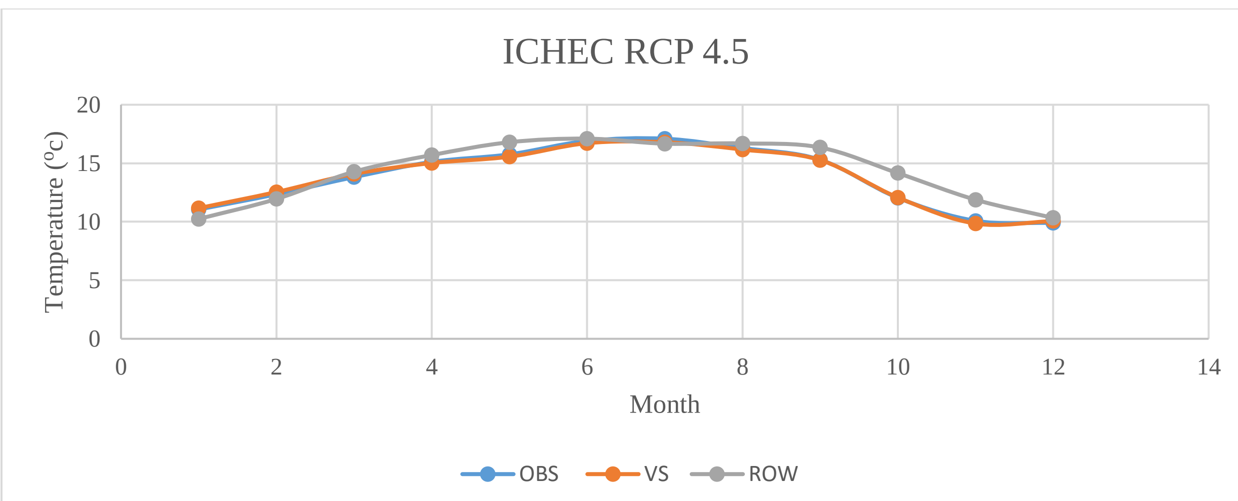

Figure 4.6: Observed (OBS), Variance Scaling (VS) Bias Corrected and Row Bias Uncorrected (ROW) Temperature Minimum Pattern of Mille Watershed

4.3 Statistical Trend Analysis of Historical Climate Variability

Trends were tested in terms of annual time series using the non-parametric Mann-Kendall trend test at significance level of 5%. According to Mann-Kendall trend test analysis, the positive and negative values of the S statistic indicates an upward and downward trend and the significance is rejected when absolute value of Z is less than tabulated Z =1.96 and the significance should be accepted (significant) when absolute value of Z is greater than 1.96 at significance level of 5%. The variation trends of annual precipitation, maximum and minimum temperature from 1986-2015 and also sediment yield of Mille watershed (1989-2002) are shown below. In the watershed, the annual precipitation and sediment yield shows insignificant decreasing trend and maximum and minimum temperature shows insignificant increasing trend during the considered historical time period.

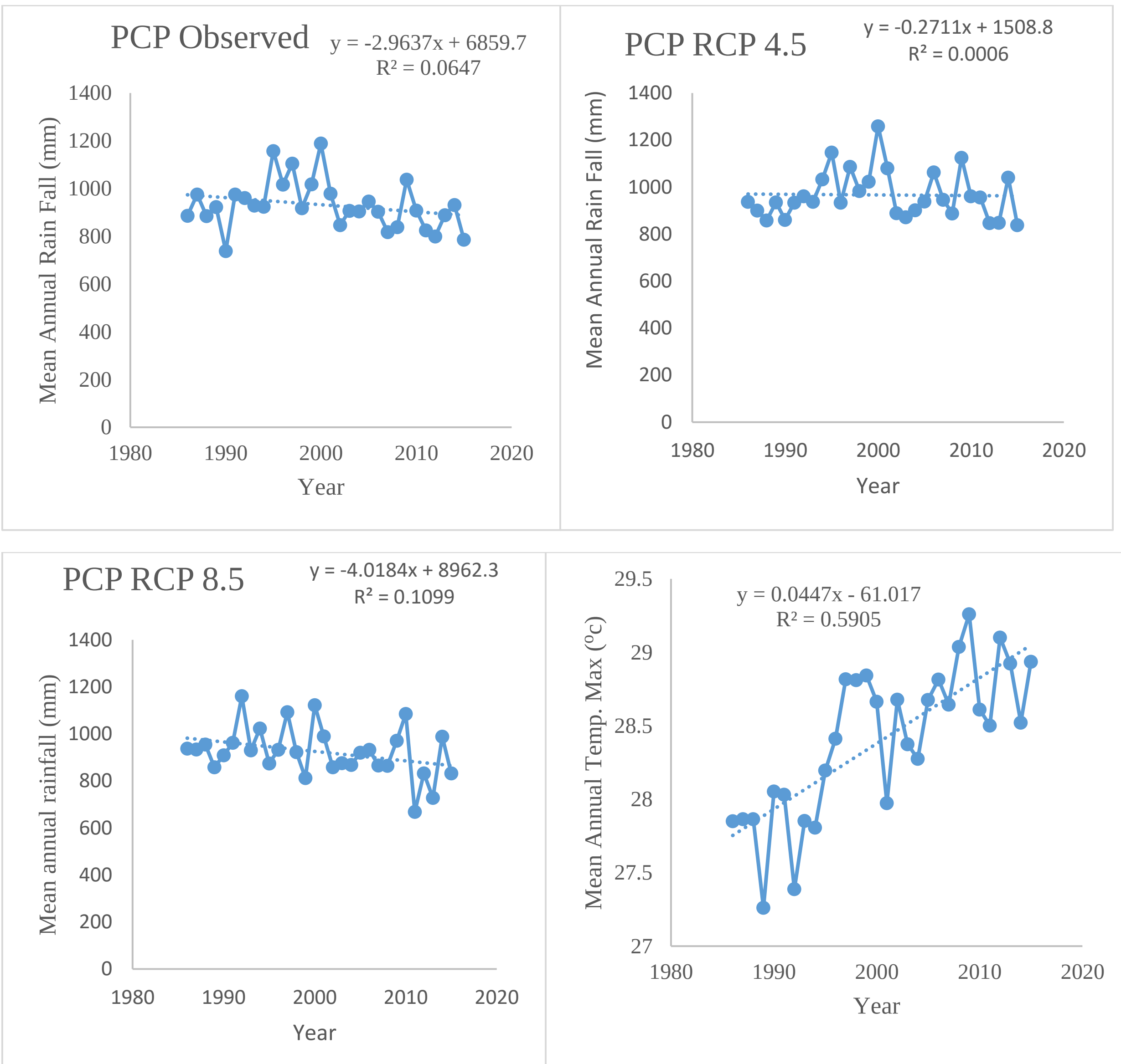

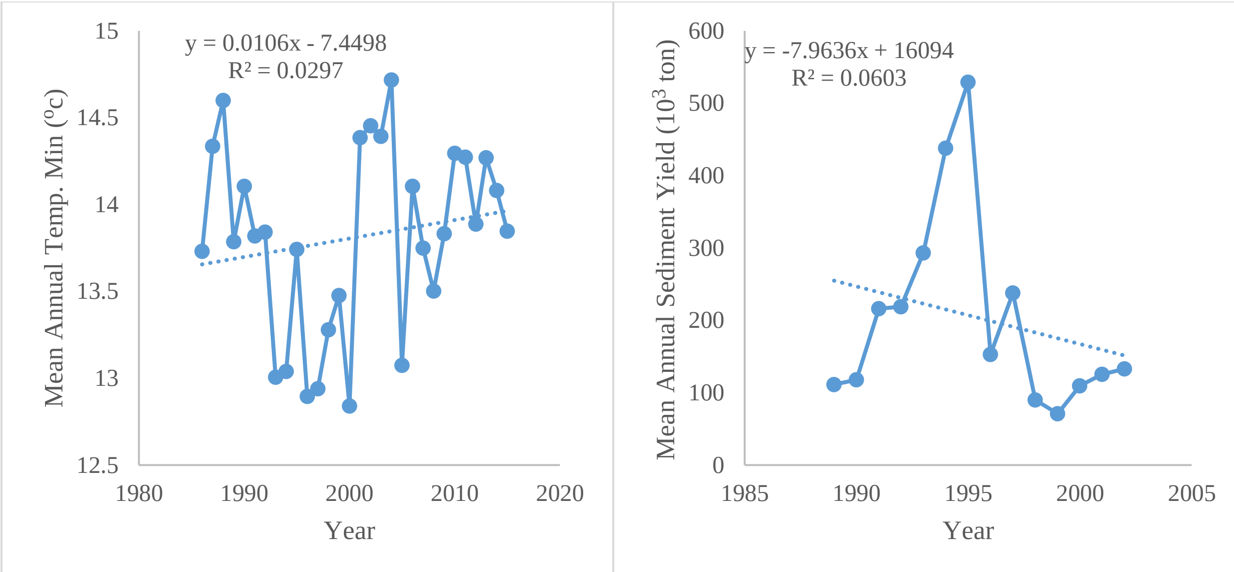

Figure 4.7: Historical Trend of Annual Precipitation, Maximum and Minimum Temperature and Sediment Yield.

Results of mean annual precipitation as well as maximum and minimum temperature were related to other researches performed in Ethiopia. Nura Boru Jilo, et al., (2019) conclude that the annual mean precipitation and sediment yield showed an insignificant decreasing trend for the period of 1971- 2000 over the Logiya watershed and also maximum and minimum temperature showed an insignificant increasing trend over the watershed for the same period of time. In addition (Atlas, (2015) reported a decreasing in precipitation and increasing temperature trend over the Afar region during 1981-2014.

4.4 Future Climate Projection

4.4.1 Projected Precipitation

The future climate data was projected using the selected climate model under RCP4.5 and RCP8.5 scenarios and two consecutive future period. This climate data arranged on average values of the two GCM/RCM climate model datasets of precipitation, maximum and minimum temperature in order to reduce errors resulted from obtaining climate data from a single climate model for impact assessment. Categorization of future time frame was made into two having 30 years of data ranges from (2031 to 2060) as 2050s which is considered as the near future time period and from (2061 to 2090) as 2070s as the far future time period. The projected future climate changes during near future and far future time frame were evaluated for both RCP4.5 and RCP8.5 scenarios in comparison with the base period (1986-2015).

The result of the study after bias corrections of raw precipitation sample showed that the mean annual precipitation in the future increases over Mille watershed (Figure 4.10). The change in mean annual precipitations for 2050s as +3.86% and for 2070s as 7.82% under RCP 4.5 climate scenario. The future precipitation increases with 4.61% and 10.57% in 2050s and 2070s respectively for RCP 8.5 climate scenario. The projected precipitation also shows increasing and decreasing monthly variation. For the month of February and April a 2.41% and 12.01% decrement observed during 2050s respectively, and an increment of precipitation ranging from 0.31% - 12.90% occurred under RCP4.5 climate scenario. August 2070s of RCP 8.5 has the Maximum increasing percentage value of 19.56% and the month November 2050s of RCP 4.5 shows the maximum decreasing value of -19.48%.

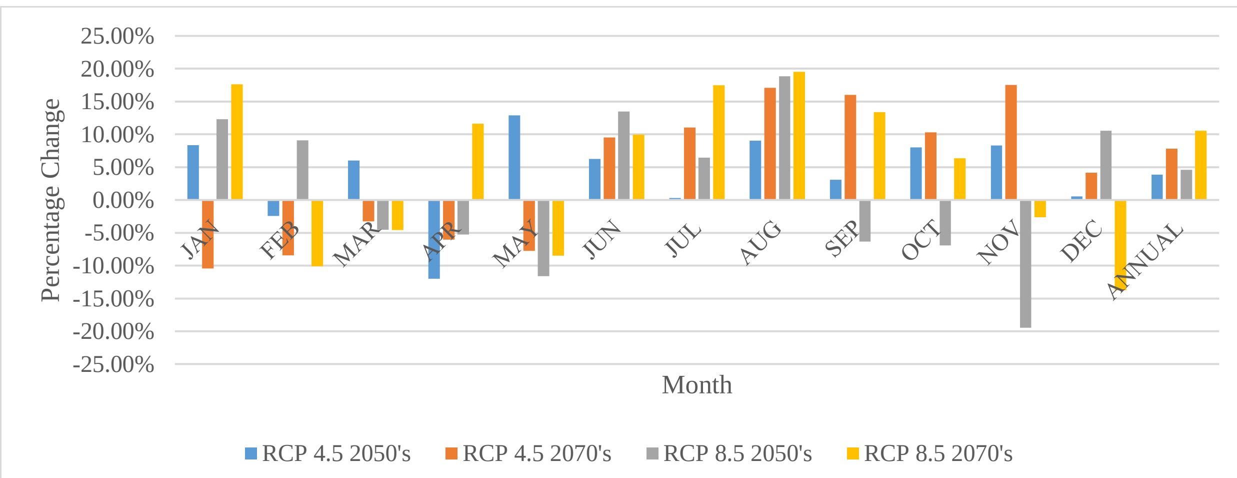

Figure 4.8: Mean Monthly and Annual Percentage Change of Precipitation

Table 4.4: Tabular Form of Mean Monthly and Annual Percentage Change of Precipitation

	JAN	FEB	MAR	APR	MAY	JUN	JUL	AUG	SEP	OCT	NOV	DEC	ANNUAL
RCP 4.5 2050's	8.37%	-2.41%	6.03%	-12.01%	12.90%	6.26%	0.31%	9.06%	3.07%	8.01%	8.32%	0.54%	3.86%
RCP 4.5 2070's	-10.41%	-8.44%	-3.26%	-6.05%	-7.73%	9.51%	11.06%	17.09%	16.04%	10.32%	17.54%	4.17%	7.82%
RCP 8.5 2050's	12.32%	9.09%	-4.52%	-5.26%	-11.58%	13.46%	6.45%	18.86%	-6.33%	-6.91%	-19.48%	10.56%	4.61%
RCP 8.5 2070's	17.62%	-10.11%	-4.58%	11.61%	-8.50%	9.97%	17.46%	19.56%	13.39%	6.33%	-2.64%	-13.77%	10.57%

At seasonal level the minor rainy season (February-May) of the watershed in most cases will experience a decreasing precipitation amount of -2.09% and -5.97% under RCP 4.5 of the 2050s and 2070s a decrement of 4.18% observed during 2050s of RCP 8.5 climate scenario respectively. Only a 1.78 percentage of increment observed for the minor rainy season of the watershed under RCP 8.5 of the 2070s. In all future time periods, *Kiremt* (wet) season (June–September) precipitation showed a percentage increment of +4.91% and +12.48% for RCP 4.5 of 2050s and 2070s and +8.44% to 14.50% for RCP 8.5 of 2050s and 2070s respectively. The *Bega* (dry) season (October- January) showed an increasing trend in all cases except the 2050s time period under RCP 8.5 climate scenario with a percentage change of -2.83%. Under RCP 4.5 the dry period of Mille watershed shows a 4.56% and 6.22% increment for the period of 2050s and 2070s respectively, and also a 2.29 percentage increment showed during the 2070s of RCP 8.5 and generally the dry season of Mille watershed shows more precipitation increment under RCP 4.5 climate scenario than RCP8.5 climate scenario and the revers situation for minor rainy season.

Generally according to this finding the minor rainy season of the watershed will experience a seasonal decrement of rainfall due to more decreasing trend on the month from February to May. Annual precipitation amount and a monthly consistent increasing detect for the month June, July, August and September, which shows the overall increment of precipitation amount for the future period over the Mille watershed.

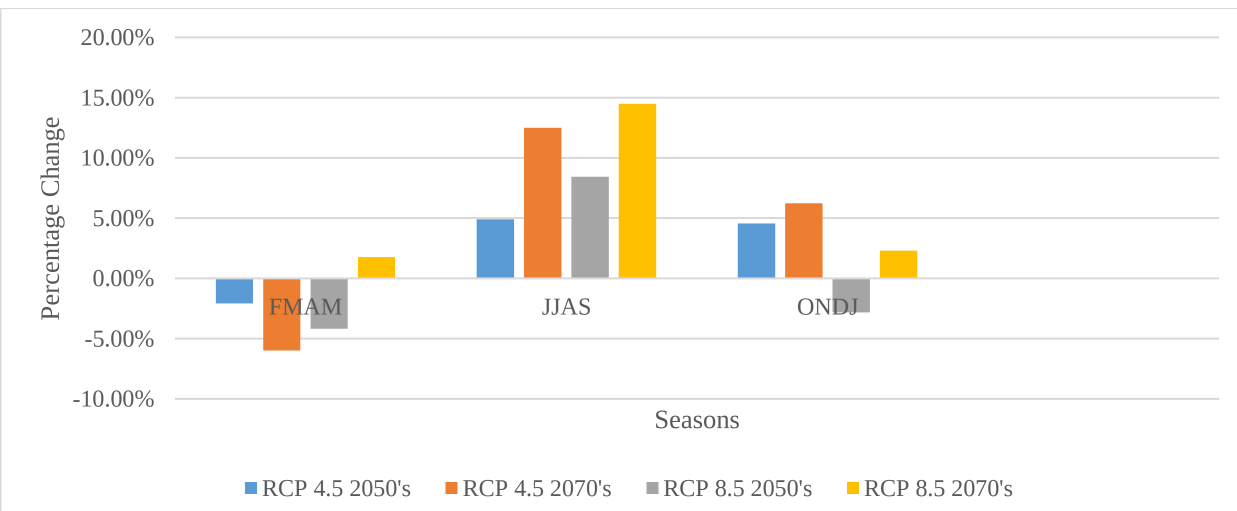

Figure 4.9: Seasonal Percentage Change of Precipitation

Table 4.5: Tabular Form of Seasonal Percentage Change

	FMAM	JJAS	ONDJ
RCP 4.5 2050's	-2.09%	4.91%	4.56%
RCP 4.5 2070's	-5.97%	12.48%	6.22%
RCP 8.5 2050's	-4.18%	8.44%	-2.83%
RCP 8.5 2070's	1.78%	14.50%	2.29%

4.4.2 Projected Temperature

In this study, the predicted temperatures in all months increases for both RCP scenarios. Under RCP 4.5, percentage changes in monthly maximum temperatures ranges from 10.61% to 16.35% with an annual average of 11.11% by the 2050s and from 8.84% to 19.48% with an annual average of 8.90% by the 2070s. For the RCP 8.5 climate scenario, the mean annual of 20.16% by the 2050s and 15.20% of increment observed in the period between 2061 to 2090 with a maximum increasing percentage value of 20.24% on the month March of 2050s.

The results also indicated that the percentage change monthly minimum temperature ranged from 2.75% to 16.94% for 2050s and from 6.71% to 24.06% for 2070s with mean annual of 9.55% and 14.50% under RCP 4.5 climate scenario respectively. On the other hand in RCP 8.5 scenario the minimum monthly temperature percentage change varies with a maximum value of 22.16% and 27.80% for 2050s and 2070s with an average annual of 13.13% for 2050's and 17.76% for 2070s under RCP 8.5 climate scenario. Figure 4.10 shows future percentage change of monthly mean temperature in both scenarios for all future time periods.

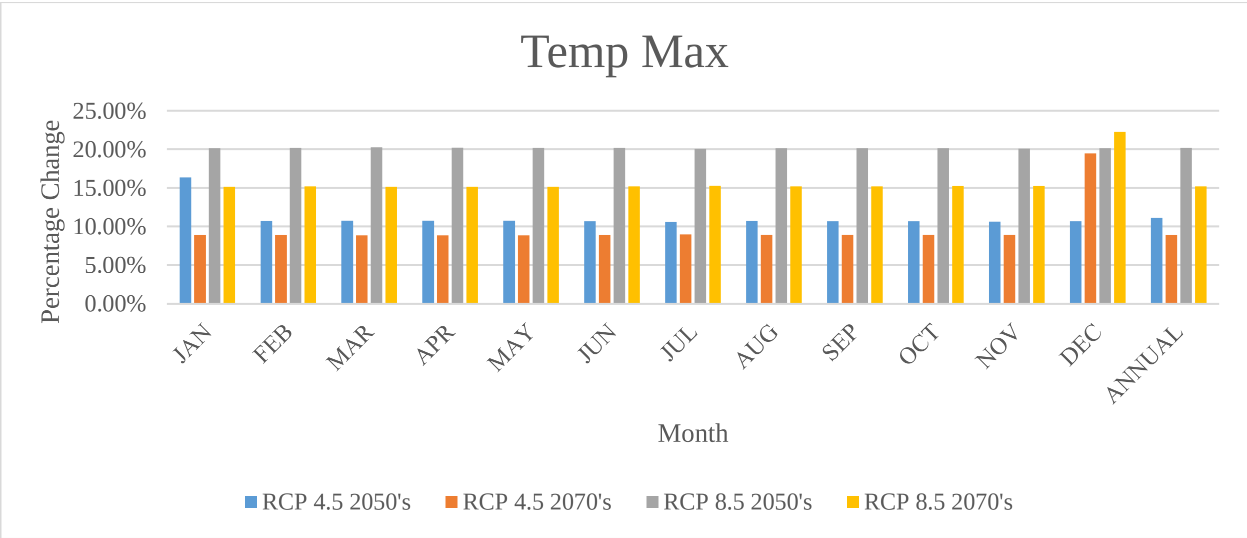

Figure 4.10: Mean Monthly and Annual Percentage Change of Temperature Maximum

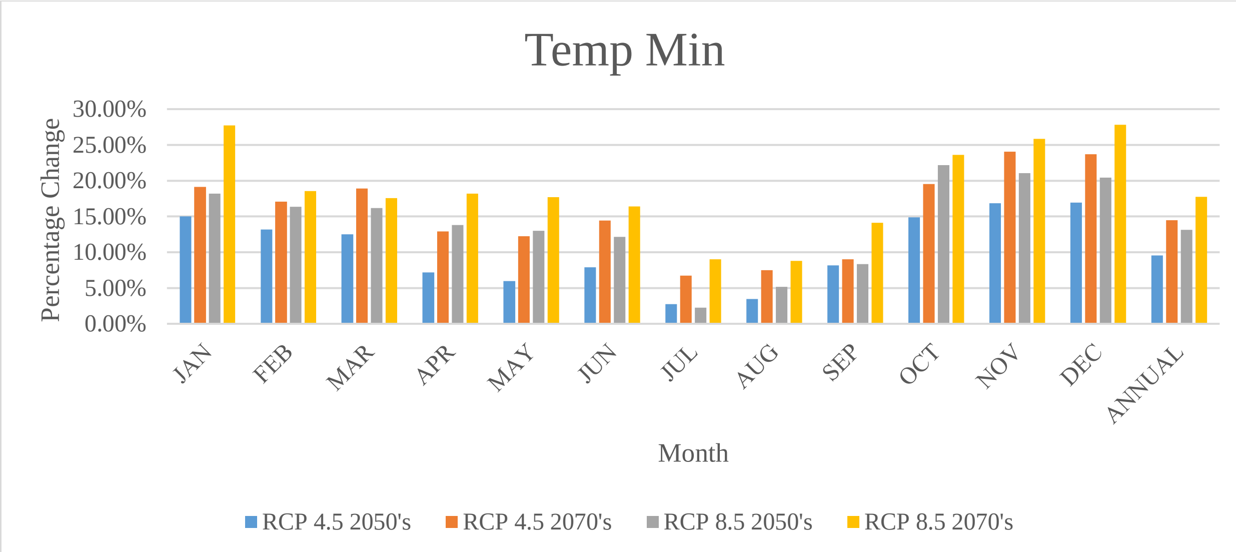

Figure 4.11: Mean Monthly and Annual Percentage Change of Temperature Minimum

According to the monthly temperature maximum basis percentage change, December month shows high increment on both RCP scenarios and all months will have a maximum increment for RCP 8.5 of the 2050s. The month January, October, November and December has maximum increasing percentage change than the other months during the two time frame and both RCP scenarios. The projected seasonal maximum and minimum temperature in the Mille watershed (Figure 4.10) indicated that a consistent increase in *Kiremt* (June-September), *Belg* (February-May) and *Bega* (October-January) in both scenarios for all time periods. Wet season of the watershed shows a maximum increment than the remaining two seasons and the dry period of the watershed exhibits the minimum seasonal increment of the maximum temperature. In contrary to this the dry period of the watershed shows the maximum incremental value for temperature minimum. Moreover, under CORDEX-Africa climate scenarios Mille watershed temperature projection RCP8.5 predicted higher temperature than that of RCP4.5.

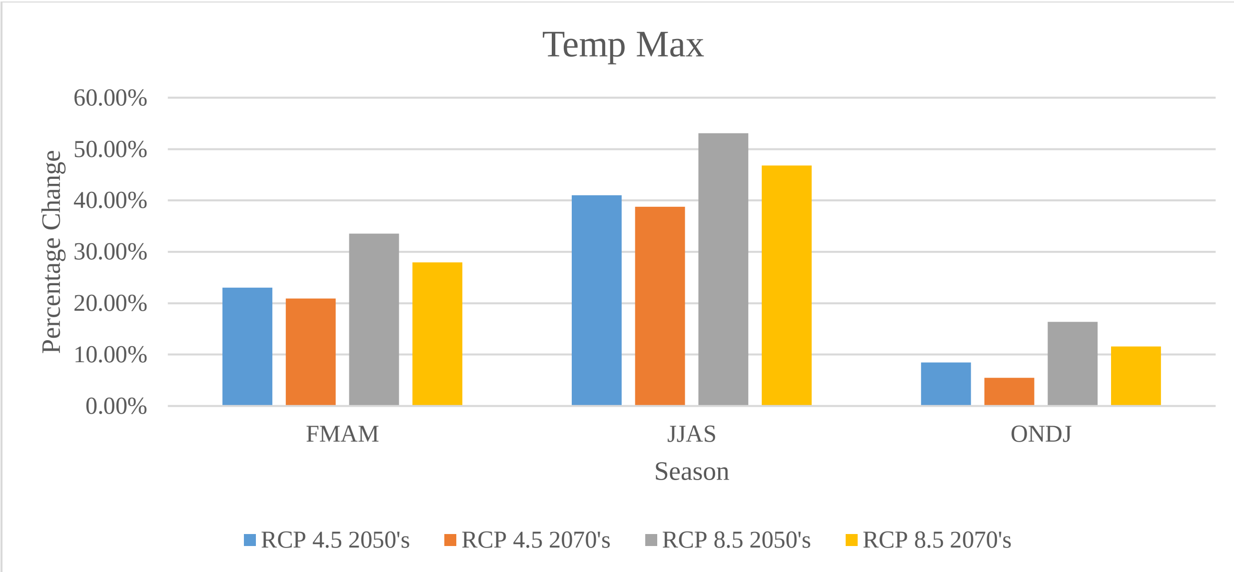

Figure 4.12: Seasonal Percentage Change of Temperature Maximum

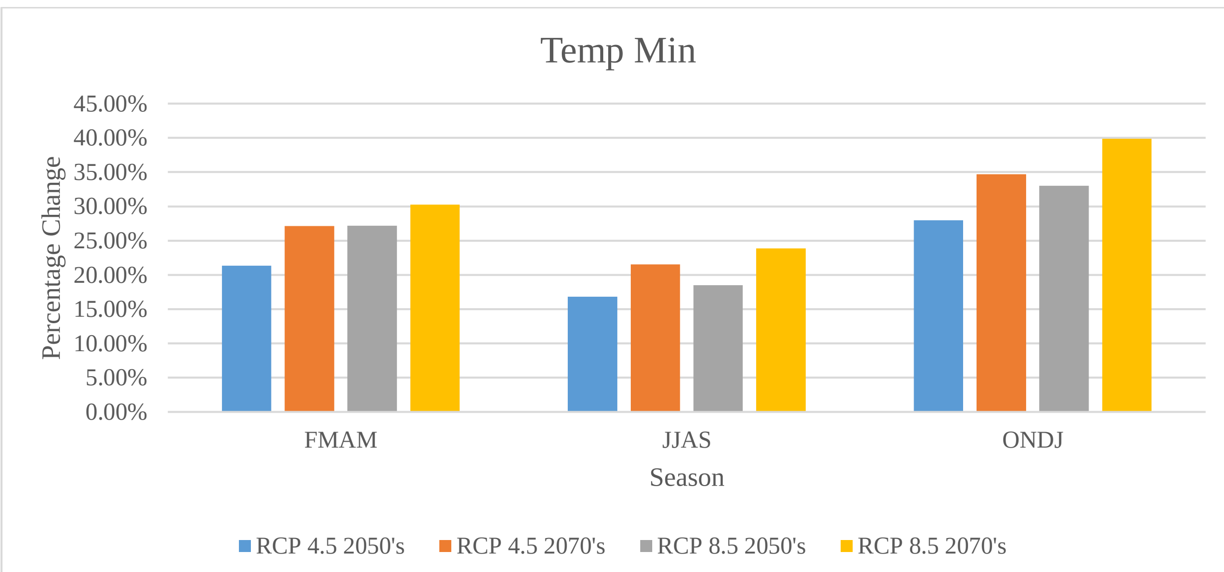

Figure 4.13: Seasonal Percentage Change of Temperature Maximum

4.5 Sensitive Parameters

The sensitivity analysis was done for flow and sediment separately since some parameters are sensitive to both flow and sediment, some sensitive to flow only and other sensitive to sediment only Abbaspour et al., (2007). Therefore, it was wise to test the sensitivity of the parameters for flow and sediment separately. Sensitivity analysis was carried out before calibrating the model to save time during calibration. Identifying sensitive parameters which affect the model output during calibration since SWAT model has a number of parameters to deal with some parameters do not have any influence on the model output while some may have little effect.

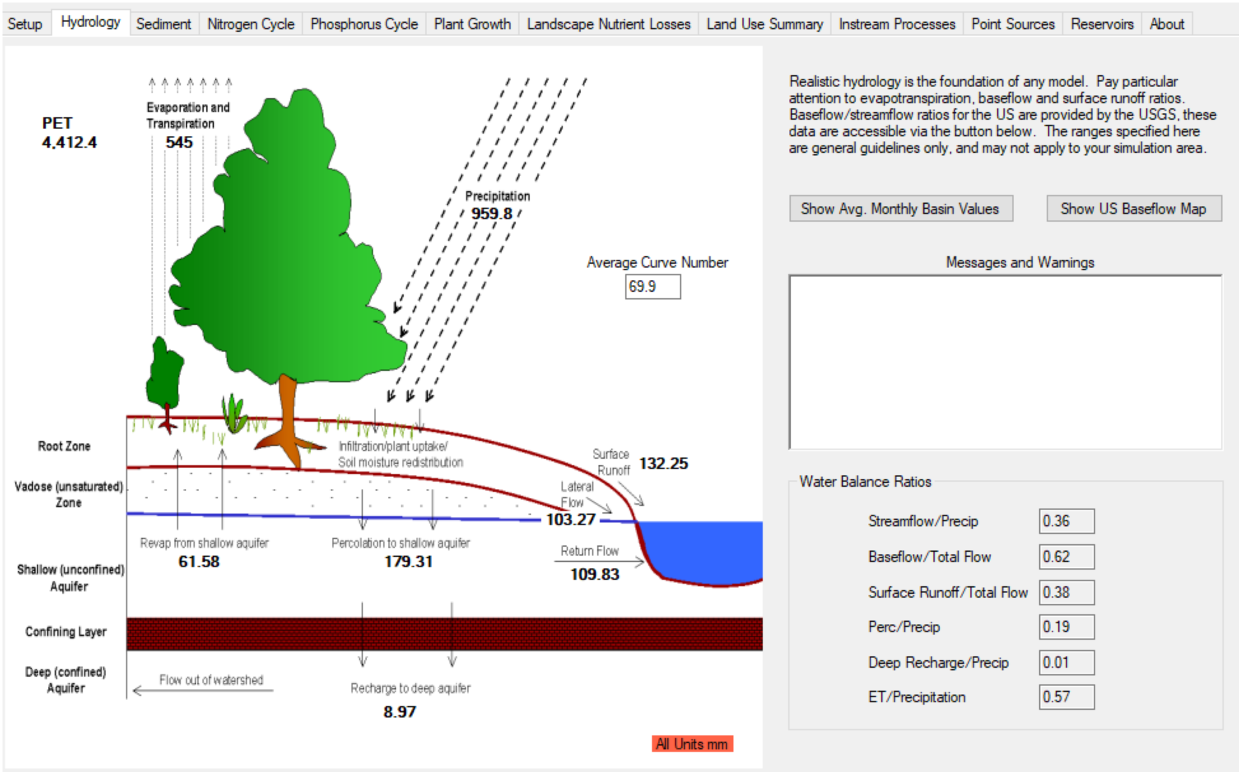

Figure 4.14: SWAT Checker Output

4.5.1 Parameters Sensitive to Flow

The 20 parameters listed in table 4.6 and figure 4.14 were used in sensitivity analysis. These parameters are used to calculate the amount of flow from the watershed. For calibration the monthly flow data from 1989 to 1997 were used.

Table 4.6: Sensitive Parameter for Flow

			Range				
No.	Parameters	Description of parameters	Min	Max	P-Value	t-Stat	Rank
1	CH_K2	Effective hydraulic conductivity in main channel alluvium	0.025	250	0.000	11.218	1
2	RCHARG_DP	Deep Aquifer percolation fraction	0	1	0.000	-8.351	2
3	CN2	SCS runoff curve no.	0	1	0.000	-6.783	3
4	SLSUBBSN	Average slope length	10	150	0.000	5.229	4

5	HRU_SLP	Average Slope Steepness	0	1	0.004	-2.938	5
6	SOL_AWC	Available water capacity of the soil layer	0	1	0.019	2.358	6
7	SURLAG	Surface runoff lag time	0.05	24	0.022	2.302	7
8	SOL_ALB	Moist Soil Albedo	0	0.25	0.055	1.929	8
9	CANMX	maximum canopy storage	0	100	0.073	1.799	9
10	REVAPMN	Threshold depth of water in "REVAP" shallow aquifer to occur	0	500	0.190	-1.313	10
11	EPCO	Plant uptake compensation factor	0	1	0.208	-1.262	11
12	ALPHA_BF	Base flow Alpha factor	0	1	0.284	1.073	12
13	GW_REVAP	Ground water "REVAP" co=efficient	0.02	0.2	0.287	1.067	13
14	LAT_TTIME	Lateral travel time	0	30	0.313	-1.010	14
15	ESCO	Soil evaporation Compensation factor	0	1	0.358	0.919	15
16	CH_N2	Manning co-efficient for main channel	0	1	0.616	0.503	16
17	GWQMN	threshold depth of water in the shallow aquifer required for return flow to occur	0	5000	0.744	-0.327	17
18	GW_DELAY	Ground water delay	0	500	0.788	0.269	18
19	OV_N	Manning "n" Value for over land flow	0.01	30	0.796	-0.258	19
20	SOL_BD	Moist bulk density	0.9	2.5	0.986	0.01	20

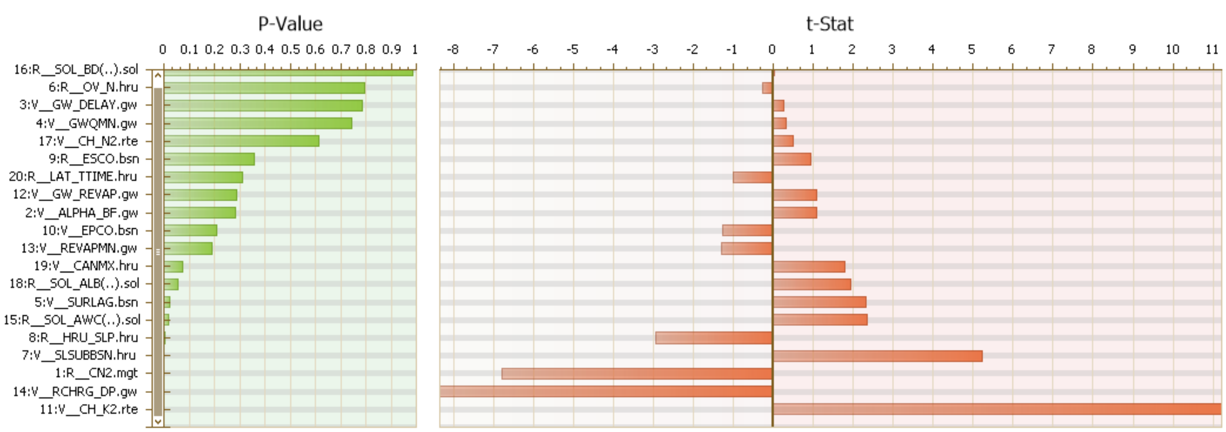

Figure 4.15: Global Sensitive Parameters for Flow

Among the 20 parameters used, Effective hydraulic conductivity in main channel alluvium (CH_K2), Deep Aquifer percolation fraction (RCHARG_DP), the SCS CN2, Average slope length (SLSUBBSN), Average Slope Steepness (HRU_SLP) and Available water capacity of the soil layer (SOL_AWC) are the highest sensitive parameters.

Table 4.7 List of flow sensitive parameters for flow and fitted values

No	Parameter Name	Fitted Value	Min Value	Max Value
1	CH_K2	2.846	-36.893	41.283
2	RCHARG_DP	0.289	0.152	0.471
3	CN2	-0.25	-0.259	-0.092
4	SLSUBBSN	21.380	20.519	28.725
5	HRU_SLP	0.229	-0.056	0.304
6	SOL_AWC	0.376	0.318	1.066

4.5.2 Parameters Sensitive to Sediment

The most sensitive parameters for erosion simulation were, the linear parameter for calculating the maximum amount of sediment that can be restrained during channel sediment routing (SPCON), average slope length (SLSUBBSN), soil available water capacity (SOL_AWC), sediment concentration in lateral flow and ground water flow (LAT_SED) and moist soil albedo (SOL_ALB).

Table 4.7: Sensitive Parameter for Sediment

			Range				
No.	Parameters	Description of parameters	Min	Max	P-Value	t-Stat	Rank
1	SPCON	Linear parameters for calculating the maximum amount of sediment that can be restored during channel sediment routing	0.0001	0.01	0.000	4.168	1
2	SLSUBBSN	average slope length	10	150	0.009	2.640	2

3	SOL_AWC	soil available water capacity	0	1	0.012	-2.519	3
4	LAT_SED	sediment concentration in lateral flow and ground water flow	0.44	1.32	0.029	2.189	4
5	SOL_ALB	moist soil albedo	0	0.25	0.037	2.091	5
6	RSDIN	initial residue cover	0.76	1.12	0.065	-1.852	6
7	SPEXP	Exponent parameters for calculating sediment retirement in channel sediment routing	1	1.5	0.175	1.359	7
8	BIOMIX	Biological mixing efficiency	-0.1	+0.1	0.185	-1.329	8
9	HRU_SLP	average slope steepness	0	1	0.309	-1.018	9
10	CH_COV2	channel cover factor	0.097	0.11	0.415	0.816	10
11	CH_ERODMO	channel erodability factor	0	1	0.473	0.719	11
12	USLE_P	USLE support practice factor	0	1	0.495	-0.683	12
13	CN2	SCS runoff curve no.	-0.25	0.25	0.560	-0.583	13
14	SED_CON	sediment concentration in runoff after urban BMP is applied	252.2	340	0.643	-0.464	14
15	CH_N2	base flow alpha factor for bank of storage	-0.16	0.16	0.699	0.387	15
16	USLE_K	USLE soil erodabilty factor	0	0.01	0.726	-0.357	16
17	CH_BED_BD	channel bed bulk density	0.9	2.5	0.975	0.031	17

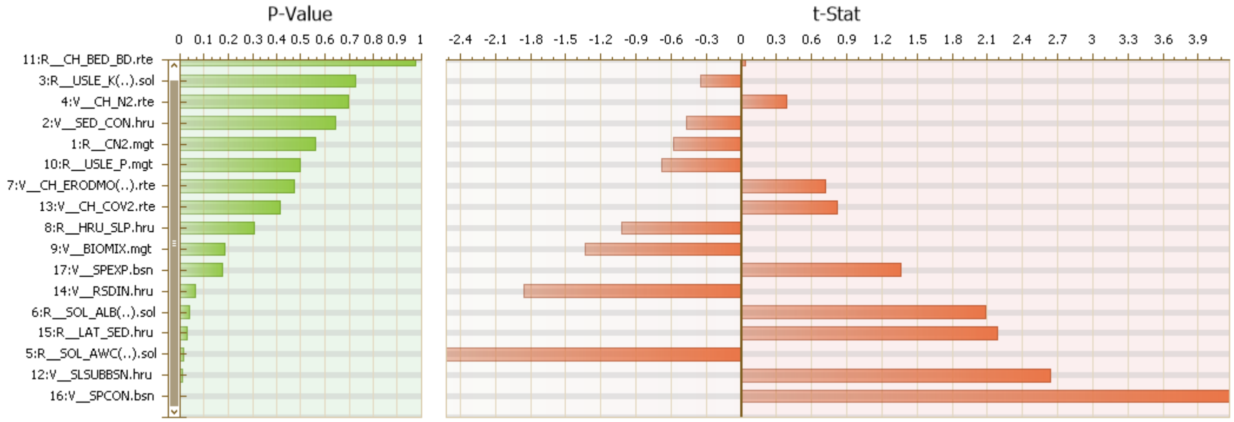

Figure 4.16: Global Sensitive Parameters for Sediment

Other parameters including in the table below were also affecting the soil erosion simulation from the catchment from upland and from channel. The parameters that were used to evaluate the sensitivity to sediment are shown into see which parameters are sensitive to sediment based on their P value and t-Stat.

Table 4.7 List of flow sensitive parameters for sediment and fitted values

No.	Parameters	Fitted Value	Min Value	Max Value
1	SPCON	0.001	0.000	0.002
2	SLSUBSN	81.669	50.537	88.580
3	SOL_AWC	0.637	0.422	0.691
4	LAT_SED	0.842	0.597	1.086
5	SOL_ALB	0.170	0.111	0.177

4.6 Model Calibration and Validation

4.6.1 Flow Calibration

SWAT 2012 model was calibrated and validated using measured stream flow data from Mille near Mille village gauge station. The flow data of Mille watershed was included from the period January 1989 to December 2002. From those stream flow data tow-third was used for calibration purpose and one-third of data used for validation purpose. The calibration period was contain from January 1989 to December 1997, which was nine years and the validation period carried out five years from January 1998 to December 2002. The overall performance of the model during calibration has been measured coefficient of determination (R^2) and Nash Efficiency (NS) value as 0.68 and 0.54 respectively. Figure 4.16 shows below the observed and simulated values after SWAT CUP calibration process.

Table 4.8: Simulated and Observed Mean Monthly flow Calibration

Time	Average Flow (m^3/sec)		Model efficiency	
Jan 1989-Dec 1997	Simulated	Observed	R2	NS
	8.05	11.45	0.68	0.54

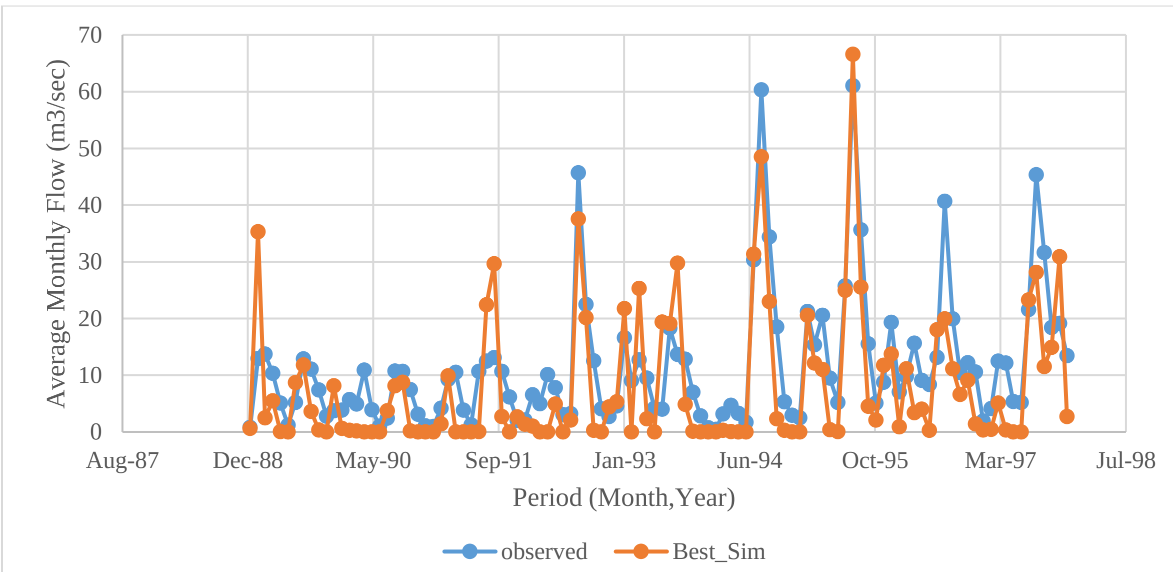

Figure 4.17: Observed and Simulated Monthly Flow for Calibration

As shown in the fig the model over estimate the peak events of the month during the period of 1996 and 1999 where as underestimates during the period of 1997,1998 and 2000. This variation can arise because of weather data quality used as input in the model or guaged flow used for calibration. In addition to this some guaging station do have missing cliamte data, which were left to be filled by the weateh generator. However the overall flow trend for Mille watershed is well simulated by the Arc-SWAT model.

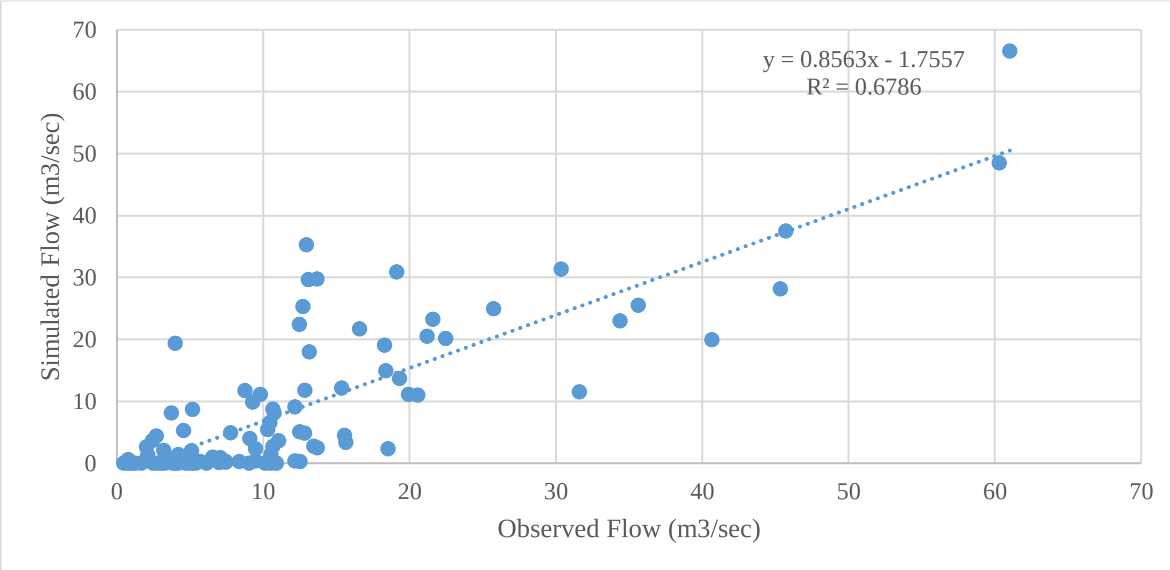

Figure 4.18: Fitted Line Between Observed and Simulated Stream Flow for Calibration.

4.6.2 Flow Validation

Model validation results is necessary to increase user confidence. It involves re-running the model using the input data and without any adjustment of calibration parameters at different time period. Therefore, for this study the model validation carried out using five years monthly flow from January 1998 to December 2002. Figure 4.18 shows below the observed and simulated values after SWAT CUP validation process. the out come of validation shows a performance evaluation of statstical measures between simulated and observed flow based on monthly time scale with coefficent of determination (R2) of 0.75, Nash Stucliff efficiency (NS) of 0.6.

Table 4.9: Simulated and Observed Mean Monthly Flow Validation

Time	Average Flow (m^3/sec)		Model efficency	
Jan 1998-Dec 2002	Simulated	Observed	R2	NS
	15.63	14.00	0.75	0.6

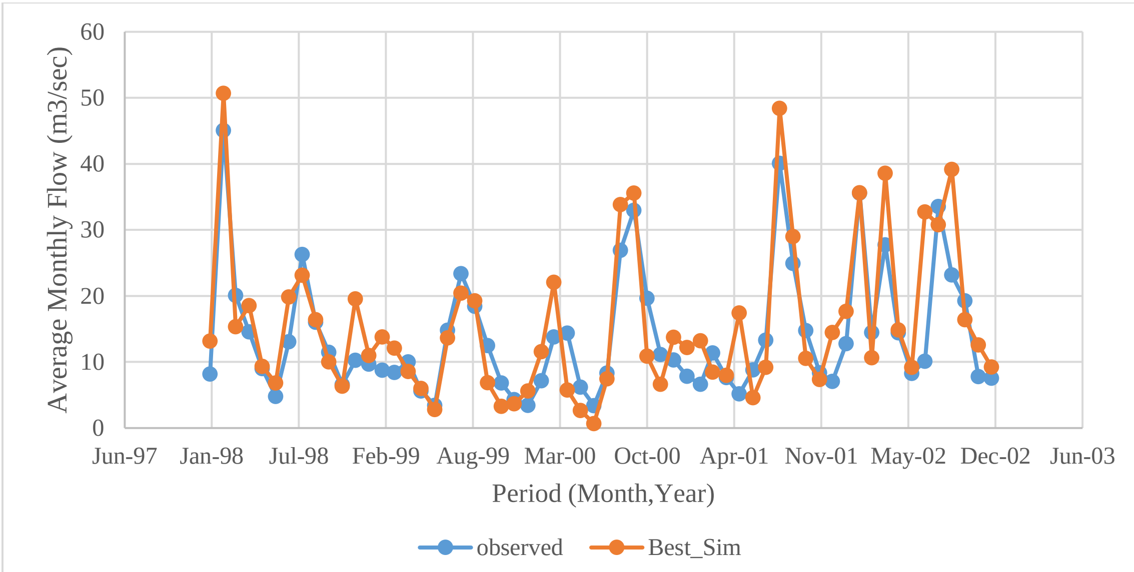

Figure 4.19: Observed and Simulated Monthly Flow for Calibration

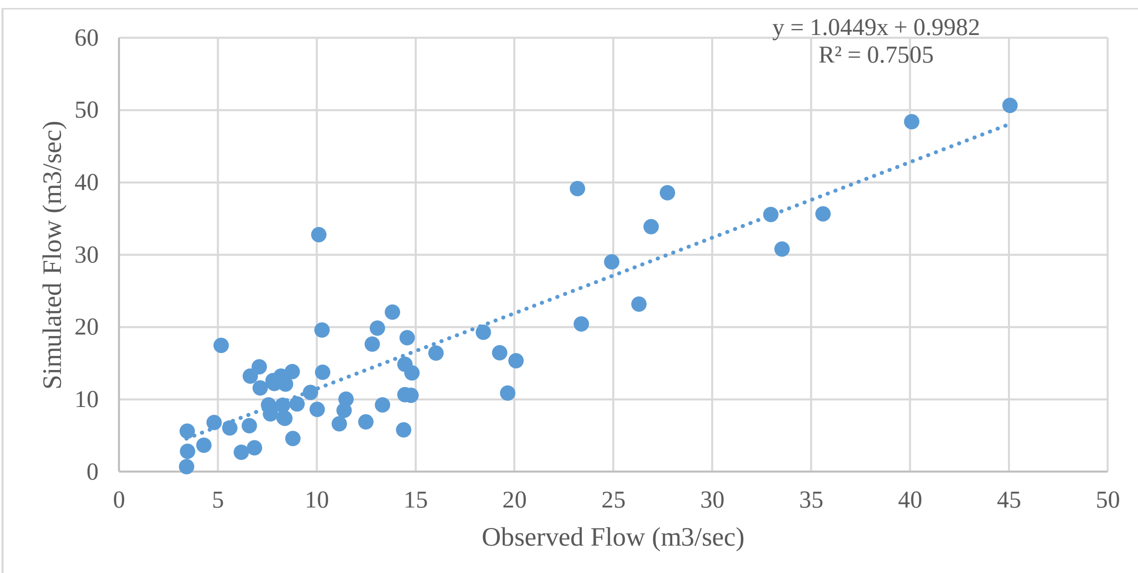

Figure 4.20: Fitted Line Between Observed and Simulated Stream Flow for Calibration.

4.6.3 Sediment Calibration

SWAT model were calibrated for monthly sediment yield where after calibration and valiadation of stream flow. The observed sediemnt data also collected from Mille near Mille Guage station and due to the short recored and missed values sediment rating curve was generated and the data for calibration and validation of sediment from SWAT model was arranged. The model was comparing observed and simulated sediment for the calibration period of 1989 to 1997.the SWAT model perfromace evaluation for the calibration of sediment for the Mille watershed based on the statstical parameter of coeffecient of determination (R^2) with a value of 0.81, Nash Stucliff efficiency (NS) of 0.81. the graphical comparison of measured and simulated sediment yield shown in figure 4.20.

Table 4.10: Simulated and Observed Mean Monthly Sediment Calibration

Time	Average sediment (ton)		Model efficency	
Jan 1989-Dec 1997	Simulated	Observed	R2	NS
	270050.84	257166.2	0.81	0.81

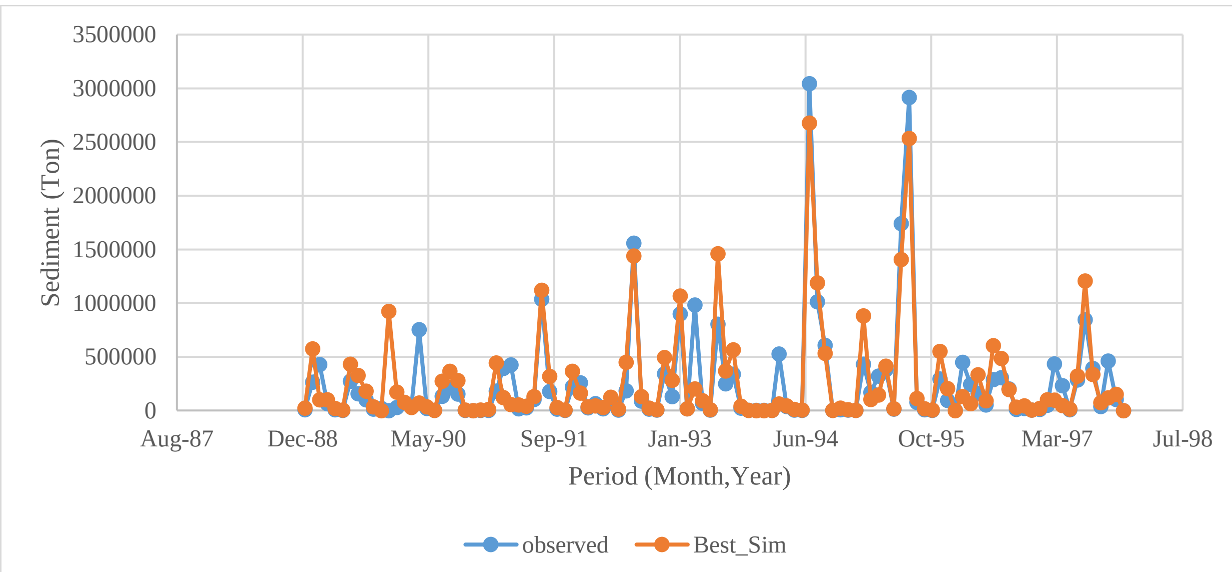

Figure 4.21: Observed and Simulated Monthly Sediment for Calibration

As shown in the above figure the SWAT model shows some over estimation and under estimation during different months and years. In the year 1993 and 1994 and both over estimation and under estimation of sediment yield occurred at sifferent month. In addition for year 1989 and 1997 the model simulate some what slight higer values and during 1990 some under estimated values simulated. In general SWAT shows a better result during calibration of sedimemt.

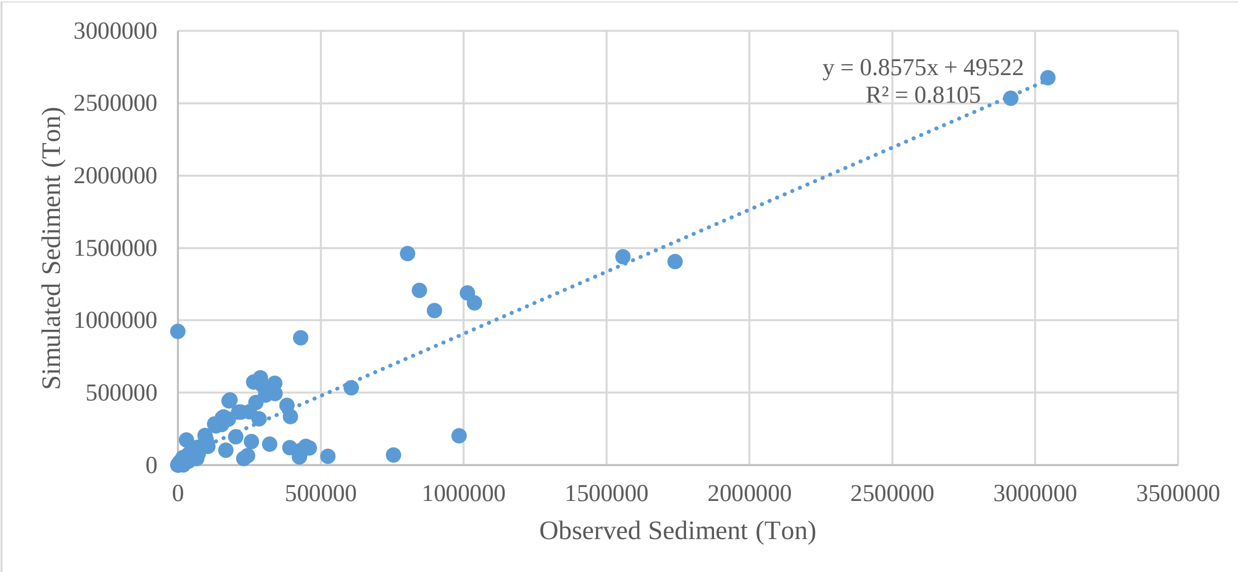

Figure 4.22: Fitted Line Between Observed and Simulated Stream Sediment for Calibration.

4.6.4 Sediment Validation

SWAT model monthly sediment validation was done after sediment calibartion without further parameter adjustment. Model validtaion was performed for the consequative five years starting from January 1998 to December 2002. The correlation coefficent (R^2) is 0.80, Nash Sutcliffe Effciency (NS) is 0.79. Those values shows that a god agreement between obsreved and simulated sediment.figure 4.9 and 4.10 shows the model monthly observed and simulated for validation and the fitted line of observed and simulated sediment for validation period respectively.

Table 4.11: Simulated and Observed Mean Monthly Sediment Validation

Time	Average sediment (ton)		Model efficency	
Jan 1998-Dec 2002	Simulated	Observed	R2	NS
	113819.72	105722.1	0.80	0.79

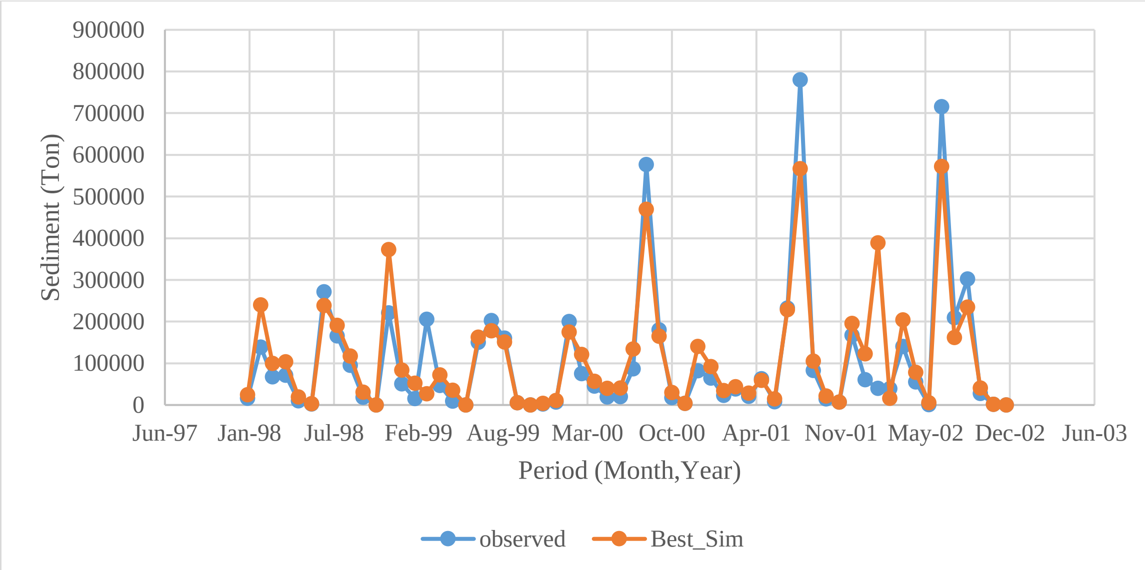

Figure 4.23: Observed and Simulated Monthly Sediment for Validation

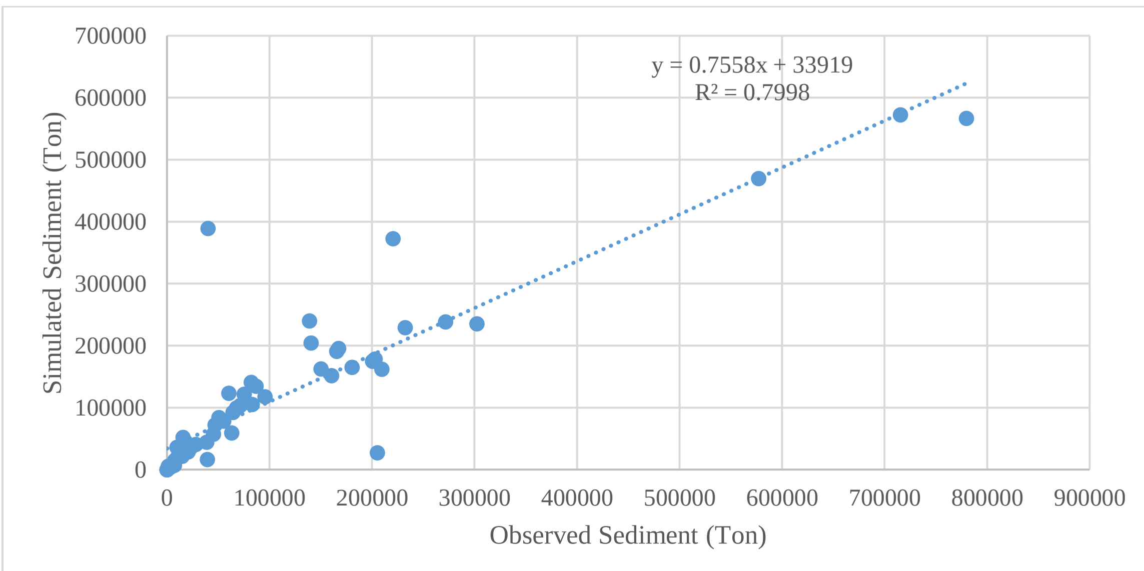

Figure 4.24: Fitted Line Between Observed and Simulated Stream Sediment for Validation

According to this finding, it was found that the average annual basin values of total sediment loading was about 2,436,948.48 ton/year for Mille watershed. the total watershed area delinated is 4640.43 km^2 . therefore, the annual specific sediemnt yield from the watershed can be calculated as the total sediemnt yield divided by the area of the watershed which equals to 525.16 $ton/km^2/year$ for the base period time.

Based on the report sediemnt measures and control of the Awash basin Halcrow., (2006), different watersheds were investigated on their sediemnt source, amount and their impacts on different hydraulic structures along the river. Mille river also one of the river watershed under the investigation and they resulted an amunt of 480 ton/km^2/year sediemnt yield and has a direct impact/ deposition on the Tendaho reservoir.

Estimation of sediment yield at Chacha dam reservoir of the upper Abbay sub-bsin using sediment rating curve output resluted that a 144.28 ton/km^2/year from the watershed area of 577.5 km^2 Weldetensay S. (2019). According to Mengistu, (2017) the Gelena catchment annual sediemnt yield was estimated as 89.14 ton/km^2/year form the catchment area of 644.28 km^2. In addition to this Tufa, (2016) estimate the estimate 106.178ton/km^2/year average annual sediemnt yield of Gibe-I reservoir having area coverage of 3602km^2.

4.7 Impact of Climate Change on Sediment Yield

SWAT successfully simulate monthly streamflow and sediment yield with a reasonable accuracy. Hence, the calibrated and validated SWAT model forced to run for historical and future climate scenarios to generate future flow in streams and sediment yield for both RCP4.5 and RCP8.5 climate scenarios to assess the impact of climate change. The effect of climate change on annual, monthly and seasonal sediment yield was also investigated as a percentage change with respect to the baseline period (1989–2002) under the two scenarios and two time periods of 2050s (2031–2060), and 2070s (2061–2090).

For all future time periods, both climate scenarios produced a moderate increase in mean annual sediment yield which is due to projected increase in future precipitation. Under RCP4.5, the mean annual percentage change of sediment yield will increase by 5.85% and 10.11% in the 2050s and 2070s, respectively. Similarly, for RCP8.5, the mean annual percentage change of sediment yield increases to 8.99% and 14.25% in the 2050s and 2070s, respectively.

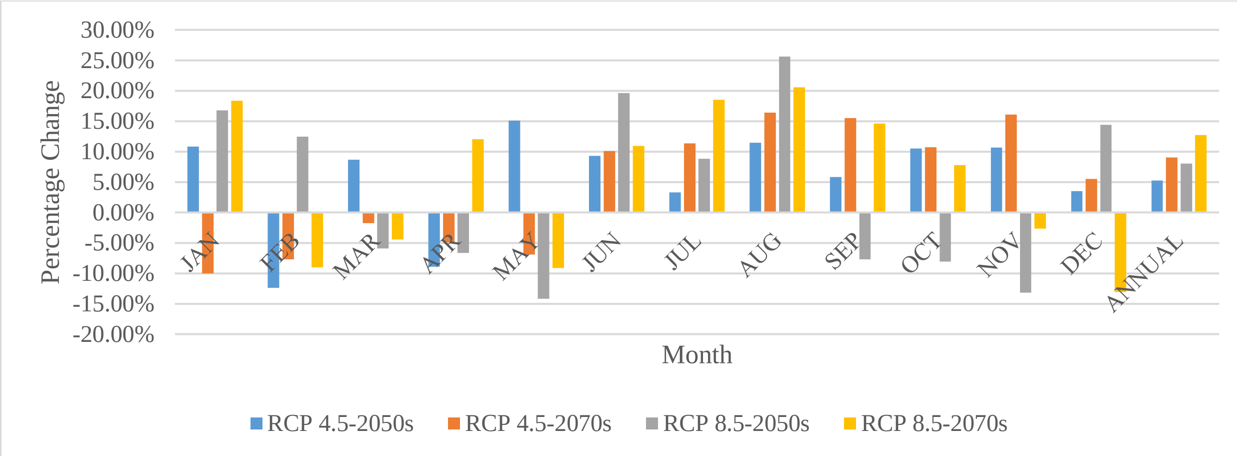

Figure 4.25: Mean Monthly and Mean Annual Percentage Change of Sediment Yield

The monthly sediment yielded from SWAT simulation using the future projected climate data shows a decrease and increase trend over the watershed. March and May months yield sediment having a percentage change of 8.67% and 15.11% more from the reference period only during the 2050s of RCP 4.5, in contrary to this months of September and October during the 2050s of RCP 8.5 showed exceptional decrement on the amount of sediment with a value of -7.68% and -8.09%. For all time frame the month June, July and August have an increased value sediment yield ranging from 3.29% to 11.44% under RCP 4.5 and from 10.10% to 16.40% for RCP 8.5. Mean annual stream flows were predicted to increase by 2.84% and 5.27% for RCP 4.5 in 2050s and the 2070s, respectively. For the RCP 8.5 scenario the model showed an increase of 3.91% by 2050s and 9.45% by 2060s. This implied that sediment yield at the outlet of the watershed was influenced by streamflow. In general the month February, March, April and May generate a decreased amount of sediment which also lead to a decreased sediment yield of the minor rainy season sediment amount and the moths of major rainy season shows a consistent sediment yield increment. Other months of the year has a mixed increasing and decreasing trend on sediment generation over the watershed and The results indicated that precipitation and sediment yield had strong relationship and this agreed with the previous findings Azim F. et al., (2006) Mullan D. et al., (2013) and Cousino L. K. et al., (2015). Overall, both RCP scenarios showed fairly similar patterns of increment in projected monthly precipitation, streamflow and sediment yield in a fair amount in the study area. Similar results were reported by Shrestha B. et al., (2013) Adem A. et al., (2015) and Azari M. et al., (2016) all of whom showed increasing streamflow proportional to increasing sediment yield. Figure 4.24 displays the projected mean monthly sediment yield at the out let of the Mille watershed under all RCP scenarios.

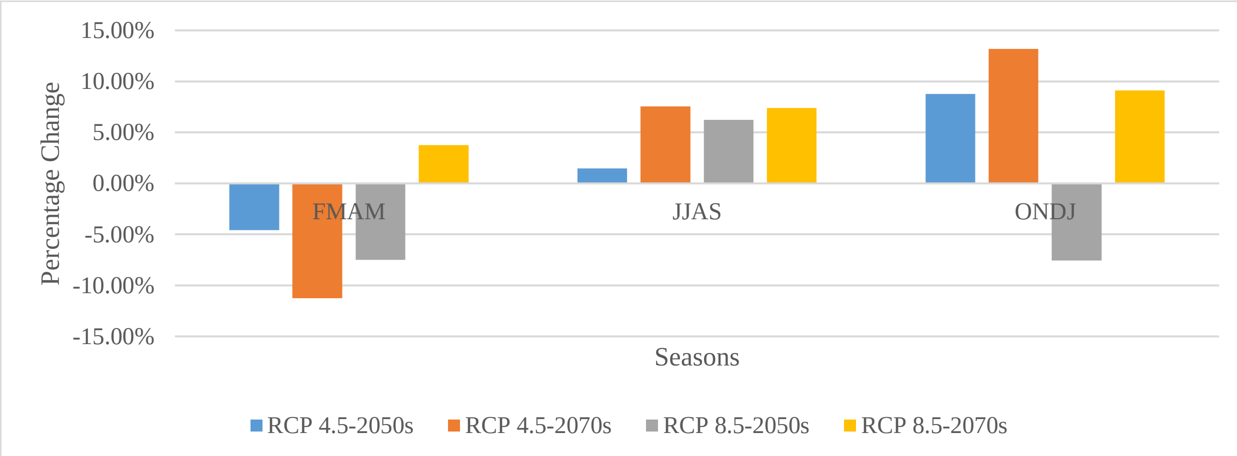

Figure 4.26: Seasonal Percentage Change of Sediment Yield

Seasonal projection shows a mixed increasing and decreasing trend for minor rainy season and dry period of the watershed. Season of the 2070s having a month combination February, March, April and May only shows an increasing trend of sediment yield over the watershed with a percentage change of 3.74 under RCP 8.5 climate scenario and the 2050s and 2070s of RCP 4.5 and also the 2050s of RCP8.5 shows a decrement over the Mille watershed in terms of sediment generation. Dry period of the 2050s, 2070 of RCP 4.5 and 2070s of RCP 8.5 on the other hand increases and the 2050s of RCP 8.5 only generate less amount of sediment with a value of 5.57% than the base period yielded. Kiremt which is the main rainy season of the shows an increase trend over the watershed during the two time frame and both RCP scenarios with a value of 1.46% and 7.54% under RCP 4.5 as well as 6.24% and 7.38% of increment under RCP8.5 of the 2050s and 2070s respectively.

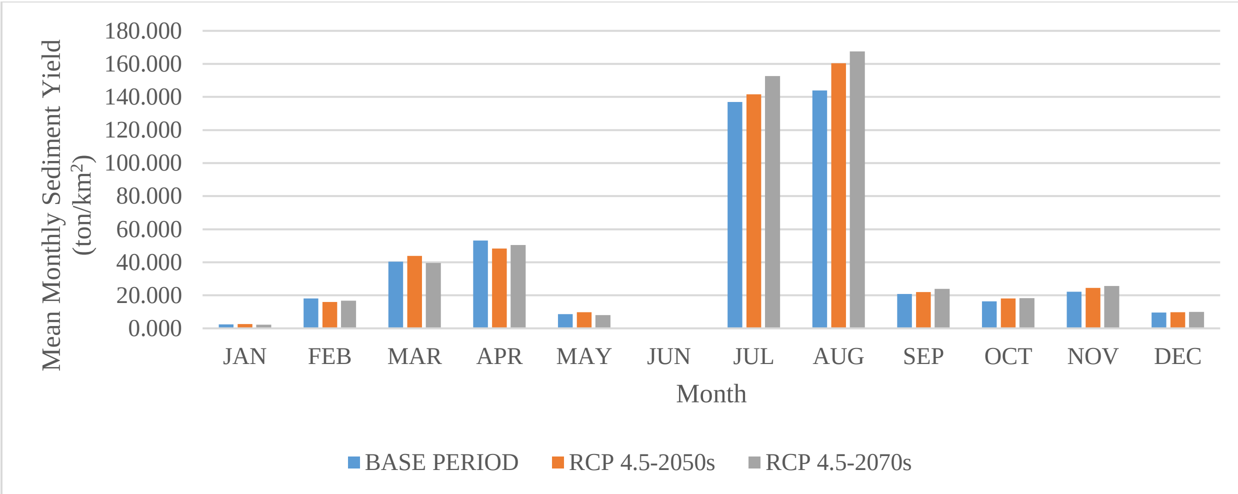

Figure 4.27: Mean Monthly Sediment Yield of the 2050s and 2070s under RCP 4.5 Climate Scenario

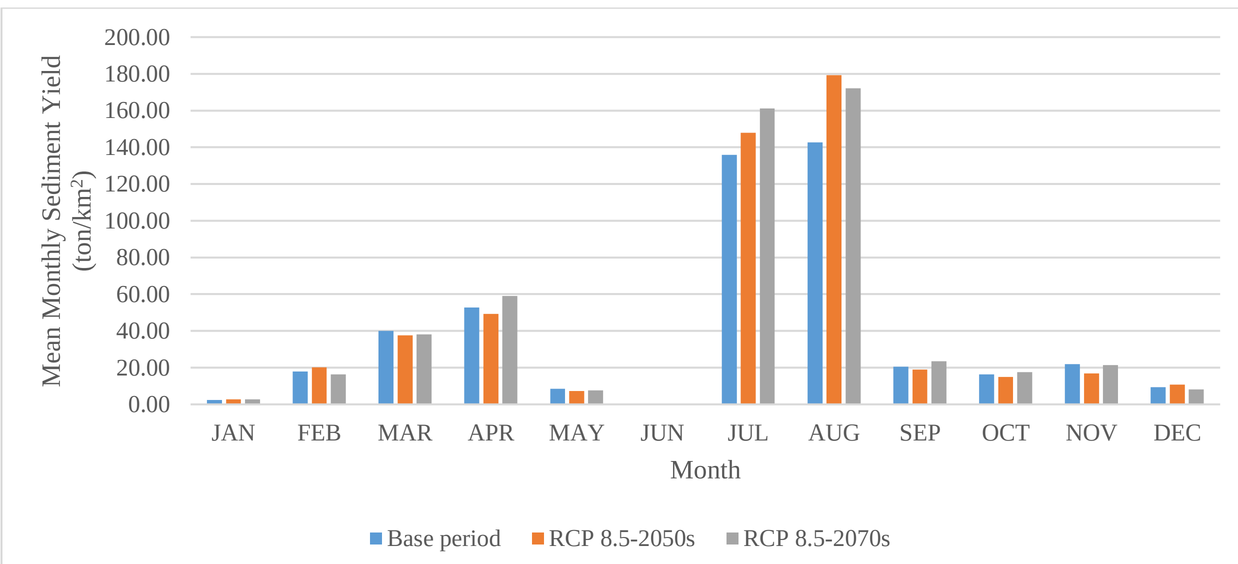

Figure 4.28: Mean Monthly Sediment Yield of the 2050s and 2070s under RCP 8.5 Climate Scenario

4.8 Spatial Variation of Sediment Yield under Different Climate Scenarios

It was found that the swat model is advantageous in providing quantitative estimation of soil loss and sediment yield and their spatial variation in different sub-watershed by considering HRU. This results plays a critical role for detailed understanding evaluation of the amount of sediment yield as well as for designing an appropriate management scenario at each sub-watershed. The spatially distributed sediment yield in each sub-watershed under different climate scenarios is demonstrated in figure 4.28 and 4.29. During the observed period, the rate of sediment yield ranged from 0.23 t/ha to 50.92 t/ha, which corresponds to the sub-basin 2 and 6 of the Mille watershed, respectively.

Besides, the projected sediment yield estimated under both RCP 4.5 and RCP 8.5 scenarios showed the spatial variation across the watershed. Severally eroded areas were situated at upper, middle and lower parts of the study area. For RCP 4.5, by the 2050s and the 2070s annual average sediment yield ranging from 0.14 t/ha to 51.13t/ha and 0.778 t/ha to 51.56 t/ha respectively and for RCP 8.5 the mean annual sediment yield from each sub-basin varies from 0.776 t/ha to 51.36 t/ha and 0.814 t/ha to 51.89 t/ha respectively, in both time serious data. In the case of the Mille watershed one third (34 % percent of the study area) of the observed soil loss rate was above the tolerable erosion limit suggested by Hurni et al., (1985) for various agro climactic zones of Ethiopia, ranging from 2 t/ha/yr to 18 t/ha/yr. Based on these, classes were assigned depending on their annual average sediment yield loading per coverage.

Table 4.12 class of tolerable soil loss level Hurni (1985).

Class	**Sediment Yld (ton/ha/yr.)**	**Remarks**
1	0-6	Low
2	6-12	moderate
3	12-18	High
4	Above 18	Severe

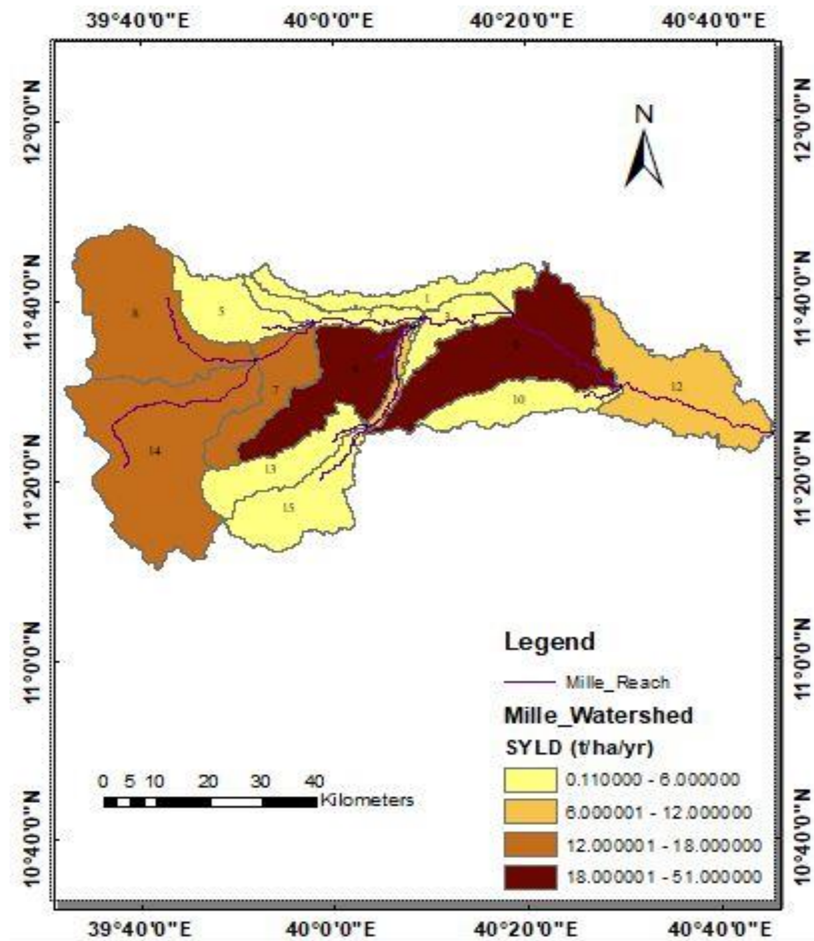

Figure 4.29: Spatial Variation Map of Base Period Sediment Yield

The average sediment yield of Mille river watershed under this particular study generate 12.446 ton of sediment per hectare during the reference period of the simulation. Modelling of runoff and sediment yield were undertaken for Kessem watershed, Middle Awash sub-basin in order to determine the sediment yield of the watershed Tesfu. A and Bogale G. et al., (2019). Based on the study on Kessem watershed has 11.43 ton/ha average watershed sediment yield. In addition to this sediment source evaluation section of the Halcrow sediment source and control measures report Halcrow ., (2006) using both sediment discharge relation and USLE prediction shows similar resulted which is 11.56 ton/ha of sediment yield over the Mille watershed. Therefore this study has an agreement with other findings which was performed with in and out of the watershed.

Table 4.13: Sub-Basins Base Period Sediment Yield

Sub-Basin	Sediment Load (ton/ha)	Sub-Basin	Sediment Load (ton/ha)
1	0.588	9	27.83
2	0.23	10	2.74
3	0.35	11	14.553
4	4.137	12	9.84
5	2.667	13	5.34
6	50.92	14	13.87
7	18.133	15	1.77
8	17.43		

In addition, the results indicate that more sever erosion occurred in the middle and upper parts so the watershed. This shows the soil erosion was serious phenomenon in the different sub-basins in the study area during observed and projected time serious. During the observed time period the maximum sediment load occurred in sub-basin 6 and during the projected time serious the maximum sediment load generated from sub-basin 6, 8 and 9 under the two RCP climate scenarios and both time frame and also some sub-basins showed some increment in sediment yield from time to time and such impacts occurred due to the increase in precipitation amount in combination with the land use land cover change, soil and slope combination of the sub-basins. For all time period the dominant LULC class of the sub-basins 6 and 9 was bare land and Eutric Regosols also cover most of the area with in sub-basin 8 and 9. This indicate that the LULC and soil type is more sensitive to soil erosion with combined effect of slope class in these sub-basins. It can be understood that Eutric Regosols soil type mostly occurs in desert regions, and it occupies around 25% of the area and barre land also cover around 39% of the total area. Kefalew et al., (2003) indicate that the lower Awash basin was highly affected by flood and soil erosion year to year.

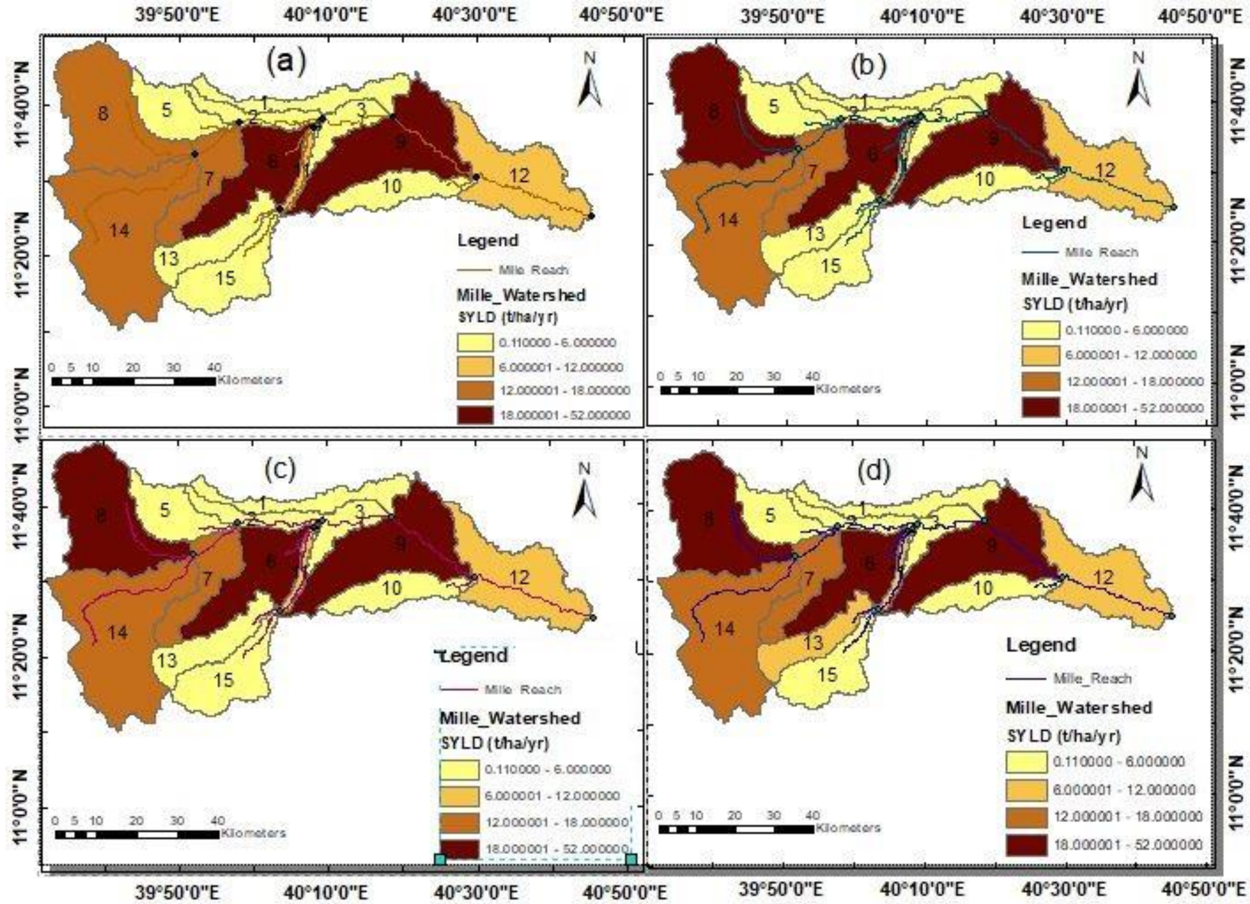

Figure 4.30: Spatial Variation Map of (a) 2050s RCP 4.5 (b) 2070s RCP 4.5 (c) 2050s RCP 8.5 (d) 2070s RCP 8.5

5. CONCLUSION AND RECOMMENDATION

5.1 Conclusion

The present study investigated the impacts of climate change on sediment yield from the Mille watershed in the Lower Awash Basin, Ethiopia. RCMs of RACMO-22 and CCLM-4 in CORDEX-Africa derived from the HadGEM2-ES and ICHEC-ES Global Climate Model were used for RCP4.5 and RCP8.5 by the 2050s and by the 2070s as compared to the baseline period (1986–2015). The SWAT hydrological model was used to simulate present and future changes in sediment yield, and the SUFI-2 algorithm in the SWAT-CUP program was used for parameter adjustment. Calibration, validation, and uncertainty analyses for sediment suggested that the SWAT model could be applied to simulate future changes in sediment yields due to ultimate climate change.

- Results indicated that mean annual precipitation as well as maximum and minimum temperatures would increase under RCP4.5 and RCP8.5 scenarios. The projected annual precipitations of RCP4.5 in the 2050s and the 2070s would increase by 3.86% and 7.85%, respectively. In the RCP8.5 scenario would increase from 4.61% and 10.57% for the 2050s and the 2050s, respectively.
- The RCP8.5 scenario was changed by a higher magnitude than the RCP4.5 scenario because RCP8.5 had a higher greenhouse gas emission scenario with a higher degree of global.
- Results of climate change impacts on sediment yield clearly showed that sediment loss would increase in all RCP scenarios. The mean annual sediment yields were predicted to increase by 5.85% by the 2050s and by 10.11% by the 2070s under RCP4.5 and also for RCP8.5, they were found to be 8.99% and 14.25% by the 2050s and the 2070s, respectively. Therefore climate change has an impact on sediment yield of watershed.
- Finally, the results showed that the amount of sediment load would vary in each sub-watershed due to changes in precipitation and temperature in the 2050s and the 2070s for both RCP4.5 and RCP8.5 scenarios. The maximum and the minimum sediment yields would occur in sub-basins 6 and 2 in the watershed.

5.2 Recommendation

- This investigation was done based on weather data gathered from meteorological agency used as an input in model simulation, however these data's have series of gaps which are missed thus can influence the result of model output. However; it is recommended the responsible organization gives more attention on recording of observed data for the future period.
- The sediment data used for this study were generated from sediment rating curves developed from limited sediment measurement data. Therefore, possible discrepancy of actual sediment and sediment data derived based on rating curves. However, superior results can be obtained if detail suspended sediment data are used. Hence, responsible bodies should give due attention to the time and frequency of sampling, method of sampling and recording of reliable sediment data together with flow measurement for future time.
- The identified critical sub basins showed of serious vulnerability to erosion and generate a huge amount of sediment at the outlet of the watershed and this can endanger the service life of Tendaho dam reservoir which is found just downstream of the outlet. Thus it needs urgent sustainable management practices. In addition to this, integration of terracing and contouring have shown effective way of sediment reduction from the catchment hence necessitates applying in combination.
- The model found to be good in simulating the run off and sediment for the study area thus can be used as a research tool for further analysis in the future in sediment yield estimation other different for watershed in the presence of the required input data for the model.

REFERENCE

- Abayneh, A. "Evaluation of Climate Change Impact on Extreme Case Study: Addis Ababa and Surrounding Catchment." (2011).
- Abbaspour, Karim C., Saeid Ashraf Vaghefi, and Raghvan Srinivasan. "A guideline for successful calibration and uncertainty analysis for soil and water assessment: a review of papers from the 2016 international SWAT conference." (2018).
- Abera, Fikru Fentaw, Dereje Hailu Asfaw, Agizew Nigussie Engida, and Assefa M. Melesse. "Optimal operation of hydropower reservoirs under climate change: The case of Tekeze reservoir, Eastern Nile." *Water* 10, no. 3 (2018): 273.
- Alemseged, Tamiru Haile, and Rientjes Tom. "Evaluation of regional climate model simulations of rainfall over the Upper Blue Nile basin." *Atmospheric research* 161 (2015): 57-64.
- Alliance, African Climate Change Resilience. "Climate trends in Ethiopia: Summary of ACCRA research in three sites." (2011).
- Arnold, Jeffrey G., Raghavan Srinivasan, Ranjan S. Muttiah, and Jimmy R. Williams. "Large area hydrologic modeling and assessment part I: model development 1." *JAWRA Journal of the American Water Resources Association* 34, no. 1 (1998): 73-89.
- Asres, Meqaunint Tenaw, and Seleshi B. Awulachew. "SWAT based runoff and sediment yield modelling: a case study of the Gumera watershed in the Blue Nile basin." *Ecohydrology & Hydrobiology* 10, no. 2-4 (2010): 191-199.
- Azari, Mahmood, Hamid Reza Moradi, Bahram Saghafian, and Monireh Faramarzi. "Climate change impacts on streamflow and sediment yield in the North of Iran." *Hydrological Sciences Journal* 61, no. 1 (2016): 123-133.
- Azim, Farooq, Abdul Sattar Shakir, and Afshan Kanwal. "Impact of climate change on sediment yield for Naran watershed, Pakistan." *International Journal of Sediment Research* 31, no. 3 (2016): 212-219.
- Bagnold, R. A. "Bed load transport by natural rivers." *Water resources research* 13, no. 2 (1977): 303-312.

- Batalla, Ramon J., and Maria Sala. "Temporal variability of suspended sediment transport in a Mediterranean sandy gravel-bed river." *IAHS Publications-Series of Proceedings and Reports-Intern Assoc Hydrological Sciences* 224 (1994): 299-306.
- Belete, B., and A. Semu. "Background report: hydro-meteorological trends." *Awash River Basin Water Audit (ARBWA) Project. Addis Ababa, Ethiopia* (2013).
- Berhanu, Belete, Yilma Seleshi, Solomon S. Demisse, and Assefa M. Melesse. "Bias correction and characterization of climate forecast system re-analysis daily precipitation in Ethiopia using fuzzy overlay." *Meteorological Applications* 23, no. 2 (2016): 230-243.
- Beven*, Keith. "How far can we go in distributed hydrological modelling?." *Hydrology and Earth System Sciences* 5, no. 1 (2001): 1-12.
- Bhuiyan, Faruk, ed. *Sediment Transport: Flow and Morphological Processes*. BoD–Books on Demand, 2011.
- Biagini, Emilio. "Hickin, Edward J., River geomorphology." *GeoJournal* 44.2 (2004): 162-163.
- Breusers, H. N. C. "Lecture notes on sediment transport 1." *IHE lecture note* (1983).
- Bui, Van Hieu, Minh Duc Bui, and Peter Rutschmann. "Advanced numerical modeling of sediment transport in gravel-bed rivers." *Water* 11, no. 3 (2019): 550.
- Campos, Rogério. "Three-dimensional reservoir sedimentation model." PhD diss., University of Newcastle upon Tyne, 2001.
- Change, IPCC Climate. "Synthesis Report. Cambridge, UK: IPCC." (2007).
- Chen, Jie, François P. Brissette, Diane Chaumont, and Marco Braun. "Finding appropriate bias correction methods in downscaling precipitation for hydrologic impact studies over North America." *Water Resources Research* 49, no. 7 (2013): 4187-4205.
- Corner, Adam, Lorraine Whitmarsh, and Dimitrios Xenias. "Uncertainty, scepticism and attitudes towards climate change: biased assimilation and attitude polarisation." *Climatic change* 114, no. 3 (2012): 463-478.
- Daba, M.; Tadele, K.; Shimelis, A.; Melesse, A. "Hydrological Response to climate change impacts and Adaptation Strategies of Upper Awash Sub-basin, in the Awash Basin, Ethiopia." In Proceedings of the International Conference on Climate-Change Impacts for Scientists & Stakeholders, Postdam, Germany, 11–13 October 2017.

- Deressa, Temesgen Tadesse, Rashid M. Hassan, and Claudia Ringler. "Perception of and adaptation to climate change by farmers in the Nile basin of Ethiopia." *The Journal of Agricultural Science* 149, no. 1 (2011): 23-31.
- Di Falco, Salvatore, Marcella Veronesi, and Mahmud Yesuf. "Does adaptation to climate change provide food security? A micro-perspective from Ethiopia." *American Journal of Agricultural Economics* 93, no. 3 (2011): 829-846.
- Emerta, A. "Climate Change, Growth and Poverty in Ethiopia. The Robert S." *Strauss Center for international security and Law: CCAPS* (2013).
- Engelund, Frank, and Eggert Hansen. "A monograph on sediment transport in alluvial streams." *Technical University of Denmark 0stervoldgade 10, Copenhagen K.* (1967).
- Fang, G. H., J. Yang, Y. N. Chen, and C. Zammit. "Comparing bias correction methods in downscaling meteorological variables for a hydrologic impact study in an arid area in China." *Hydrology and Earth System Sciences* 19, no. 6 (2015): 2547-2559.
- FAO and MoWIE . "Developing a Water Audit for Awash River Basin." GCP/INT/072/ITA Addis Ababa, Ethiopia (2013).
- Fowler, Hayley J., Stephen Blenkinsop, and Claudia Tebaldi. "Linking climate change modelling to impacts studies: recent advances in downscaling techniques for hydrological modelling." *International Journal of Climatology: A Journal of the Royal Meteorological Society* 27, no. 12 (2007): 1547-1578.
- Francipane, Antonio, Simone Fatichi, Valeriy Y. Ivanov, and Leonardo V. Noto. "Stochastic assessment of climate impacts on hydrology and geomorphology of semiarid headwater basins using a physically based model." *Journal of Geophysical Research: Earth Surface* 120, no. 3 (2015): 507-533.
- Fujino, Junichi, Rajesh Nair, Mikiko Kainuma, Toshihiko Masui, and Yuzuru Matsuoka. "Multi-gas mitigation analysis on stabilization scenarios using AIM global model." *The Energy Journal* Special Issue# 3 (2006).
- Garcia, Marcelo, ed. "Sedimentation engineering: processes, measurements, modeling, and practice." American Society of Civil Engineers, 2008.
- Gebrie, Tesfa, and Minichil Jemberie. "Sediment Yield Modeling of Dedissa Sub Basin, Abay Basin, South-Western Ethiopia." *Environment and Earth Science* 6, no. 10 (2016): 120-127.

- Giorgi, Filippo, Colin Jones, and Ghassem R. Asrar. "Addressing climate information needs at the regional level: the CORDEX framework." *World Meteorological Organization (WMO) Bulletin* 58, no. 3 (2009): 175.
- Girma, Endalkachew. "Climate change impact on surface water sources of Addis Ababa: a case study in Legedadi-Dire-Gefersa catchments and reservoirs." PhD diss., School of Graduate Study, Addis Ababa University, 2012.
- Green, W. H., & Ampt, G. A. (1911). Studies on soil physics, 1. The flow of air and water through soils. Journal of Agricultural Science, 4(1), pp. 1-24.
- Guyot, Jean Loup, Jacques Bourges, and Jose Cortez. "Sediment transport in the Rio Grande, an Andean river of the Bolivian Amazon drainage basin." *IAHS Publications-Series of Proceedings and Reports-Intern Assoc Hydrological Sciences* 224 (1994): 223-232.
- Hampson, L. *Sediment transport analysis, Carmel river near carmel water years 1992-1995*. No. 97-03. technical memorandum, 1997.
- Hernández-Díaz, Leticia, René Laprise, Laxmi Sushama, Andrey Martynov, Katja Winger, and Bernard Dugas. "Climate simulation over CORDEX Africa domain using the fifth-generation Canadian Regional Climate Model (CRCM5)." *Climate Dynamics* 40, no. 5-6 (2013): 1415-1433.
- Houghton, John T., Y. Ding, D. J. Griggs, M. Noguer, P. J. Van Der Linden, X. Dai, K. Maskell, and C. A. Johnson. "Climate Change 2001: The science of climate change." *Contribution of the Working Group I to the Third Assessment Report of the Intergovernmental Panel on Climate Change Cambridge University Press, Cambridge, United Kingdom and New York, NY* (2001): 881.
- Intergovernmental Panel on Climate Change (IPCC). (2014).V. R. Barros, C. B. Field, D. J. Dokken, M. D. Mastrandrea, K. J. Mach, T. E. Bilir, M. Chatterjee, K. L. Ebi, Y. O. Estrada, R. C. Genova, B. Girma, E. S. Kissel, A. N. Levy, S. MacCracken, P. R. Mastrandrea, & L. L. White (Eds.). Cambridge University Press.
- Jacob, Daniela, Alberto Elizalde, Andreas Haensler, Stefan Hagemann, Pankaj Kumar, Ralf Podzun, Diana Rechid et al. "Assessing the transferability of the regional climate model REMO to different coordinated regional climate downscaling experiment (CORDEX) regions." *Atmosphere* 3, no. 1 (2012): 181-199.

- Jaroot, Eltayeb Ahmed Khalifa. "The Effect of the Sediment Accumulation in Reservoirs: Case of the Roseires." PhD diss., UOFK, 2015.
- Jones, Colin, Filippo Giorgi, and Ghassem Asrar. "The Coordinated Regional Downscaling Experiment: CORDEX–an international downscaling link to CMIP5." *CLIVAR exchanges* 16, no. 2 (2011): 34-40.
- Kleinn, Jan, Christoph Frei, Joachim Gurtz, Daniel Lüthi, Pier Luigi Vidale, and Christoph Schär. "Hydrologic simulations in the Rhine basin driven by a regional climate model." *Journal of Geophysical Research: Atmospheres* 110, no. D4 (2005).
- Kumar, Vijay, Sharad K. Jain, and Yatveer Singh. "Analysis of long-term rainfall trends in India." *Hydrological Sciences Journal–Journal des Sciences Hydrologiques* 55, no. 4 (2010): 484-496.
- Laprise, René. "Regional climate modelling." *Journal of Computational Physics* 227, no. 7 (2008): 3641-3666.
- Lenderink, Geert, Adri Buishand, and W. van Deursen. "Estimates of future discharges of the river Rhine using two scenario methodologies: direct versus delta approach." *Hydrology and Earth System Sciences* 11, no. 3 (2007): 1145-1159.
- Lu, X. X., L. S. Ran, S. Liu, T. Jiang, S. R. Zhang, and J. J. Wang. "Sediment loads response to climate change: A preliminary study of eight large Chinese rivers." *International Journal of Sediment Research* 28, no. 1 (2013): 1-14.
- McSweeney, C., M. New, and G. Lizcano. "UNDP climate change country profiles: Ethiopia." *Profiles for 52 countries* (2008).
- Ménard, R. "Bias Estimation, in: Data Assimilation, edited by: Lahoz, W., Khattatov, B., and Menard, R." Springer Berlin Heidelberg, (2010): 113–135.
- Moriasi, Daniel N., Jeffrey G. Arnold, Michael W. Van Liew, Ronald L. Bingner, R. Daren Harmel, and Tamie L. Veith. "Model evaluation guidelines for systematic quantification of accuracy in watershed simulations." *Transactions of the ASABE* 50, no. 3 (2007): 885-900.
- Moss, Richard H., Jae A. Edmonds, Kathy A. Hibbard, Martin R. Manning, Steven K. Rose, Detlef P. Van Vuuren, Timothy R. Carter et al. "The next generation of scenarios for climate change research and assessment." *Nature* 463, no. 7282 (2010): 747-756.

- Nash, J. Eamonn, and Jonh V. Sutcliffe. "River flow forecasting through conceptual models part I—A discussion of principles." *Journal of hydrology* 10, no. 3 (1970): 282-290.
- Ndomba, Preksedis Marco, and Ann van Griensven. "Suitability of SWAT model for sediment yields modelling in the Eastern Africa." *Advances in Data, Methods, Models and Their Applications in Geoscience, InTech, China* (2011): 261-284.
- Nearing, M. A., F. F. Pruski, and M. R. O'neal. "Expected climate change impacts on soil erosion rates: a review." *Journal of soil and water conservation* 59, no. 1 (2004): 43-50.
- Neitsch, Susan L., Jeffrey G. Arnold, Jim R. Kiniry, and Jimmy R. Williams. *Soil and water assessment tool theoretical documentation version 2009*. Texas Water Resources Institute, 2011.
- Nill, Dieter, U. Schwertmann, U. Sabel-Koschella, M. Bernhard, and J. Breuer. "Soil erosion by water in Africa." *Principles, prediction and protection* (1996).
- NMA, " Convention on Climate Change (UNFCCC)", National Meteorological Services Agency, Addis Ababa, Ethiopia, (2001).
- Parry, Martin, Martin L. Parry, Osvaldo Canziani, Jean Palutikof, Paul Van der Linden, and Clair Hanson, eds. *Climate change 2007-impacts, adaptation and vulnerability: Working group II contribution to the fourth assessment report of the IPCC*. Vol. 4. Cambridge University Press, 2007.
- Riahi, Keywan, Arnulf Grübler, and Nebojsa Nakicenovic. "Scenarios of long-term socio-economic and environmental development under climate stabilization." *Technological Forecasting and Social Change* 74, no. 7 (2007): 887-935.
- Sahilu Geremew and Nigussie Agizew. "Climate Modeling of the Impact of Climate Change on Sugarcane and Cotton for Project on 'a Climate Resilient Production of Cotton and Sugar in Ethiopia" Climate Change and Modeling. EDRI Research Report 21. Addis Ababa: Ethiopian Development Research Institute, (2015).
- Setegn, Shimelis G., Bijan Dargahi, Ragahavan Srinivasan, and Assefa M. Melesse. "Modeling of Sediment Yield From Anjeni-Gauged Watershed, Ethiopia Using SWAT Model 1." *JAWRA Journal of the American Water Resources Association* 46, no. 3 (2010): 514-526.

- Shabalova, M. V., W. P. A. Van Deursen, and T. A. Buishand. "Assessing future discharge of the river Rhine using regional climate model integrations and a hydrological model." *Climate research* 23, no. 3 (2003): 233-246.
- Shrestha, B., M. S. Babel, S. Maskey, A. van Griensven, S. Uhlenbrook, A. Green, and I. Akkharath. "Impact of climate change on sediment yield in the Mekong River basin: a case study of the Nam Ou basin, Lao PDR." *Hydrology and Earth System Sciences* 17, no. 1 (2013): 1-20.
- Singh, Vijay P., and David A. Woolhiser. "Mathematical modeling of watershed hydrology." *Journal of hydrologic engineering* 7, no. 4 (2002): 270-292.
- Stocker, Thomas F., Dahe Qin, G-K. Plattner, Melinda MB Tignor, Simon K. Allen, Judith Boschung, Alexander Nauels, Yu Xia, Vincent Bex, and Pauline M. Midgley. "Climate Change 2013: The physical science basis. contribution of working group I to the fifth assessment report of IPCC the intergovernmental panel on climate change." (2014).
- Terink, W., R. T. W. L. Hurkmans, P. J. J. F. Torfs, and R. Uijlenhoet. "Evaluation of a bias correction method applied to downscaled precipitation and temperature reanalysis data for the Rhine basin." *Hydrology and earth system sciences* 14, no. 4 (2010): 687-703.
- Teutschbein, Claudia, and Jan Seibert. "Bias correction of regional climate model simulations for hydrological climate-change impact studies: Review and evaluation of different methods." *Journal of hydrology* 456 (2012): 12-29.
- Themeßl, Matthias Jakob, Andreas Gobiet, and Georg Heinrich. "Empirical-statistical downscaling and error correction of regional climate models and its impact on the climate change signal." *Climatic Change* 112, no. 2 (2012): 449-468.
- Thornton, Philip K., Peter G. Jones, Polly J. Ericksen, and Andrew J. Challinor. "Agriculture and food systems in sub-Saharan Africa in a 4 C+ world." *Philosophical Transactions of the Royal Society A: Mathematical, Physical and Engineering Sciences* 369, no. 1934 (2011): 117-136.
- Tibebe, Mahtsente, Assefa M. Melesse, and Dereje Hailu. "Rainfall-runoff relation and runoff estimation for Holetta River, Awash subbasin, Ethiopia using SWAT model." *International Journal of Water Resources and Environmental Engineering* 9, no. 5 (2017): 102-112.

- Tu, Jun. "Combined impact of climate and land use changes on streamflow and water quality in eastern Massachusetts, USA." *Journal of Hydrology* 379, no. 3-4 (2009): 268-283.
- Van Rijn, Leo C. *Principles of sediment transport in rivers, estuaries and coastal seas*. Vol. 1006. Amsterdam: Aqua publications, 1993.
- Van Vuuren, Detlef P., Jae Edmonds, Mikiko Kainuma, Keywan Riahi, Allison Thomson, Kathy Hibbard, George C. Hurtt et al. "The representative concentration pathways: an overview." *Climatic change* 109, no. 1 (2011): 5-31.
- Vanoni, Vito A. "Sedimentation engineering: Theory, measurements, modeling, and practice." *American Society of Civil Engineers (ASCE), Reston, Virginia, USA* (2006).
- Walling, Des E. "The changing sediment load of the Mekong River." *Ambio* (2008): 150-157.
- White, R. H., and R. Toumi. "The limitations of bias correcting regional climate model inputs." *Geophysical Research Letters* 40, no. 12 (2013): 2907-2912.
- Wischmeier, Walter H., and Dwight David Smith. *Predicting rainfall erosion losses: a guide to conservation planning*. No. 537. Department of Agriculture, Science and Education Administration, 1978.
- Wood, Andrew W., Lai R. Leung, Venkataramana Sridhar, and D. P. Lettenmaier. "Hydrologic implications of dynamical and statistical approaches to downscaling climate model outputs." *Climatic change* 62, no. 1 (2004): 189-216.
- Zhang, Shanghong, Zehao Li, Xiaonan Lin, and Cheng Zhang. "Assessment of climate change and associated vegetation cover change on watershed-scale runoff and sediment yield." *Water* 11, no. 7 (2019): 1373.
- Zhang, Xunchan C., and Mark A. Nearing. "Impact of climate change on soil erosion, runoff, and wheat productivity in central Oklahoma." *Catena* 61, no. 2-3 (2005): 185-195.
- Zollo, Alessandra L., Guido Rianna, Paola Mercogliano, Paolo Tommasi, and Luca Comegna. "Validation of a simulation chain to assess climate change impact on precipitation induced landslides." In *Landslide Science for a Safer Geoenvironment*, pp. 287-292. Springer, Cham, 2014.

APPENDECES

(A) Areal Precipitation RCP 4.5 2050s (2031-2060)

PCP	JAN	FEB	MAR	APR	MAY	JUN	JULY	AUG	SEP	OCT	NOV	DEC
2031	19.50	13.76	63.31	63.86	81.86	42.80	404.34	289.11	85.00	2.72	0.01	33.62
2032	8.71	6.86	30.76	67.71	82.74	51.16	316.01	219.40	44.53	37.58	3.27	5.36
2033	51.30	5.68	162.67	102.09	70.25	40.34	375.08	226.31	162.84	18.28	0.02	0.75
2034	5.91	30.79	49.02	56.38	71.50	40.20	137.77	182.49	100.32	4.16	0.29	4.05
2035	13.50	8.42	68.45	49.17	118.48	54.73	166.17	334.05	46.93	41.38	0.53	2.92
2036	30.49	30.20	143.12	101.95	171.47	29.62	630.32	557.91	130.84	30.99	0.73	32.80
2037	75.45	12.43	86.44	69.92	96.58	51.21	331.18	178.34	206.08	10.38	4.32	61.10
2038	0.15	33.39	83.15	104.14	63.74	39.63	185.94	210.33	123.78	39.96	39.62	3.16
2039	84.42	16.27	81.10	65.64	39.14	27.55	107.31	234.07	58.46	16.66	7.91	14.60
2040	15.39	31.80	101.38	85.76	60.99	10.45	206.80	208.28	97.69	39.03	1.09	6.95
2041	37.78	25.35	86.57	96.72	83.04	53.95	175.95	349.02	56.96	21.18	5.68	8.56
2042	62.65	31.66	112.13	71.81	186.68	38.75	296.71	426.98	113.87	29.58	1.38	15.96
2043	16.62	35.17	83.82	69.47	50.22	5.91	202.69	395.43	104.79	18.05	5.14	65.08
2044	51.80	36.59	111.29	76.26	52.00	5.45	171.96	248.13	44.33	32.49	24.13	0.17
2045	2.97	48.29	125.85	91.97	71.56	26.45	108.34	224.36	56.54	74.19	0.00	17.27
2046	6.02	51.01	83.78	76.10	69.75	20.66	184.16	306.55	32.28	11.44	14.35	0.92
2047	5.52	23.13	58.29	70.01	36.06	20.57	148.33	300.68	239.65	29.34	8.10	72.51
2048	25.89	17.69	58.33	88.56	68.12	6.52	226.20	289.48	11.11	2.67	6.01	56.78
2049	37.56	57.99	127.86	66.34	63.95	2.65	226.98	211.48	67.02	13.22	1.95	28.88
2050	26.08	37.62	97.69	70.05	46.72	12.28	167.33	159.18	73.51	49.44	34.92	31.17
2051	30.02	33.17	143.96	58.90	44.93	0.74	87.96	88.27	60.09	75.71	586.27	28.95
2052	21.10	27.05	72.73	36.16	37.88	18.16	137.10	156.83	94.88	44.89	1.89	14.27
2053	31.09	37.63	75.58	39.88	67.23	37.15	176.66	261.26	114.95	85.37	1.31	9.71
2054	26.15	56.30	54.21	94.03	39.47	14.06	303.08	193.81	64.83	19.42	1.79	23.77
2055	25.66	35.34	53.81	87.81	47.63	2.82	251.62	391.10	70.36	197.31	7.59	15.55
2056	48.17	45.71	74.06	39.90	44.46	11.09	139.96	321.61	77.80	3.55	3.26	55.25
2057	21.69	62.57	120.67	13.78	1.80	8.61	197.37	256.59	70.11	21.96	23.78	102.54
2058	37.36	44.37	46.33	18.90	44.34	21.74	201.25	178.19	90.70	59.59	7.29	43.27
2059	32.81	41.13	37.48	108.12	16.43	9.07	112.84	205.12	132.09	45.74	5.30	29.17
2060	27.41	15.11	41.41	35.46	74.17	5.27	117.48	149.70	174.46	105.83	16.20	7.93

Areal Precipitation RCP 4.5 2070s (2061-2090)

PCP	JAN	FEB	MAR	APR	MAY	JUN	JULY	AUG	SEP	OCT	NOV	DEC
2061	42.35	129.16	110.77	138.95	134.18	9.01	171.05	169.05	61.32	9.61	21.01	136.78
2062	41.02	12.61	22.81	63.98	161.03	6.15	349.05	164.43	66.94	17.78	16.16	27.32
2063	27.18	4.30	37.98	81.85	52.23	11.14	118.39	219.26	102.94	65.58	12.67	52.91
2064	8.27	23.62	4.97	63.00	86.09	14.38	80.39	100.32	87.71	37.81	100.81	40.25
2065	9.76	69.05	128.10	92.73	99.21	2.28	94.07	210.10	56.70	40.44	135.96	25.72
2066	74.21	8.06	69.38	11.08	76.11	19.24	229.62	194.32	78.72	28.68	6.57	63.72
2067	16.27	23.46	52.29	112.87	26.26	19.54	121.18	219.39	53.59	42.19	10.70	7.10
2068	13.64	20.08	159.76	49.78	37.03	17.66	286.97	287.78	98.07	52.57	15.88	31.38
2069	77.42	52.62	152.22	23.19	18.92	0.59	257.76	159.53	116.04	51.13	21.45	51.44
2070	11.48	32.72	135.91	86.55	34.85	3.28	149.83	272.27	132.83	30.67	2.88	19.41
2071	30.41	34.38	90.64	42.72	13.57	28.66	239.42	345.31	91.46	19.63	40.17	8.09
2072	18.53	21.21	161.69	79.06	63.53	3.90	279.84	140.84	137.38	56.26	6.80	1.92
2073	25.33	10.84	11.81	19.77	16.31	39.76	270.70	210.78	131.18	28.50	20.69	10.95
2074	0.11	29.35	160.47	70.60	3.89	10.01	202.60	215.67	119.58	32.03	9.55	44.35
2075	10.42	41.91	12.49	11.22	19.03	3.02	252.53	192.13	138.20	45.43	9.66	10.61
2076	19.84	18.76	78.75	98.44	107.54	23.50	266.39	314.44	105.96	76.16	5.55	4.79
2077	9.01	14.91	45.51	11.97	53.12	30.67	258.72	322.05	146.71	54.64	13.07	9.81
2078	15.49	20.05	68.08	77.82	49.57	36.40	257.31	290.65	109.52	49.08	2.85	12.47
2079	15.00	41.33	137.66	89.69	19.51	52.52	229.08	339.13	120.14	33.89	189.37	19.24
2080	35.71	35.42	25.00	129.62	54.10	8.76	311.43	381.25	126.92	14.63	157.83	21.98
2081	75.69	36.64	29.24	65.93	13.15	8.13	221.43	399.54	118.22	57.06	5.63	5.86
2082	3.78	12.94	93.54	48.85	34.59	47.81	274.29	290.63	146.92	18.43	23.48	13.60
2083	34.59	30.75	4.71	125.53	70.44	8.12	306.65	324.80	137.62	6.31	2.33	24.58
2084	11.13	58.02	105.90	92.16	51.59	31.85	255.92	320.93	70.70	52.82	40.03	66.15
2085	41.68	50.61	99.47	127.18	91.39	51.41	262.51	353.53	99.84	44.63	0.80	18.18
2086	7.90	6.10	66.82	138.50	59.55	30.15	294.32	389.24	121.22	64.97	0.08	43.84
2087	2.45	4.97	42.52	11.77	26.64	54.90	264.04	388.76	127.04	84.84	7.31	0.40
2088	16.94	21.48	1.28	105.75	43.89	37.21	310.58	391.94	53.90	10.40	0.02	0.18
2089	16.08	5.94	137.09	37.28	94.52	50.82	269.19	363.20	94.16	70.95	2.02	38.84
2090	15.14	22.33	66.27	109.58	25.29	70.36	305.87	353.41	108.34	10.30	2.09	9.82

Areal Precipitation RCP 8.5 2050s (2031-2060)

PCP	JAN	FEB	MAR	APR	MAY	JUN	JULY	AUG	SEP	OCT	NOV	DEC
2031	3.55	8.75	34.32	77.45	31.18	49.17	351.11	404.48	44.48	18.04	19.57	4.76
2032	8.64	46.26	71.90	75.91	71.57	53.06	346.99	250.21	45.32	9.87	0.06	14.90
2033	8.79	54.85	53.51	105.68	60.67	57.32	331.81	356.34	30.68	16.19	21.10	20.97
2034	3.23	0.77	61.42	69.36	84.94	54.04	269.65	285.49	103.88	18.18	0.58	27.13
2035	19.75	26.43	68.91	107.81	65.89	34.56	239.21	458.98	146.90	4.69	5.81	6.45
2036	24.41	35.67	78.57	81.67	84.81	31.57	259.22	192.83	131.00	36.85	47.25	26.41
2037	65.56	12.81	82.50	84.57	73.26	51.26	159.28	223.24	124.20	83.28	4.30	13.95
2038	61.38	40.29	105.51	95.96	65.02	37.57	199.99	293.42	48.59	12.78	14.96	0.28
2039	11.91	33.42	76.72	78.45	74.52	34.58	202.44	293.80	14.60	29.75	0.49	53.39
2040	24.41	37.61	73.54	105.33	108.26	8.58	306.49	226.01	55.36	16.98	20.87	32.05
2041	24.74	13.52	54.06	89.53	46.54	4.85	153.52	305.20	91.13	7.94	0.01	0.30
2042	8.65	44.99	76.50	96.23	53.56	44.89	341.78	179.78	116.75	18.36	19.27	4.33
2043	6.97	36.64	80.70	88.76	45.10	1.29	179.27	158.89	176.59	63.11	12.00	67.28
2044	2.78	40.89	78.65	86.56	47.06	11.37	339.48	309.06	48.61	16.45	18.30	3.83
2045	22.39	28.75	54.88	93.98	29.19	23.27	117.49	458.17	176.11	11.11	3.82	74.18
2046	57.72	53.41	102.38	99.17	28.11	10.47	313.20	159.72	40.95	18.61	22.87	66.18
2047	33.22	19.55	71.28	74.59	21.48	4.87	297.66	173.43	53.95	106.90	1.14	31.29
2048	37.67	36.56	70.22	96.44	73.54	23.62	144.07	247.31	67.29	58.52	9.62	14.84
2049	16.77	38.08	67.65	104.61	8.13	12.04	128.08	427.97	149.33	42.35	11.05	70.53
2050	28.02	48.30	91.91	55.16	74.46	21.79	218.01	213.55	12.69	68.29	3.86	15.65
2051	35.31	33.53	81.11	51.26	19.02	23.36	122.00	275.51	95.57	86.80	15.30	14.88
2052	77.28	68.91	80.82	27.40	33.69	1.13	170.36	131.37	38.65	21.54	1.44	4.52
2053	29.07	25.60	121.86	41.05	20.08	7.74	83.28	73.50	12.28	4.02	99.61	25.64
2054	77.91	63.23	61.00	60.03	50.36	9.16	358.13	339.13	131.58	11.98	6.94	12.94
2055	14.38	38.60	44.12	13.99	14.82	12.85	347.66	237.53	22.69	24.26	19.00	89.62
2056	89.92	38.91	103.18	97.31	95.32	36.83	226.07	181.69	91.56	74.81	84.75	14.61
2057	7.73	45.42	91.13	5.00	12.14	16.18	335.42	540.55	210.52	10.86	19.16	20.34
2058	28.74	27.71	86.54	83.37	76.52	13.84	84.09	386.67	42.57	11.08	8.62	61.18
2059	38.39	33.54	108.57	39.94	45.88	3.67	89.16	222.25	160.95	55.17	80.04	39.31
2060	41.93	31.77	49.52	49.54	53.67	62.72	177.98	444.74	65.94	60.12	33.35	40.32

Areal Precipitation RCP 4.5 2070s (2061-2090)

PCP	JAN	FEB	MAR	APR	MAY	JUN	JULY	AUG	SEP	OCT	NOV	DEC
2061	72.05	119.38	17.53	16.01	110.51	3.60	140.35	154.16	80.17	70.50	21.87	56.11
2062	35.32	18.24	56.16	32.80	31.99	14.54	219.47	155.33	54.49	33.12	19.55	69.04
2063	61.02	79.27	180.85	189.13	30.57	5.11	114.93	368.42	6.31	4.79	42.89	30.82
2064	55.96	0.56	225.78	41.60	38.46	19.45	195.57	134.73	75.15	19.05	64.29	33.38
2065	51.66	12.82	12.94	27.13	46.07	5.62	65.75	126.47	114.12	18.85	61.18	37.17
2066	52.31	16.14	26.42	99.00	20.42	36.19	319.30	317.68	106.63	123.31	37.49	61.84
2067	31.58	10.08	9.68	15.21	72.40	4.97	207.51	266.58	144.10	114.89	64.23	14.07
2068	63.83	53.14	114.57	38.82	144.23	6.78	100.38	280.24	99.90	30.78	43.64	20.98
2069	57.49	0.20	226.05	188.78	1.41	5.63	219.62	172.21	71.25	28.91	12.78	22.93
2070	34.66	24.74	56.12	22.23	2.99	26.38	176.43	146.73	73.46	21.39	21.91	24.09
2071	15.17	1.32	36.36	31.92	107.15	61.29	152.51	206.64	109.23	28.48	32.07	18.44
2072	15.51	28.51	24.29	127.28	91.49	34.72	248.87	159.86	85.05	19.30	21.68	33.74
2073	52.90	73.83	45.94	78.78	44.33	8.63	177.68	207.34	115.59	53.17	12.00	23.42
2074	55.96	21.15	54.12	25.66	9.09	17.52	185.73	363.74	111.31	42.31	9.72	33.60
2075	53.06	0.11	89.77	45.93	55.51	11.24	183.73	288.66	110.06	45.36	117.02	33.34
2076	30.22	0.00	115.90	73.02	20.06	27.82	150.89	327.34	107.83	68.31	7.67	13.36
2077	3.68	25.99	28.71	53.18	134.64	14.10	320.11	291.76	135.24	87.13	1.32	0.29
2078	10.17	7.33	130.83	106.65	25.01	19.50	240.75	254.38	121.15	31.98	2.81	35.48
2079	7.94	58.08	86.37	192.96	144.38	2.51	199.32	299.18	142.88	17.60	14.56	4.37
2080	5.03	73.87	19.19	183.25	29.76	11.40	293.63	343.43	131.68	21.17	2.47	4.11
2081	6.44	14.10	56.81	78.23	24.69	18.19	237.68	344.96	131.53	24.19	9.47	15.34
2082	15.20	7.48	31.33	17.32	24.02	7.72	335.56	391.13	132.29	25.62	8.87	4.57
2083	26.66	12.29	1.50	131.67	82.83	28.03	277.80	368.43	111.47	13.89	5.31	22.97
2084	7.62	7.79	111.01	142.26	35.58	25.10	379.93	407.85	124.50	17.52	0.24	10.76
2085	47.46	5.50	198.07	119.16	63.41	36.96	394.91	310.21	90.16	29.52	58.34	21.90
2086	13.71	35.71	32.09	148.77	40.17	18.89	431.47	413.88	108.69	30.29	2.67	10.46
2087	14.88	22.37	104.17	117.23	49.64	96.25	411.56	285.56	114.76	18.35	2.88	15.86
2088	17.37	93.10	46.24	83.00	42.43	29.69	362.77	356.94	60.05	71.48	31.06	0.40
2089	19.97	52.57	75.22	49.39	31.41	31.82	449.06	363.56	102.38	43.97	1.74	0.60
2090	19.37	1.69	67.67	157.91	68.88	104.71	412.40	392.78	116.22	8.58	0.03	6.71

(B) Areal Temperature Maximum RCP 4.5 2050s (2031-2060)

	JAN	FEB	MAR	APR	MAY	JUN	JUL	AUG	SEP	OCT	NOV	DEC
2031	29.18	28.41	30.56	31.68	33.30	34.99	32.99	31.02	31.61	30.65	29.17	27.82
2032	28.87	28.67	29.13	32.10	30.96	35.25	34.47	31.68	32.59	30.84	29.02	27.88
2033	29.30	28.47	31.77	32.13	35.08	35.81	32.22	30.27	30.69	29.91	28.44	27.61
2034	27.56	26.72	28.36	28.04	32.57	35.68	34.02	32.18	31.37	30.86	29.60	26.51
2035	27.97	25.63	28.23	30.41	34.84	37.10	33.83	33.10	32.68	31.44	29.82	28.92
2036	29.90	28.24	29.12	32.18	33.84	36.44	33.06	31.42	31.90	30.45	29.31	27.96
2037	28.23	27.01	29.21	32.44	34.31	35.77	33.56	30.26	29.74	29.13	28.30	27.18
2038	27.72	25.71	30.49	29.29	31.76	35.49	34.25	33.06	32.67	31.39	30.40	29.16
2039	30.45	30.08	30.34	33.44	27.65	36.70	32.73	30.88	31.18	30.42	29.13	27.87
2040	30.05	28.90	29.86	30.78	33.64	36.07	32.98	31.65	32.13	31.55	30.21	28.17
2041	28.66	30.39	30.48	32.10	32.28	34.76	34.00	32.27	32.82	32.09	29.90	29.18
2042	28.95	30.01	30.70	31.54	34.93	35.64	34.35	33.53	34.54	30.99	29.89	29.18
2043	28.95	28.55	30.21	33.98	35.31	38.48	33.49	31.59	32.50	32.00	30.83	28.26
2044	29.12	31.43	30.22	34.34	35.61	37.10	33.37	31.99	31.95	30.85	29.76	28.74
2045	30.11	31.10	32.64	33.49	34.59	36.82	34.01	31.26	31.61	30.61	28.77	27.34
2046	27.10	29.06	28.87	32.46	34.44	35.77	33.62	31.22	31.24	31.33	29.05	28.74
2047	27.50	29.16	30.99	32.29	35.88	37.00	35.57	32.61	31.51	31.99	30.49	27.29
2048	27.98	29.74	31.16	32.25	35.08	36.58	33.74	31.45	31.95	31.28	29.60	27.44
2049	29.65	28.60	31.05	30.77	34.93	33.63	34.29	32.75	32.40	31.01	30.36	27.58
2050	29.00	31.41	31.84	32.24	32.55	36.07	33.44	32.15	32.90	30.84	30.32	29.58
2051	30.57	30.15	31.27	30.59	34.75	37.00	33.95	32.17	32.17	31.82	30.60	29.23
2052	28.41	29.86	32.44	33.07	36.29	34.79	32.33	31.99	32.23	31.51	29.86	29.06
2053	30.07	29.11	32.83	33.87	35.64	36.90	35.09	32.63	32.52	31.36	28.94	28.27
2054	29.56	30.22	32.10	32.97	36.04	37.45	33.68	33.03	33.40	31.81	31.10	28.76
2055	29.76	29.87	29.89	32.94	34.61	37.10	33.91	31.84	32.16	32.09	29.81	27.55
2056	28.73	29.81	30.33	34.27	33.75	36.09	34.06	31.34	32.07	31.84	29.45	28.31
2057	30.55	29.09	32.12	32.33	35.32	37.85	35.39	32.01	31.74	31.01	30.76	29.85
2058	30.64	30.80	32.23	33.58	35.42	35.89	33.84	30.77	32.68	31.25	30.19	28.45
2059	29.98	28.51	31.62	33.14	33.03	36.52	35.42	31.75	31.63	30.40	29.85	28.50
2060	28.87	31.23	32.76	34.90	35.19	36.24	36.76	32.28	30.39	29.95	28.85	28.27

Areal Temperature Maximum RCP 4.5 2070s (2061-2090)

	JAN	FEB	MAR	APR	MAY	JUN	JUL	AUG	SEP	OCT	NOV	DEC
2061	27.32	27.95	30.06	31.16	32.76	34.42	32.45	30.52	31.09	30.15	28.69	27.37
2062	27.00	28.22	28.57	31.48	30.42	34.65	34.04	31.14	32.09	30.41	28.54	27.57
2063	27.30	28.01	31.17	31.57	34.37	35.31	31.78	29.78	30.22	29.48	28.03	27.18
2064	25.77	26.34	27.90	27.59	32.04	35.10	33.46	31.66	30.86	30.36	29.12	26.08
2065	26.22	25.21	27.77	29.92	34.27	36.50	33.28	32.56	32.15	30.93	29.33	28.45
2066	27.96	27.81	28.59	31.50	33.23	35.88	32.63	30.96	31.31	30.01	28.86	27.60
2067	26.45	26.55	28.73	31.76	33.71	35.19	33.19	29.73	29.29	28.69	27.89	26.69
2068	25.86	25.41	29.99	28.82	31.24	34.91	33.69	32.53	32.14	30.88	29.90	28.69
2069	28.50	29.59	29.84	32.89	27.20	36.10	32.20	30.37	30.68	29.93	28.66	27.42
2070	28.10	28.47	29.17	30.33	33.07	35.37	32.62	31.10	31.64	31.07	29.77	27.76
2071	26.79	29.79	29.98	31.54	31.71	34.08	33.55	31.83	32.22	31.65	29.42	28.76
2072	27.04	29.49	30.20	31.03	34.36	35.06	33.79	32.99	33.97	30.49	29.41	28.71
2073	27.08	28.09	29.71	33.43	34.74	37.85	32.95	31.07	31.97	31.48	30.33	27.80
2074	27.25	30.96	29.61	33.77	34.93	36.62	32.79	31.57	31.42	30.33	29.35	28.33
2075	28.18	30.49	32.07	32.96	33.89	36.28	33.53	30.75	31.14	30.14	28.33	26.94
2076	25.41	28.52	28.40	31.93	33.88	35.18	33.07	30.72	30.73	30.82	28.58	28.28
2077	25.76	28.69	30.49	31.77	35.30	36.40	34.99	32.08	31.00	31.47	30.00	26.84
2078	26.22	29.28	30.60	31.73	34.34	36.03	33.32	30.93	31.44	30.83	29.08	27.02
2079	27.87	28.01	30.54	30.18	34.29	33.15	33.70	32.24	31.89	30.57	29.97	27.18
2080	27.12	30.79	31.33	31.71	32.02	35.49	32.90	31.62	32.36	30.34	29.82	29.10
2081	28.61	29.66	30.76	30.10	34.19	36.40	33.40	31.65	31.65	31.31	30.10	28.76
2082	26.62	29.32	31.88	32.45	35.75	34.23	31.86	31.42	31.78	30.99	29.43	28.62
2083	28.19	28.49	32.15	33.27	35.08	36.23	34.72	32.07	32.06	30.90	28.47	27.80
2084	27.67	29.70	31.57	32.44	35.45	36.84	33.13	32.49	32.86	31.29	30.59	28.29
2085	27.83	29.38	29.41	32.40	34.05	36.50	33.36	31.32	31.64	31.57	29.32	27.10
2086	26.88	29.23	29.82	33.67	33.15	35.52	33.68	30.74	31.51	31.36	29.21	27.69
2087	28.64	28.79	31.40	31.71	34.62	37.28	34.87	31.59	31.24	30.51	30.27	29.40
2088	28.62	30.29	31.71	33.03	34.85	35.31	33.29	30.26	32.14	30.74	29.70	27.99
2089	28.06	28.05	31.10	32.61	32.49	35.93	34.85	31.23	31.12	29.91	29.36	28.03
2090	27.04	30.68	32.15	34.31	34.64	35.63	36.27	31.78	29.99	29.41	28.44	27.81

Areal Temperature Maximum RCP 8.5 2050s (2031-2060)

	JAN	FEB	MAR	APR	MAY	JUN	JUL	AUG	SEP	OCT	NOV	DEC
2031	30.15	30.83	33.17	34.40	36.15	37.98	35.80	33.67	34.30	33.26	31.65	30.20
2032	29.80	31.11	31.61	34.86	33.60	38.26	37.40	34.38	35.37	33.48	31.49	30.26
2033	30.28	30.90	34.49	34.88	38.07	38.86	34.97	32.85	33.30	32.45	30.86	29.97
2034	28.47	28.99	30.78	30.43	35.35	38.72	36.92	34.92	34.05	33.49	32.13	28.77
2035	28.92	27.81	30.64	33.01	37.81	40.28	36.72	35.93	35.48	34.13	32.37	31.40
2036	30.85	30.65	31.59	34.93	36.73	39.56	35.89	34.10	34.62	33.05	31.81	30.36
2037	29.20	29.30	31.71	35.22	37.24	38.83	36.42	32.84	32.27	31.61	30.71	29.50
2038	28.57	27.90	33.09	31.79	34.47	38.53	37.18	35.89	35.47	34.08	33.01	31.67
2039	31.45	32.66	32.94	36.30	29.93	39.84	35.53	33.52	33.85	33.02	31.63	30.26
2040	31.02	31.37	32.41	33.40	36.51	39.15	35.79	34.35	34.87	34.25	32.80	30.58
2041	29.58	32.99	33.08	34.85	35.04	37.73	36.91	35.03	35.63	34.85	32.47	31.69
2042	29.86	32.58	33.33	34.24	37.92	38.70	37.29	36.40	37.50	33.65	32.45	31.68
2043	29.88	30.99	32.79	36.90	38.34	41.78	36.36	34.29	35.27	34.74	33.48	30.68
2044	30.07	34.13	32.80	37.28	38.65	40.27	36.23	34.72	34.68	33.49	32.31	31.21
2045	31.09	33.77	35.44	36.36	37.55	39.97	36.92	33.93	34.31	33.23	31.22	29.66
2046	28.01	31.55	31.33	35.23	37.38	38.82	36.49	33.88	33.90	34.01	31.53	31.20
2047	28.41	31.65	33.64	35.05	38.95	40.17	38.61	35.39	34.20	34.72	33.10	29.61
2048	28.93	32.29	33.82	35.01	38.08	39.71	36.62	34.14	34.68	33.95	32.13	29.78
2049	30.65	31.03	33.70	33.40	37.92	36.56	37.22	35.55	35.16	33.66	32.95	29.93
2050	29.96	34.10	34.56	34.98	35.33	39.16	36.30	34.89	35.71	33.47	32.92	32.10
2051	31.56	32.72	33.94	33.20	37.72	40.17	36.85	34.92	34.91	34.54	33.21	31.73
2052	29.36	32.41	35.21	35.90	39.40	37.76	35.09	34.72	34.98	34.20	32.42	31.54
2053	31.04	31.60	35.64	36.77	38.69	40.05	38.08	35.41	35.29	34.04	31.41	30.68
2054	30.54	32.81	34.84	35.79	39.12	40.65	36.55	35.84	36.25	34.52	33.75	31.22
2055	30.71	32.42	32.44	35.75	37.57	40.28	36.82	34.57	34.90	34.83	32.36	29.90
2056	29.66	32.35	32.92	37.20	36.64	39.18	36.97	34.00	34.80	34.56	31.97	30.73
2057	31.55	31.57	34.87	35.09	38.33	41.06	38.42	34.74	34.45	33.65	33.39	32.40
2058	31.62	33.44	34.99	36.45	38.45	38.99	36.73	33.39	35.46	33.91	32.77	30.88
2059	30.96	30.94	34.31	35.97	35.84	39.64	38.45	34.45	34.32	32.99	32.40	30.93
2060	29.83	33.90	35.56	37.86	38.17	39.33	39.91	35.03	32.98	32.50	31.31	30.68

Areal Temperature Maximum RCP 8.5 2070s (2061-2090)

	JAN	FEB	MAR	APR	MAY	JUN	JUL	AUG	SEP	OCT	NOV	DEC
2061	28.90	29.57	31.80	32.97	34.65	36.41	34.33	32.28	32.89	31.90	30.35	28.95
2062	28.56	29.86	30.22	33.30	32.18	36.66	36.01	32.94	33.94	32.16	30.19	29.17
2063	28.88	29.63	32.97	33.40	36.36	37.35	33.62	31.50	31.96	31.18	29.65	28.75
2064	27.26	27.86	29.51	29.18	33.89	37.13	35.40	33.49	32.65	32.11	30.80	27.58
2065	27.73	26.67	29.38	31.65	36.25	38.61	35.20	34.45	34.01	32.72	31.03	30.10
2066	29.58	29.41	30.24	33.32	35.15	37.95	34.51	32.75	33.12	31.75	30.53	29.19
2067	27.98	28.08	30.39	33.59	35.67	37.22	35.11	31.45	30.99	30.35	29.50	28.24
2068	27.35	26.89	31.73	30.48	33.05	36.93	35.64	34.41	34.00	32.67	31.63	30.35
2069	30.15	31.30	31.57	34.80	28.77	38.19	34.06	32.13	32.45	31.66	30.32	29.01
2070	29.73	30.12	30.86	32.08	34.99	37.42	34.51	32.89	33.47	32.86	31.49	29.37
2071	28.34	31.52	31.71	33.36	33.55	36.05	35.49	33.67	34.08	33.48	31.13	30.43
2072	28.61	31.20	31.95	32.82	36.35	37.09	35.75	34.90	35.94	32.25	31.11	30.37
2073	28.65	29.71	31.43	35.36	36.75	40.04	34.85	32.87	33.82	33.30	32.09	29.41
2074	28.82	32.75	31.32	35.72	36.95	38.74	34.68	33.39	33.24	32.09	31.05	29.96
2075	29.81	32.25	33.93	34.87	35.85	38.38	35.47	32.53	32.94	31.89	29.96	28.49
2076	26.88	30.17	30.05	33.77	35.84	37.22	34.99	32.49	32.51	32.60	30.23	29.91
2077	27.25	30.34	32.25	33.60	37.34	38.51	37.02	33.94	32.79	33.29	31.73	28.40
2078	27.74	30.97	32.37	33.56	36.33	38.12	35.25	32.72	33.26	32.61	30.76	28.58
2079	29.48	29.63	32.31	31.92	36.27	35.07	35.65	34.11	33.73	32.34	31.70	28.75
2080	28.69	32.57	33.14	33.55	33.87	37.54	34.80	33.45	34.24	32.09	31.55	30.78
2081	30.26	31.37	32.54	31.84	36.16	38.50	35.33	33.48	33.48	33.12	31.84	30.42
2082	28.16	31.01	33.72	34.32	37.82	36.21	33.71	33.24	33.62	32.78	31.13	30.27
2083	29.82	30.14	34.01	35.19	37.11	38.33	36.72	33.93	33.91	32.69	30.12	29.41
2084	29.27	31.42	33.40	34.31	37.50	38.97	35.04	34.37	34.76	33.10	32.36	29.93
2085	29.44	31.08	31.11	34.27	36.02	38.61	35.29	33.14	33.47	33.39	31.02	28.66
2086	28.44	30.92	31.55	35.62	35.07	37.57	35.63	32.52	33.33	33.17	30.90	29.29
2087	30.29	30.46	33.21	33.54	36.62	39.44	36.89	33.42	33.05	32.27	32.02	31.09
2088	30.28	32.04	33.54	34.94	36.86	37.35	35.21	32.01	34.00	32.52	31.42	29.61
2089	29.68	29.67	32.90	34.49	34.37	38.00	36.86	33.03	32.92	31.63	31.06	29.65
2090	28.61	32.46	34.01	36.29	36.64	37.69	38.36	33.62	31.72	31.11	30.08	29.42

Areal Temperature Minimum RCP 4.5 2050s (2031-2060)

	JAN	FEB	MAR	APR	MAY	JUN	JUL	AUG	SEP	OCT	NOV	DEC
2031	12.39	13.24	16.34	16.63	16.90	16.62	16.16	16.27	15.04	13.77	11.52	11.01
2032	12.70	14.63	17.21	17.21	16.38	18.67	14.82	12.61	15.33	13.77	11.72	11.55
2033	12.94	14.42	14.94	15.58	15.94	18.23	15.20	14.69	17.11	13.33	11.79	10.31
2034	12.64	14.53	16.59	15.81	16.38	18.45	16.22	16.11	17.26	14.02	11.68	10.78
2035	13.00	14.90	16.68	16.33	16.51	18.66	15.16	16.92	17.55	14.44	11.33	11.20
2036	12.93	15.70	15.74	15.44	16.00	18.59	14.99	15.41	14.89	13.11	10.65	10.34
2037	12.41	16.04	15.34	15.39	16.05	17.56	15.41	16.01	15.57	13.23	11.67	9.91
2038	12.89	14.39	15.69	14.56	16.38	20.32	15.82	14.20	16.28	13.75	11.75	10.71
2039	12.85	13.88	14.02	16.24	16.85	15.90	17.02	15.83	17.12	13.92	11.56	11.35
2040	12.95	14.12	14.79	16.11	16.59	19.37	15.81	16.95	18.66	13.77	11.51	10.66
2041	12.68	14.52	15.42	16.66	17.31	18.26	16.72	16.09	17.88	13.53	11.14	11.05
2042	12.40	14.76	14.94	16.14	17.27	19.34	15.13	18.11	18.01	12.80	10.89	10.87
2043	12.84	13.34	15.81	16.88	17.36	19.55	16.48	14.08	13.31	13.51	10.77	10.75
2044	12.92	14.14	15.40	16.63	17.15	17.53	19.23	16.06	20.19	14.02	11.54	11.93
2045	12.40	14.02	15.07	17.10	16.16	19.76	17.50	20.41	16.25	13.72	12.02	11.35
2046	12.19	12.60	15.01	16.34	16.87	19.36	20.09	17.11	19.07	13.40	11.23	11.82
2047	12.49	14.01	16.01	17.23	18.41	20.19	16.46	16.81	17.40	13.93	11.76	11.20
2048	12.53	13.21	15.46	16.07	16.17	17.84	21.44	17.50	15.89	13.06	11.20	12.41
2049	13.16	12.03	14.48	16.78	16.72	19.35	19.52	20.21	17.62	13.65	11.81	11.59
2050	12.89	12.69	15.40	16.68	17.72	17.72	18.67	17.00	16.72	13.16	11.55	11.88
2051	12.84	13.52	15.18	15.54	16.74	16.80	18.30	15.72	15.26	14.35	12.50	12.39
2052	12.56	13.47	15.75	16.47	16.92	18.28	17.63	15.80	17.27	14.19	12.24	12.18
2053	12.50	13.53	15.27	16.90	16.73	16.87	18.46	18.62	16.22	13.91	12.16	11.77
2054	11.90	12.80	16.50	14.94	15.99	16.90	19.80	17.27	15.40	13.19	11.78	12.40
2055	12.61	13.61	15.81	15.30	15.45	18.88	18.76	17.35	14.96	13.74	11.48	12.13
2056	12.46	14.90	16.19	16.30	16.37	16.73	21.82	20.90	17.32	14.72	12.25	12.85
2057	13.40	12.85	14.73	16.58	17.68	18.28	18.79	17.64	14.70	14.29	12.28	12.61
2058	12.65	15.05	15.60	17.73	16.72	17.80	17.43	16.93	14.98	14.54	12.54	12.27
2059	13.10	14.66	15.86	14.42	16.91	17.23	18.64	17.92	16.06	14.93	13.46	13.43
2060	13.01	13.62	15.02	16.05	16.36	18.26	19.52	19.56	17.20	15.30	13.56	12.45

Areal Temperature Minimum RCP 4.5 2070s (2061-2090)

	JAN	FEB	MAR	APR	MAY	JUN	JUL	AUG	SEP	OCT	NOV	DEC
2061	11.97	14.07	16.05	15.39	14.78	20.19	22.10	17.96	14.58	14.09	12.83	12.58
2062	12.32	15.90	17.00	16.83	15.83	19.77	20.74	18.05	15.97	13.53	12.64	12.50
2063	12.70	14.22	17.05	16.14	16.70	20.16	19.17	16.94	16.66	14.40	12.41	12.38
2064	12.48	16.08	16.83	16.96	17.19	20.78	17.70	16.16	17.14	14.60	13.00	12.43
2065	12.94	13.04	14.96	15.82	15.92	19.00	20.31	14.78	17.48	15.45	13.06	12.96
2066	13.15	15.68	15.91	17.86	17.19	18.74	18.63	17.77	15.47	14.26	12.86	12.62
2067	13.16	15.48	16.17	16.44	16.84	21.20	19.15	17.77	18.94	14.99	12.73	12.87
2068	13.02	15.04	14.89	16.46	17.59	21.41	16.45	16.42	16.74	14.40	12.62	12.49
2069	13.49	14.10	15.23	16.37	17.90	18.54	16.67	17.13	16.70	14.59	13.05	12.20
2070	13.39	13.50	15.30	15.60	17.51	19.06	16.93	19.16	17.48	15.06	12.63	12.21
2071	13.08	12.54	14.96	16.18	17.81	17.49	17.30	16.66	18.73	13.91	12.05	11.92
2072	13.72	12.93	14.11	15.93	16.87	17.51	17.82	18.30	19.14	14.77	13.01	12.42
2073	12.67	15.25	16.52	17.60	18.28	20.35	16.78	18.45	18.66	14.36	12.67	12.30
2074	13.68	14.17	15.13	16.41	18.22	22.53	18.66	19.09	16.72	14.83	12.91	12.20
2075	14.10	12.97	16.54	18.00	18.74	19.69	19.24	19.32	18.28	14.22	13.06	11.87
2076	13.57	13.40	15.61	16.69	17.02	20.25	16.38	18.70	18.78	14.81	12.62	12.59
2077	13.20	14.11	15.84	18.13	18.25	19.10	16.45	16.96	16.41	13.71	12.12	11.47
2078	13.43	14.73	15.94	17.49	18.73	17.73	18.05	19.60	18.32	14.78	12.60	12.38
2079	12.85	14.45	15.51	17.23	18.44	17.64	19.40	15.86	16.79	14.84	12.43	12.22
2080	13.49	14.58	17.08	17.40	17.17	19.78	19.97	16.95	16.21	14.59	12.19	12.24
2081	13.80	14.96	17.51	17.77	19.16	19.82	16.89	17.82	14.70	14.65	12.04	11.34
2082	12.91	15.23	16.80	17.73	18.26	17.82	18.82	16.21	15.98	14.22	12.16	11.92
2083	13.65	12.23	17.91	16.18	17.11	16.72	20.49	19.17	15.43	14.74	12.19	12.12
2084	13.35	14.86	16.76	17.27	18.03	18.70	19.32	17.69	12.36	14.21	12.72	13.17
2085	13.18	14.37	16.81	17.23	18.15	18.43	17.11	16.48	17.33	14.19	11.99	12.09
2086	13.15	14.42	17.32	17.57	18.25	18.75	16.94	18.03	14.24	14.12	12.09	11.73
2087	13.49	14.93	17.88	19.04	19.10	19.88	15.69	15.57	16.33	13.76	12.02	11.85
2088	12.52	15.09	18.67	17.99	18.13	18.69	19.04	19.49	17.82	13.67	11.93	12.11
2089	12.93	15.84	17.93	18.44	18.29	20.34	16.88	18.05	14.45	13.94	12.29	11.97
2090	13.54	15.58	18.56	17.84	19.18	20.35	18.24	15.29	16.51	14.08	12.18	12.00

Areal Temperature Minimum RCP 8.5 2050s (2031-2060)

	JAN	FEB	MAR	APR	MAY	JUN	JUL	AUG	SEP	OCT	NOV	DEC
2031	12.86	15.31	17.14	17.99	18.19	18.87	14.20	13.61	16.58	14.20	11.94	10.91
2032	12.43	14.37	15.95	16.20	16.56	18.97	15.27	15.09	15.57	14.32	11.97	11.40
2033	12.19	14.55	16.83	17.82	17.80	19.72	13.92	13.42	13.65	14.54	11.69	11.51
2034	12.77	16.99	16.66	16.30	17.25	20.19	14.65	15.84	16.43	14.85	12.27	11.02
2035	13.61	14.90	16.77	16.55	17.60	20.36	14.57	15.46	15.54	14.73	11.69	10.60
2036	13.03	13.55	16.43	16.74	17.71	20.51	14.91	12.64	14.83	14.62	12.01	10.89
2037	12.69	13.94	16.50	16.36	17.29	16.81	14.19	16.01	15.85	14.81	11.92	11.05
2038	13.21	13.72	14.73	16.41	18.17	19.01	16.67	16.68	18.66	14.54	11.90	11.30
2039	13.26	14.67	15.71	16.86	18.44	19.80	16.27	17.01	18.62	14.48	11.42	11.68
2040	13.58	14.03	16.11	17.44	17.82	18.38	16.04	16.87	16.04	14.38	11.78	11.61
2041	13.63	13.98	16.41	17.32	17.98	18.27	17.89	19.56	19.12	14.81	11.69	11.09
2042	12.07	14.46	15.98	16.50	17.84	21.53	15.65	16.20	16.20	14.01	12.13	10.59
2043	13.83	14.98	15.87	15.94	17.69	19.64	16.52	18.03	16.10	14.90	12.08	11.25
2044	13.62	14.25	15.62	17.13	19.24	20.33	19.51	17.82	17.68	13.77	11.53	11.91
2045	13.16	14.76	15.66	17.51	19.42	19.04	17.65	18.62	15.56	14.79	11.39	11.01
2046	13.39	14.26	15.32	17.77	18.26	18.65	17.39	17.39	16.51	14.19	11.80	11.99
2047	13.86	13.68	15.63	17.31	18.39	19.87	17.40	18.56	18.61	14.68	12.57	12.56
2048	12.51	14.26	15.81	18.15	17.53	18.28	17.52	17.95	17.15	14.60	12.10	11.75
2049	13.03	14.41	16.09	16.70	18.57	18.99	16.78	17.45	13.82	14.79	11.64	11.49
2050	12.79	13.57	15.55	18.46	16.87	17.41	18.16	18.65	17.99	14.31	12.24	13.24
2051	12.92	14.15	15.79	17.25	17.75	18.64	18.96	15.66	16.43	14.82	12.25	12.18
2052	13.33	13.19	16.31	18.44	17.27	18.04	19.40	20.21	18.06	15.14	12.96	12.76
2053	12.79	13.70	15.60	17.38	17.40	19.02	22.07	16.52	17.18	14.91	12.79	13.74
2054	13.22	13.94	15.84	17.56	17.99	19.18	19.82	19.52	17.02	14.14	12.06	12.46
2055	12.99	14.33	16.97	18.89	18.82	18.49	19.02	17.29	15.26	14.15	12.33	12.81
2056	12.48	13.95	15.88	16.77	16.30	17.19	17.74	16.72	15.76	14.63	12.91	12.72
2057	13.27	14.36	16.20	18.70	18.67	17.98	19.66	18.15	16.98	14.49	11.92	11.70
2058	12.53	15.36	15.66	15.97	16.53	18.83	21.42	18.83	16.46	15.83	13.01	13.10
2059	13.79	15.30	15.87	16.88	17.72	18.93	19.64	20.33	17.61	16.69	14.24	13.28
2060	12.95	14.18	16.59	16.78	17.23	17.96	21.47	18.18	16.03	16.19	13.76	13.88

Areal Temperature Minimum RCP 8.5 2070s (2061-2090)

	JAN	FEB	MAR	APR	MAY	JUN	JUL	AUG	SEP	OCT	NOV	DEC
2061	13.13	13.04	15.60	17.67	17.16	19.33	17.39	15.45	15.03	14.60	12.58	12.51
2062	13.22	14.19	15.95	17.26	17.51	19.42	19.15	17.05	15.78	14.21	12.57	12.69
2063	13.10	13.36	14.95	15.93	16.82	19.37	21.76	17.77	16.67	14.40	12.14	13.40
2064	13.24	15.06	15.02	16.34	17.09	19.63	19.40	17.19	17.26	14.62	12.90	13.01
2065	13.49	15.67	16.66	17.36	17.69	20.56	19.39	16.63	16.74	15.41	13.05	12.82
2066	13.65	14.01	16.11	17.69	17.21	20.00	18.19	14.96	15.76	14.21	12.76	12.95
2067	13.93	14.75	16.84	17.72	17.53	18.89	16.29	16.22	17.37	15.19	12.21	11.86
2068	13.54	15.02	15.18	16.67	16.95	20.29	18.98	17.00	17.58	15.19	12.61	12.36
2069	14.44	15.20	14.41	15.75	18.38	19.28	17.23	17.43	17.66	14.82	13.20	12.90
2070	14.14	13.69	15.43	17.66	18.83	17.79	19.16	17.29	16.76	15.31	13.19	13.31
2071	13.79	14.95	16.15	18.32	18.26	18.70	18.78	17.40	16.65	15.19	12.32	12.12
2072	14.11	12.89	15.96	16.68	18.20	18.80	18.27	17.61	17.41	14.74	13.18	12.63
2073	14.49	14.84	14.98	17.54	17.94	20.43	17.22	17.01	16.35	15.12	13.36	12.58
2074	13.89	13.79	15.71	17.88	19.18	18.00	18.34	17.89	17.14	15.02	12.62	12.78
2075	15.12	14.55	15.75	17.49	19.13	17.84	17.52	18.89	16.78	15.16	13.01	12.66
2076	13.97	14.89	15.61	17.97	19.30	18.96	17.84	17.52	18.53	15.37	12.83	12.42
2077	13.85	14.59	16.42	17.72	18.35	20.70	17.56	19.64	19.71	13.98	12.50	12.43
2078	14.48	15.06	15.80	18.22	19.24	20.38	18.78	18.87	15.76	15.12	12.92	12.41
2079	14.41	13.16	15.51	17.81	17.84	18.63	19.91	19.41	17.23	15.41	12.83	12.22
2080	14.62	13.56	16.65	17.51	19.15	21.51	19.16	19.48	18.70	15.28	12.45	12.47
2081	14.46	14.59	16.59	18.45	19.83	21.30	19.41	17.67	18.15	15.33	12.62	12.91
2082	14.86	14.55	16.65	19.34	19.72	20.30	18.68	18.11	17.73	15.08	12.17	12.38
2083	14.09	14.96	18.09	18.82	18.12	19.71	19.67	18.90	17.36	15.12	12.58	12.50
2084	14.57	15.21	17.36	18.92	20.02	20.25	19.21	19.00	18.21	15.18	12.39	12.47
2085	13.97	14.48	15.99	18.25	19.09	19.51	17.57	16.76	17.81	14.81	12.54	12.80
2086	14.97	13.65	17.36	19.20	20.02	18.37	18.10	18.21	16.00	14.50	12.42	12.43
2087	14.83	16.54	17.26	18.85	19.26	19.83	18.87	17.26	18.59	14.54	12.60	13.08
2088	14.74	15.28	17.56	19.03	19.25	21.61	18.48	17.04	18.92	15.03	12.80	13.15
2089	14.49	15.51	17.65	19.31	19.50	17.84	19.42	18.82	20.35	14.35	12.71	12.55
2090	13.80	18.07	18.05	18.66	19.90	23.24	19.35	19.59	19.84	14.28	12.42	12.61

(C)Base Period Observed Stream Flow (m^3/sec) (1989-2002)

Year	Jan	Feb	Mar	Apr	May	Jun	Jul	Aug	Sep	Oct	Nov	Dec
1989	0.763	12.966	13.657	10.314	5.107	1.156	5.173	12.869	11.309	7.465	2.731	0.000
1990	3.832	5.839	4.871	0.000	0.000	1.055	2.439	10.943	10.753	7.489	3.117	1.087
1991	0.941	4.200	9.414	10.637	0.000	0.000	0.000	12.613	13.065	10.607	6.140	2.017
1992	2.133	6.534	4.885	10.267	7.775	3.020	3.235	45.950	22.526	12.567	4.084	2.677
1993	4.549	16.708	9.028	12.728	9.455	4.146	3.995	18.532	12.425	12.813	6.985	2.788
1994	0.716	0.470	3.116	4.716	3.345	1.661	30.551	60.452	34.377	18.965	5.371	2.974
1995	2.415	21.373	15.542	20.585	9.450	5.263	25.392	61.626	35.447	15.587	5.520	8.521
1996	19.416	7.092	9.787	15.423	9.053	8.524	13.164	40.585	19.834	10.455	12.375	10.720
1997	1.903	4.036	12.593	12.241	5.371	5.268	21.411	45.408	31.474	18.382	19.138	13.783
1998	8.150	30.036	20.085	14.680	9.078	4.787	13.050	26.153	16.636	11.718	6.679	10.265
1999	9.611	8.700	8.454	10.459	5.838	3.728	14.554	23.175	18.733	12.467	6.741	4.760
2000	3.494	7.194	13.908	14.398	6.174	3.422	8.817	16.874	22.941	19.851	11.520	10.873
2001	7.607	6.573	11.691	7.709	5.716	8.793	13.844	36.194	24.589	14.646	8.422	7.015
2002	12.654	15.599	14.643	22.301	14.743	8.405	10.198	33.706	23.313	19.410	7.770	7.493

(D) Base Period Sediment Data From Rating Curve (ton) (1989-2002)

Year	Jan	Feb	Mar	Apr	May	Jun	Jul	Aug	Sep	Oct	Nov	Dec
1989	7917.12	264700	428423	63465.4	7211.4	1020.81	272533	155621	98748.4	14742.8	19101	110.688
1990	29683.6	71771.3	37426.4	754383	20588	1009.77	132588	211954	153635	3096.51	34.7372	1057.17
1991	2573.25	179138	391566	425580	17351.9	24241.4	104522	1037741	176383	14040.8	1255.85	220126
1992	256900	24044.1	65505.9	15970.5	69620.3	4024.67	182479	1557030	88039.3	14084.8	5349.77	340331
1993	128824	898104	16460.9	983529	66117.1	3867.86	803625	250232	338766	23391	1768.26	978.947
1994	817.825	599.974	525179	38914.2	6081.96	1513.31	3044678	1013634	606696	1813.18	9050.17	3401.46
1995	776.362	429686	167436	321106	381783	12324	1739888	2914506	76554.6	8600.69	3045.85	295092
1996	94702.9	1125.08	447701	243407	160314	53161.6	288601	306738	202854	11186.1	19593.4	3780.34
1997	11102.4	48233.2	432646	230733	7652.24	284201	845149	393556	37069.8	460096	102677	114.521
1998	15980	138900	67960	71700	10120	2348	271900	165700	95600	18393.1	141.797	220650
1999	50722.2	15763.4	205382	47020.9	9688.22	380.302	150196	202915	160641	5589.31	156.59	2369.22
2000	6846.93	200639	75326.1	45313.4	19173.1	20255.4	86971.2	577220	180549	18007	3882.25	82237.3
2001	64351.6	22947.8	38699.3	20828.7	63120.8	7597.81	232287	779925	83219.9	14671.4	7227.18	167568
2002	60380.9	39918	39565.9	140465	55216.3	1175.37	715643	209677	302271	28137.5	1679.39	115

(E) Data Collected for the development of rating curve

River / Stream	Basin	Flow (m3/sec)	Sed con (mg/l)	sed (t/day)
Mille	Awash	14.387	25538.38	31745.14615
Mille	Awash	14.387	25696.23	31941.35951
Mille	Awash	14.387	25788.63	32056.21611
Mille	Awash	15.796	4652.17	6349.16252
Mille	Awash	15.796	4571.43	6238.970635
Mille	Awash	15.796	4500.00	6141.4848
Mille	Awash	15.000	4218.75	5467.5
Mille	Awash	15.000	4033.33	5227.19568
Mille	Awash	15.000	4000.00	5184
Mille	Awash	9.020	2500.00	1948.32
Mille	Awash	9.020	2500.00	1948.32

Mille	Awash	9.020	2677.42	2086.588374
Mille	Awash	0.535	237.04	10.95693696
Mille	Awash	0.535	266.90	12.3371856
Mille	Awash	0.535	691.67	31.97175408
Mille	Awash	0.563	428.00	20.8192896
Mille	Awash	0.563	345.26	16.79455123
Mille	Awash	0.563	310.45	15.10128144
Mille	Awash	3.374	9858.85	2873.988855
Mille	Awash	3.374	9826.43	2864.537984
Mille	Awash	3.374	9599.46	2798.373143
Mille	Awash	1.098	2565.56	243.3874936
Mille	Awash	1.098	2662.37	252.5715873
Mille	Awash	1.098	2726.36	258.6421394
Mille	Awash	0.834	489.75	35.2902096
Mille	Awash	0.834	521.67	37.59028819
Mille	Awash	0.834	575.65	41.47995744
Mille	Awash	0.540	281.00	13.110336
Mille	Awash	0.540	285.48	13.31935488
Mille	Awash	0.540	299.57	13.97673792
Mille	Awash	0.058	377.59	1.892179008
Mille	Awash	0.058	510.08	2.556112896
Mille	Awash	0.058	410.95	2.05935264
Mille	Awash	0.451	975.56	38.01406118
Mille	Awash	0.451	916.40	35.70880896
Mille	Awash	0.451	892.83	34.79037091
Mille	Awash	0.818	670.10	47.35945152
Mille	Awash	0.818	679.20	48.00259584
Mille	Awash	0.818	717.74	50.72641805
Mille	Awash	0.711	322.58	19.81621843
Mille	Awash	0.711	325.00	19.96488
Mille	Awash	0.711	304.35	18.69634224
Mille	Awash	34.993	39726.49	120108.8792
Mille	Awash	34.993	40522.86	122516.6204
Mille	Awash	34.993	32455.26	98125.0773
Mille	Awash	9.418	8295.83	6750.442968
Mille	Awash	9.418	8201.57	6673.742173
Mille	Awash	9.418	8283.81	6740.662111
Mille	Awash	29.990	5839.21	15130.18724
Mille	Awash	29.990	6243.43	16177.57624
Mille	Awash	29.990	5627.50	14581.61784
Mille	Awash	11.258	1301.35	1265.811693

Mille	Awash	11.258	1295.93	1260.539707
Mille	Awash	11.258	1316.22	1280.275611
Mille	Awash	8.032	456.85	317.0378189
Mille	Awash	8.032	464.48	322.3327703
Mille	Awash	8.032	502.80	348.9255014
Mille	Awash	7.029	21697.59	13177.06791
Mille	Awash	7.029	22407.24	13608.04233
Mille	Awash	7.029	22464.00	13642.513
Mille	Awash	28.287	36483.71	89166.07049
Mille	Awash	28.287	32716.04	79957.89707
Mille	Awash	28.287	41106.50	100464.1545
Mille	Awash	71.263	32014.35	197116.2971
Mille	Awash	71.263	26828.72	165187.7343
Mille	Awash	71.263	26479.35	163036.6202
Mille	Awash	47.565	26100.00	107260.9776
Mille	Awash	47.565	26347.55	108278.313
Mille	Awash	47.565	28677.64	117854.0882
Mille	Awash	306.069	2185.60	57796.79671
Mille	Awash	306.069	53245.00	1408030.033
Mille	Awash	306.069	37055.69	979914.0657
Mille	Awash	763.033	39225.94	2586011.329
Mille	Awash	764.033	40879.71	2698569.861
Mille	Awash	765.033	42999.85	2842240.687
Mille	Awash	46.942	1073.24	4352.834772
Mille	Awash	46.942	13972.06	56667.72446
Mille	Awash	46.942	18379.18	74542.0724
Mille	Awash	65.590	3822.58	21662.46912
Mille	Awash	65.590	7200.00	40802.2272
Mille	Awash	65.590	4000.00	22667.904
Mille	Awash	58.911	17483.87	88991.33175
Mille	Awash	58.911	15944.44	81155.77098
Mille	Awash	58.911	1029.41	5239.604665
Mille	Awash	39.134	16189.78	54740.52148
Mille	Awash	39.134	1486.49	5026.086691
Mille	Awash	39.134	1132.35	3828.676455
Mille	Awash	24.877	18822.58	40456.74148
Mille	Awash	24.877	13932.43	29945.98608
Mille	Awash	24.877	2914.29	6263.895657
Mille	Awash	91.320	2957.14	23331.97654
Mille	Awash	91.320	13561.64	107001.9906
Mille	Awash	91.320	17814.29	140555.6032

Mille	Awash	49.288	1611.11	6860.884868
Mille	Awash	49.288	18250.00	77717.3184
Mille	Awash	49.288	16508.20	70299.89236
Mille	Awash	28.570	17492.54	43179.42538
Mille	Awash	28.570	16220.59	40039.68294
Mille	Awash	28.570	14666.67	36203.91223
Mille	Awash	71.088	16549.30	101645.8536
Mille	Awash	71.088	17880.60	109822.7024
Mille	Awash	71.088	16123.29	99029.29877
Mille	Awash	45.782	940.30	3719.417581
Mille	Awash	45.782	12028.17	47578.20586
Mille	Awash	45.782	17287.88	68383.32959
Mille	Awash	16.256	17764.71	24950.86207
Mille	Awash	16.256	14868.42	20882.96947
Mille	Awash	16.256	15394.74	21622.19559
Mille	Awash	19.431	7657.53	12855.75541
Mille	Awash	19.431	17861.54	29986.63924
Mille	Awash	19.431	10375.00	17417.9484
Mille	Awash	77.301	7402.99	49443.13699
Mille	Awash	77.301	6352.94	42430.05633
Mille	Awash	77.301	16314.29	108959.9845
Mille	Awash	35.119	8852.94	26862.31295
Mille	Awash	35.119	8850.75	26855.66787
Mille	Awash	35.119	575.76	1747.017974
Mille	Awash	16.988	10924.76	16034.9607
Mille	Awash	16.988	10338.73	15174.80743
Mille	Awash	16.988	9000.00	13209.8688
Mille	Awash	0.406	262.49	9.207729216
Mille	Awash	0.406	265.49	9.312964416
Mille	Awash	0.406	222.22	7.795122048